January 2012

Neuroglial Mechanisms Involved In The Anti-Inflammatory Effect Of Acetate Supplementation

Mahmoud Lotfy Soliman

NEUROGLIAL MECHANISMS INVOLVED IN THE ANTI-INFLAMMATORY EFFECT OF ACETATE SUPPLEMENTATION

by

Mahmoud Lotfy Soliman

Bachelor of Medicine and Surgery (MBBCh), Fayoum University, Egypt, 2002

A Dissertation

Submitted to the Graduate Faculty

of the

University of North Dakota

in partial fulfillment of the requirements

for the degree of

Doctor of Philosophy

Grand Forks, North Dakota
December
2012

This dissertation, submitted by Mahmoud Lotfy Soliman in partial fulfillment of the requirements for the Degree of Doctor of Philosophy from the University of North Dakota, has been read by the Faculty Advisory Committee under whom the work has been done and is hereby approved.

_____
Thad A. Rosenberger, Chairperson

_____
Othman Ghribi

_____
James Porter

_____
Keith Henry

_____
Patrick Carr

This dissertation is being submitted by the appointed advisory committee as having met all of the requirements of the Graduate School at the University of North Dakota and is hereby approved.

_____
Dr. Wayne Swisher, Dean of the Graduate School

_____
Date

PERMISSION

Title	Neuroglial Mechanisms Involved in the Anti-inflammatory Effect of Acetate Supplementation
Department	Pharmacology, Physiology and Therapeutics
Degree	Doctor of Philosophy

In presenting this dissertation in partial fulfillment of the requirements for a graduate degree from the University of North Dakota, I agree that the library of this University shall make it freely available for inspection. I further agree that permission for extensive copying for scholarly purposes may be granted by the professor who supervised my dissertation work or, in their absence, by the chairperson of the department or the dean of the Graduate School. It is understood that any copying or publication or other use of this dissertation or part thereof for financial gain shall not be allowed without my written permission. It is also understood that due recognition shall be given to me and to the University of North Dakota in any scholarly use which may be made of any material in my dissertation.

Mahmoud Lotfy Soliman
November 23, 2012

TABLE OF CONTENTS

LIST OF FIGURES

LIST OF TABLES

ACKNOWLEDGMENTS

All thanks are due to God, the Lord of all the worlds.

I would like to acknowledge the Thad Rosenberger laboratory where I thrived and learned how to become a scientist. I owe my deep gratitude to Dr. Matthew Picklo and Dr. Othman Ghribi who have been unwaveringly supportive to me on a personal level, even well before I started my graduate studies. I would also like to thank Dr. Colin Combs for his enormous scientific assistance and humbly teaching me a lot of what I now know. Thank you.

I would not be here today without my parents and siblings in Egypt who inculcated in me the passion for knowledge and the fortitude to work hard.

To my father, the late Dr. Lotfy Soliman

And my mother Dr. Amal Ali Mousa

ABSTRACT

Acetate supplementation increases brain acetyl-CoA and attenuates lipopolysaccharide (LPS)-induced neuroinflammation *in vivo*. To explain the anti-inflammatory effect of acetate treatment, we proposed that acetate treatment disrupts inflammatory signaling in microglia and astrocytes, and induces histone hyperacetylation known to be correlated with anti-inflammatory properties. To test this hypothesis, we measured the effects that LPS and acetate treatment had on histone acetylation, mitogen-activated protein kinase (MAPK), nuclear factor-kappa B (NF-κB), and eicosanoid signaling. A single oral dose of acetate treatment (6 g/kg) in normal animals induced a time- and site-specific pattern of histone hyperacetylation, associated with reduction of histone deacetylase (HDAC) activity and expression. Long-term acetate treatment over 28 days induced the same site-specific pattern of histone hyperacetylation, and reversed LPS-induced histone H3 at lysine 9 (H3K9) hypoacetylation and interleukin (IL)-1β expression. In LPS-stimulated BV-2 microglia, acetate treatment reversed LPS-induced H3K9 hypoacetylation, IL-1β, IL-6, tumor necrosis factor (TNF)-α, cyclooxygenase (Cox)-1 and 2 protein levels, and NF-κB p65 protein level and phosphorylation at serine 468. Further, acetate treatment increased IL-4 and transforming growth factor (TGF)-β1 expression, and NF-κB p65 acetylation at lysine 310. Conversely, acetate treatment did not alter LPS-induced

cytosolic (c) phospholipase A_2 (PLA_2), transiently reduced MAPK p38 and JNK phosphorylation, and increased MAPK ERK1/2 phosphorylation. In LPS-stimulated astrocyte, acetate treatment induced H3K9 hyperacetylation, reversed LPS-induced increases in IL-1β, TNF-α, NF-κB p65, and Cox-1 protein levels, MAPK p38 and $cPLA_2$ phosphorylation and PGE_2 release, and reversed LPS-induced decreases in TGF-β1 and IL-4. Moreover, acetate treatment reduced basal levels of IL-6, phosphorylated ERK1/2 and NF-κB p65 at serine 536, $sPLA_2$ IIA and PLCβ1. Acetate treatment also increased acetylated H3K9 bound to the promoters of the genes of Cox-1, Cox-2, IL-1β and NF-κB p65, but not IL-4 in BV-2 microglia, which suggests that acetate treatment-induced H3K9 hyperacetylation can potentially be involved in the alteration of the expression of these genes. These data suggest that acetate treatment has net anti-inflammatory effects *in vivo* and *in vitro* both in LPS-stimulated microglia and astrocyte cultures through neuroglial cell type-distinct mechanisms.

CHAPTER I

INTRODUCTION

Dietary Acetate Supplementation

Dietary acetate supplementation is a potentially effective therapy for the treatment of Canavan disease; a human demyelinating disease (Arun *et al.* 2010b, Madhavarao *et al.* 2009) and is effective at reducing the tremor phenotype in a rat model of this disease (Arun et al. 2010b). Acetate supplementation is also effective at maintaining adenosine triphosphate (ATP) levels in a rat model of traumatic brain injury (Arun *et al.* 2010a) and reduces neuroglial activation and cholinergic immunoreactivity in rats subjected to lipopolysaccharide (LPS)-induced neuroinflammation (Reisenauer *et al.* 2011). In the brain, acetate is converted to acetyl-CoA through the combined action of nuclear acetyl-CoA synthetase 1 (Ariyannur *et al.* 2010) and mitochondrial acetyl-CoA synthetase 2 (Fujino *et al.* 2001). A single oral dose of glyceryl triacetate increases brain and liver acetyl-CoA levels by 2.2-and 2.6-fold, respectively (Reisenauer et al. 2011). Acetyl-CoA is a widely active precursor in numerous biological processes that are central to mitochondrial energy supply, fatty acid synthesis, and lipid metabolism (Deutsch *et al.* 2002). For example, acetyl-CoA is used for oxidation in Krebs cycle and energy production after condensing with oxaloacetate to form citrate (Des Rosiers *et al.* 1991, McGarry & Foster 1980). Acetate can also be channeled into fatty acids and cholesterol synthesis, and when

present in excess as a result of an increase in fatty acid oxidation, acetyl-CoA can form ketone bodies (Fukao *et al.* 2004).

Acetylation of Histone and Non-histone Proteins

Acetyl-CoA is utilized as a substrate for protein acetylation which is increasingly appreciated as one of the major post-translational modification systems with a wide range of histone and non-histone substrates. Non-histone targets of acetylation include transcription factors, nuclear transport factors, cytoskeletal proteins and many enzymes involved in diverse metabolic and signaling transduction pathways (Polevoda & Sherman 2002). Acetylation of non-histones alters their subcellular localization, DNA binding, transcriptional activity, protein-protein interaction, and protein stability (Glozak *et al.* 2005).

Another major target of acetylation is histone proteins which are instrumental in the packaging of DNA and play a central role in transcription regulation. There are five isoforms of histones: H1, H2A, H2B, H3 and H4. The basic structural unit of eukaryotic chromosomes is a DNA-protein complex called the nucleosome which consists of a DNA molecule associated with a histone octamer comprised of pairs of the core histones H2A, H2B, H3 and H4. The nucleosomes are joined by linker DNA and histone H1 to form chromatin, and each chromosome can accommodate 147 base pairs of DNA. Each core histone has a globular region and a histone fold domain which is involved in histone-histone interactions (Arents *et al.* 1991) and the wrapping of DNA around the nucleosome core (Luger *et al.* 1997). The N-terminal tail regions extend outside of the nucleosome particle where they can interact with DNA and with other

regulatory proteins or transcription factors (Baneres *et al.* 1997, Bradbury 1992, Luger et al. 1997). Acetylation of the lysine residues on the N-terminal tail of histones neutralizes the positive charge on the lysine residue and reduces histone-DNA binding. The reduction in histone-DNA binding increases the accessibility of chromatin by transcription machinery (Anderson *et al.* 2001, Gorisch *et al.* 2005, Polach *et al.* 2000). Hyperacetylated nucleosomes also increase the flexibility of the DNA associated with the end of the nucleosomes, which is proposed as an additional way histone acetylation can alter gene expression (Krajewski & Becker 1998). Histone acetylation and methylation sites are recognized by proteins that have bromo- and chromo-domains respectively. Therefore, covalently modified histone serve as marks for binding sites to recruit other proteins that facilitate downstream events resulting in altered gene expression (Mu *et al.* 2007). The multitude of events and changes that take place during transcription are thus not due only to histone acetylation changes, but represents the outcome of synergistic actions of several factors (Eberharter & Becker 2002).

The acetylation of histone H4 is restricted to lysines 5, 8, 12, and 16 (H4K5, H4K8, H4K12 and H4K16, respectively) (Clarke *et al.* 1993). Another known post-translational modification of histone H4 is methylation, restricted to lysine 20 (Borun *et al.* 1972), which precludes acetylation at this site (Annunziato *et al.* 1995). Random histone acetylation would yield four mono-acetylated isoforms: acetylated H4K5, H4K8, H4K12 or H4K16, six di-acetylated isoforms: H4K5/H4K8, H4K5/H4K12, H4K5/H4K16, H4K8/H4K12, H4K8/H4K16 and H4K12/H4K16, four tri-acetylated isoforms: H4K5/H4K8/H4K12, H4K5/H4K12/H4K16, H4K8/H4K12/H4K16, and

H4K5/H4K8/H4K16, and one tetra-acetylated isoform. The most common mono-acetylated form is that of lysine 16 (Zhang *et al.* 2002). Histone H3 can be acetylated at lysines 9, 14, 18 and 23, of which the acetylation at lysines 9 and 14 is better understood (Sterner & Berger 2000), and can be methylated at more numerous sites including lysines 4, 9, 27, 36 and 79, and arginines 2, 17 and 26 (Mu et al. 2007). H2A has the largest number of variants including H2A.Z, MacroH2A, H2A-Bbd, H2AvD, and H2A.X which are classified based on the C-terminal sequence and length, and genomic distribution (Redon *et al.* 2002). H2B has a few variants with largely unknown roles, even though they have specialized functions in chromatin compaction and transcription repression during gametogenesis (Green *et al.* 1995). The involvement of histones H2A and H2B in inflammation is less clear than histones H3 and H4. A pubmed search using the keywords "H3 and H4 and inflammation" retrieves 54 articles, whereas using the keywords "H2A and H2B and inflammation" retrieves only 3 references. We therefore chose to focus on changes in histones H3 and H4, but this does not exclude the possibility of acetate treatment inducing covalent modifications in histones H2A and H2B with potential functional consequences. Histone proteins can also be modified by phosphorylation, ADP-ribosylation, glycosylation and ubiquitination although the most well studied modifications are acetylation and methylation (Mu et al. 2007). Throughout our studies, we focused on acetylation changes in histones which are more likely to result from altering the level of the acetyl group donor acetyl-CoA after acetate treatment.

Site-specific acetylation patterns have been linked to both physiological and pathological roles. For example, histone H4 acetylated at lysine 16 (H4K16) is essential for transcription initiation (Shogren-Knaak *et al.* 2006) and DNA repair (Li *et al.* 2010). Histone H3 acetylated at lysine 9 (H3K9) is selectively enriched at the promoters of stem cells, suggesting a role in pluripotency (Hezroni *et al.* 2011). Alterations in histone acetylation state are involved in many physiological processes including normal development (Shi & Wu 2009), cell differentiation (Haumaitre *et al.* 2009), memory formation (Peleg *et al.* 2010, Levenson *et al.* 2004), cellular lifespan (Dang *et al.* 2009), synaptic plasticity (Vecsey *et al.* 2007, Guan *et al.* 2009, Sharma 2010), and modifications of embryonic neuron differentiation (Balasubramaniyan *et al.* 2006). Therapeutically, increases in histone acetylation are associated with neuroprotective properties in animal models of cerebral ischemia (Kim *et al.* 2007), and amyotrophic lateral sclerosis (Rouaux *et al.* 2007), and reduce microglial activation in traumatic brain injury (Zhang *et al.* 2008). Furthermore, oxidative stress-induced apoptosis, a hallmark of many neurodegenerative diseases such as Alzheimer's disease, Parkinson's disease, Huntington's disease, stroke, and multiple sclerosis, is reduced upon treatment with histone deacetylase (HDAC) inhibitors suberoylanilide hydroxamic acid (SAHA) and trichostatin A (TSA) which lead to histone hyperacetylation (Ryu *et al.* 2003). Similarly, HDAC inhibitors decrease polyglutamine toxicity in a mouse motor neuron–neuroblastoma fusion cell line (McCampbell *et al.* 2001) and in Drosophila models of polyglutamine diseases (Steffan *et al.* 2001). All of which suggests a loss of neuronal function during

neurodegeneration can be restored by increasing histone acetylation. The histone acetylation state is actively maintained by the opposing activities of two enzyme families: histone acetyltransferases (HATs) and HDACs. Based on structural homology, HDACs are classified into different classes: HDAC class I is mainly located in the nucleus, HDAC class II shuttles between the nucleus and cytoplasm, and HDAC class III (sirtuins) are located in the cytoplasm (de Ruijter *et al.* 2003). HDAC classes I and II are inhibited by conventional HDAC inhibitors, while class III HDACs are nicotinamide adenine dinucleotide (NAD+)-dependent and inhibited by nicotinamide (Avalos *et al.* 2005). Likewise, HATs are classified into distinct families (general control non-derepressible 5 (GCN5), P300/cyclic adenosine monophosphate response element binding protein associated factor (PCAF), the MYST family named for its founding members in yeast and mammals, monocytic leukemia zinc finger protein (Moz), Something About Silencing protein (Sas2p), and HIV tat-interacting protein 60 (Tip60), transcription initiation factor TFIID 250 kDa subunit (TAFII250), steroid receptor coactivator proteins (SRC), and GCN5-related N-acetyltransferase (GNAT)) that show high sequence similarity within families, but poor-to-no sequence similarity between families (Marmorstein & Roth 2001). The exact correlation of individual HATs or HDACs with site-specific acetylation or deacetylation of histone lysine residues remains largely unknown due to overlapping enzyme targets (Howe *et al.* 2001, Kuo *et al.* 1996).

Neuroinflammation

Neuroinflammation, an innate immune response characterized by the release of a repertoire of inflammatory mediators including cytokines, is advantageous with regard to normal brain physiology. However, excessive and persistent neuroinflammation is detrimental and associated with numerous neurological pathologies (Glass *et al.* 2010, Mrak 2009). Cytokines have pleiotropic physiological functions that include regulating cell growth, survival, differentiation, and activities (Hopkins & Rothwell 1995, Rothwell & Hopkins 1995). Cytokine release can lead to either beneficial or deleterious outcomes depending on the dose, time and duration of secretion, and cellular target leading to enhanced cellular viability or further damage, respectively (Suzuki *et al.* 2009). Under normal conditions, cytokines serve as communication signals among different cell types in the brain, but contribute to bystander neuronal lysis in uncontrolled neuroinflammation (Tian *et al.* 2012). Excessive pro-inflammatory cytokines tumor necrosis factor-alpha (TNF-α), interleukin (IL)-1β, and IL-6 are involved in the pathogenesis of neuroinflammatory and neurodegenerative disease states such as acute cerebral ischemia (Denes et al. 2010), Alzheimer's disease (Johnston *et al.* 2011, Shaftel *et al.* 2008), Parkinson's disease (Qian *et al.* 2010), multiple sclerosis (Merson *et al.* 2010) and traumatic brain injury (Helmy *et al.* 2011). Therefore, disrupting pro-inflammatory cytokine signaling is commonly proposed as a therapeutic target. In contrast, anti-inflammatory cytokines include transforming growth factor-beta1 (TGF-β1), IL-4 and IL-10 which obviate the potential of injury due to excessive or uncontrolled inflammatory reactions through

downregulating the pro-inflammatory cytokines and induction of tissue repair (Ledeboer *et al.* 2000, Vitkovic *et al.* 2001). A dynamic balance exists between the pro- and anti-inflammatory cytokines, both of which are generated upon exposure to injury or infection. The duration and net effect of interactions between these opposing molecular groups determines the outcome of the immune response. Pathologies arise from shifting this dynamic balance in one direction or the other. For example, excessive pro-inflammatory cytokines are linked to neuroinflammation and degeneration as mentioned earlier, while excessive anti-inflammatory cytokines are conversely associated with susceptibility to systemic infections (Kasai *et al.* 1997, Munoz *et al.* 1991).

Lipopolysaccharide-induced Neuroinflammation

A well-established method of inducing neuroinflammation experimentally is through the use of LPS in whole animals or in cell cultures. LPS, an endotoxin present in the membrane of Gram-negative bacilli, binds to toll-like receptor 4 (TLR-4) found on many brain cell types and promotes an inflammatory response characterized by enhanced expression of the pro-inflammatory cytokines, neuroglial activation and neurodegeneration, and increased turnover and metabolism of brain arachidonic acid. The activities of both arachidonic acid-selective secretory (s) and cytosolic phospholipases A_2 ($cPLA_2$) also increase as do the levels of prostaglandins E_2 and D_2 (PGE_2 and D_2) with LPS stimulation. Thus, this model reproduces many of the properties associated with known modalities of neuroinflammation (Aravalli *et al.* 2007, Hauss-Wegrzyniak *et al.* 1998a, Hauss-Wegrzyniak *et al.* 1998b, Hauss-

Wegrzyniak *et al.* 2000, Lehnardt 2010, Lehnardt *et al.* 2003, Reisenauer et al. 2011, Rosenberger *et al.* 2004). LPS infusion through a cannula implanted into the fourth ventricle of the brain and connected to a subcutaneous mini-osmotic pump is commonly used as a model to study neuroinflammation *in vivo* (Hauss-Wegrzyniak et al. 1998a, Hauss-Wegrzyniak et al. 1998b, Hauss-Wegrzyniak et al. 2000, Reisenauer et al. 2011, Rosenberger et al. 2004).

Microglia and Aastrocytes in Physiology and Neuroinflammation

Microglia are the primary resident immune cells of the central nervous system that, under normal conditions, monitor the brain for any changes in the environment. When the structural or functional integrity of the brain is disturbed, microglia change into a more reactive phenotype characterized by microglial hypertrophy, loss or shortening or cellular processes, increased secretion of inflammatory mediators and enhanced phagocytic activity (Hanisch 2002, Hanisch & Kettenmann 2007, Lehnardt 2010, Lehnardt et al. 2003, Olson & Miller 2004, Ransohoff & Perry 2009, Streit *et al.* 1999). The BV-2 mouse microglia cell line, immortalized through oncogenes-carrying retrovirus, exhibit morphological, functional, and phenotypical properties similar to primary microglia (Blasi *et al.* 1990, Bocchini *et al.* 1992). Therefore, BV-2 microglial cells are commonly used as an alternative to primary microglia to study various microglial responses and interactions (Petrova *et al.* 1999, Rojanathammanee *et al.* 2011, Woo *et al.* 2003). Astrocytes are the most abundant cell type in central nervous system with essential functions in maintaining the blood-brain barrier, synaptic plasticity, provision of metabolites to neurons, and neurotransmitters homeostasis

(Sadoul *et al.* 2008, Sofroniew & Vinters 2010). Being connected via gap junctions, in injury and infections, astrocytes distribute many mediators that contribute to either detrimental or beneficial consequences (Frantseva *et al.* 2002, Nakase *et al.* 2003). In inflammatory conditions, astrocytes undergo reactive astrogliosis characterized by astrocytic hypertrophy, upregulation of intermediate filaments like vimentin and glial fibrillary acidic protein (GFAP), altered molecular expression profile, and scar formation (Kang & Hebert 2011, Pekny & Nilsson 2005, Sofroniew 2009). Although essential for proper tissue healing, excessive astrocytic reactivity contributes to the inflammatory response through production to numerous pro-inflammatory cytokines (Dong & Benveniste 2001, Gorina *et al.* 2011, Gorina *et al.* 2009) and are thus recognized as a potential target of therapeutics in many neurological disorders (Hamby & Sofroniew 2010).

Mitogen-activated Protein Kinases and Nuclear Factor-kappa B Signaling

Mitogen-activated protein kinases (MAPK) p38, c-Jun N-terminal kinase (JNK) and extracellular signal-regulated kinase (ERK) have a crucial role in the regulation of the immune and inflammatory responses, cell differentiation and survival, and the response to stress. MAPK are key regulators of the biosynthesis of pro-inflammatory cytokines TNF-α, IL-6 and IL-1β and are hence potential therapeutic targets in inflammatory and autoimmune diseases (Kumar *et al.* 2003, Pearson *et al.* 2001). When activated by phosphorylation, MAPK signaling upregulates the biosynthesis of a number of inflammatory mediators including the pro-inflammatory cytokines (Kaminska *et al.* 2009, Pearson et al. 2001). Interestingly, a certain lysine acetylation

in MAPK phosphatase-1 leads to its activation, which subsequently dephosphorylates and inactivates MAPK signaling (Cao *et al.* 2008). This provides an important link between acetylation and phosphorylation in the regulation of inflammatory signaling. Nuclear factor-kappa B (NF-κB) is another major regulator of inflammatory and immune responses downstream of TLR-4 receptors. NF-κB is a heterodimer of two subunits; most commonly p65 and p50, combined in the cytosol with inhibitors of kappa B (IκB) which mask the nuclear export motif, leading to NF-κB inactivity. Upon stimulation by pro-inflammatory cytokines, B and T cell receptor signaling, and viral and bacterial toxins, NF-κB is released from IκB and translocates to the nucleus where it binds DNA sequences and alters the transcriptional activity of genes involved in inflammatory responses and cell survival (Chen & Ghosh 1999, DiDonato *et al.* 2012, Schmitz *et al.* 2004). p65, but not p50, binds transcriptional co-activators p300 and CREB-binding protein (Perkins *et al.* 1997) and can be modified by acetylation at certain lysine residues with variable functional outcomes in terms of the affinity to IκB, nuclear translocation, DNA binding and transcriptional activity (Chen & Ghosh 1999, Chen *et al.* 2001, Chen *et al.* 2002, Huang *et al.* 2010a, Kiernan *et al.* 2003). Therefore, both MAPK and NF-κB signaling pathways are important players in inflammation that can be regulated by acetylation.

Eicosanoid Signaling

Phospholipases are a heterogeneous group of enzymes which catalyze the hydrolysis of fatty acids esterified to membrane phospholipids and release free fatty acids and lysophospholipids. The action of cyclooxygenases-1 and 2 (Cox-1 and 2) on

arachidonic acid, released from the *sn*-2 position of membrane phosphatidyl choline by the action of PLA_2, leads to the release of prostaglandins (PGs) (Smith *et al.* 2000). PLA_2 groups are classified into cytosolic (c) PLA_2 and secretory (s) PLA_2 which require calcium for activity, and calcium-independent PLA_2 ($iPLA_2$) (Balboa *et al.* 2002, Dennis 1994). $sPLA_2$ is divided into type I (also called pancreatic type) and type II (also called inflammatory type) (Sun *et al.* 2010), the most well studied of which is type IIA $sPLA_2$ expressed in most areas of rat brain and whose levels are elevated after inflammatory conditions like ischemia and endotoxic shock (Fujimori *et al.* 1992, Lauritzen *et al.* 1994). PLCs, structurally divided into PLCβ, γ, δ, and ε, hydrolyze fatty acids esterified at the *sn*-3 position of phosphatidyl inositol 4, 5-bisphosphate to release diacyl glycerol and inositol 1, 4 and 5- trisphosphate which eventually increase intracellular calcium and activate protein kinase C (Farooqui & Horrocks 2005). The physiological functions of phospholipases in the brain include phospholipid metabolism, exocytosis, removal of phospholipid peroxides, neurotransmitter release, long-term potentiation, neural cell proliferation, and the release of neurotransmitters (Farooqui *et al.* 1997, Balboa et al. 2002, Dennis 1994). Eicosanoid signaling is upregulated by LPS, pro-inflammatory cytokines IL-1β, IL-6 and TNF-α, NF-κB, and MAPK p38, ERK and JNK, all of which are major players in neuroinflammation (Farooqui & Horrocks 2005, Sun et al. 2010, Fujimori et al. 1992, Lauritzen et al. 1994, Lima *et al.* 2012, Phillis & O'Regan 2004, Farooqui et al. 1997, Smith et al. 2000, Balboa et al. 2002, Dennis 1994, Hiller & Sundler 1999, Kramer *et al.* 1996, Adibhatla & Hatcher 2007, Jupp *et al.* 2003). $cPLA_2$ is activated by phosphorylation, especially

by MAPK, which is followed by translocation from the cytosol to the membrane (Hiller & Sundler 1999, Kramer et al. 1996). In pathological conditions, phospholipases and eicosanoid signaling has a role in neuronal injury because of altered membrane permeability, accumulation of free fatty acids and lipid peroxides and are therefore involved in a number of neuroinflammatory and degenerative conditions (Lima et al. 2012, Phillis & O'Regan 2004).

Our Work and Findings

Acetate supplementation increases plasma and tissue levels of acetate and brain levels of acetyl-CoA, and attenuates LPS-induced microglia and astroglial activation and the loss of cholinergic immunoreactivity in a rat model of neuroinflammation (Reisenauer et al. 2011). In addition, acetate treatment is effective therapy for the treatment of a human demyelinating disease Canavan disease (Arun et al. 2010b, Madhavarao et al. 2009) and is effective at reducing the tremor phenotype in a rat model of this disease (Arun et al. 2010b). Acetate supplementation is also effective at maintaining ATP levels in a rat model of traumatic brain injury (Arun et al. 2010a) . This body of work represents an attempt to understand the mechanisms of the anti-inflammatory effects of acetate supplementation in inflammation. No reports are available that describe a decline in brain acetate levels in response to LPS or neurological pathologies. Consequently, rather than replenishing endogenous acetate stores, we propose that acetate supplementation acts to increase intracellular levels of acetyl-CoA as an inducer of metabolic and molecular processes that ultimately result in the reduction of inflammatory phenotype. Our overall hypothesis is that acetate

treatment in *in vivo* and *in vitro* models of inflammation shifts the cytokine balance toward a more anti-inflammatory state and disrupts inflammatory signaling, which is associated with acetylation of histone and non-histone targets. To begin to test this hypothesis, we tested the effect that a single oral dose of glyceryl triacetate, used to induce acetate supplementation, has on brain histone acetylation. We treated normal rats once with oral gavage of 6 g/kg glyceryl triacetate and used Western blot analysis to determine the level of acetylated histone H3 at lysine 9 and 14 (H3K9 and H3K14), and histones H4 at lysine 5, 8, 12 and 16 (H4K5, H4K8, H4K12 and H4K16). We chose this dose of glyceryl triacetate based on earlier reports showing that this is the dose that leads to the highest increase in plasma and tissue acetate levels (Mathew *et al.* 2005). Our goal was to induce the highest possible acetyl-CoA level derived from acetate treatment to identify the metabolic and inflammatory processes that can be modulated downstream to acetyl-CoA formation. Thereafter, the dose of acetate can be scaled down to determine the smallest acetate concentration that still leads to the desired therapeutic effects. We found that acetate treatment induced a pattern of site- and time-specific histone hyperacetylation in the brain. Acetate supplementation increased the acetylation state of brain H4K8 at 2 and 4 h, H4K16 at 4 and 24 h, and H3K9 at 4 h following treatment. No changes in other forms of brain H3 and H4 acetylation state were found at any post-treatment times measured. To determine the mechanism by which a single acetate supplementation alters histone acetylation, we measured the effect of a single acetate treatment on the HAT and HDAC enzymic activities. We found that while HAT activity was not altered by a single oral dose of

acetate treatment, HDAC activity was reduced at 2 and 4 hrs that was associated with reduced HDAC2 protein level. Based on these data, we conclude that a single oral dose of acetate supplementation can indeed alter histone acetylation, which is mainly due to reduction in HDAC activity.

The hypothesis that long-term acetate supplementation reverses LPS-induced histone acetylation changes and pro-inflammatory expression in the brain, proceeded to be tested. The objective of this study was to demonstrate the association of histone hyperacetylation with functional consequences in terms of alteration of inflammatory gene expression in a rat model of neuroinflammation. Sprague-Dawley rats underwent surgeries to install LPS or artificial cerebrospinal fluid (aCSF) subcutaneous minipumps connected to a cannula implanted into the 4^{th} ventricle. Afterwards, animals were treated orally daily with either water or glyceryl triacetate (6 g/kg). After 28 days of treatment, animals were killed and the brains were collected. Using Western blot analysis, we measured histone acetylation changes as well as the expression of IL-1β protein. Parallel studies were performed to quantify IL-1β mRNA using quantitative real-time polymerase chain reaction (qrt-PCR). We found that long-term acetate supplementation increased the proportion of brain H3K9, H4K8 and H4K16, similar to that found with a single oral dose. However, unlike a single dose of glyceryl triacetate, long-term treatment increased HAT activity and had no effect on HDAC activity, with variable effects on brain HDAC class I and II expression. In agreement with our hypothesis, neuroinflammation reduced the proportion of brain H3K9 acetylation by 50%, which was effectively reversed with acetate supplementation. Further, in rats

subjected to LPS-induced neuroinflammation, IL-1β protein and mRNA levels were increased by 1.3- and 10-fold, respectively, and acetate supplementation reduced this expression to control levels. Based on these results, we conclude that dietary acetate supplementation effectively reduces pro-inflammatory cytokine expression by a mechanism that may involve a distinct site-specific pattern of histone acetylation in the brain.

An *in vitro* system that is conducive to examining the effect of acetate treatment on certain inflammatory signaling pathways in primary and BV-2 microglia and primary astrocyte cultures was then designed. We proposed that in microglia and astrocytes, acetate supplementation reverses LPS-induced changes in histone acetylation, pro- and anti-inflammatory cytokines, and MAPK, NF-κB, and eicosanoid signaling. In order to test that, we measured the effects of LPS and acetate treatment on the proportion of acetylated H3K9, the expression of IL-1β, IL-6, TNF-α, TGF-β1, IL-4 and IL-10, the phosphorylation of MAPK p38, JNK and ERK1/2, NF-κB p65 total protein and modification, $cPLA_2$ phosphorylation, the protein levels of $sPLA_2$ IIA, PLCβ1, PLCγ1, PLCδ1, Cox-1 and Cox-2, and the release of PGE_2. We treated primary microglia for 4 hours with either 6.25 ng/ml LPS and/or 12 mM sodium acetate and compared the results to 12 mM NaCl as a control group. The rationale for using this acetate concentration is based on unpublished data showing that 12 mM sodium acetate is the highest concentration that does not cause significant cell death compared to cells grown in serum-free media. The rationale for using this LPS concentration is based on the dose-response study showing that this LPS concentration produced 50%

H3K9 hypoacetylation in microglia similar to that found *in vivo*, and increased all the pro-inflammatory cytokines measured in microglia. NaCl was used as a control group as well as together with LPS treatment to make sure all treatment groups had similar osmolarity to that of 12 mM sodium acetate. Acetate supplementation increased H3K9 acetylation starting at 2 hours in BV-2 microglia and at 1 hr in astrocytes, so we chose 4 hr for later treatments to ensure protein expression after treatment.

We observed distinct neuroglial-cell type specific differences both with acetate treatment and LPS challenge. In LPS-stimulated microglia, acetate treatment induced H3K9 hyperacetylation and reversed LPS-induced H3K9 hypoacetylation similar to that found *in vivo*. LPS also increased IL-1β, IL-6 and TNF-α mRNA and protein, while acetate treatment returned the protein to control levels and only partially attenuated IL-6 mRNA. In contrast, acetate treatment increased mRNA levels of TGF-β1 and both IL-4 mRNA and protein. LPS increased p38 MAPK and JNK phosphorylation at 4 and 2-4 hr respectively, while acetate treatment reduced p38 MAPK and JNK phosphorylation only at 2 hr. In addition, acetate treatment reversed the LPS-induced elevation of NF-κB p65 protein and phosphorylation at serine 468 and induced hyperacetylation at lysine 310. Acetate treatment did not alter the LPS-induced 1.7-fold increase in the $cPLA_2$ phosphorylation, reversed to control levels the LPS-induced 2-fold reduction in PLCβ1 protein levels and 1.5-fold increase in Cox-1 protein level, and only partially attenuated the LPS-induced 4-fold increase in Cox-2 protein level. The protein levels of total $cPLA_2$, $sPLA_2$ IIA, PLCγ1 and PLCδ1, and PGE_2 release were not altered by either acetate treatment or LPS. Because acetate

treatment induces H3K9 hyperacetylation, reverses LPS-induced H3K9 hypoacetylation, and alters inflammatory gene expression *in vivo* (Soliman *et al.* 2012b) and *in vitro* (Soliman *et al.* 2012a), we proposed that acetate treatment increases the enrichment levels of acetylated H3K9 at the promoters of Cox-1 and 2, NF-κB, pro-inflammatory cytokine IL-1β and anti-inflammatory cytokine IL-4. Using chromatin immunoprecipitation analysis in LPS-stimulated BV-2 microglia, acetylated H3K9 was found to be increased with acetate treatment at the promoter regions of these genes except IL-4. It is therefore possible that acetate treatment-mediated increase in acetylated H3K9 bound to the promoters of certain inflammatory genes is potentially involved in altering their expression. These data suggest that acetate metabolism shifts inflammatory cytokine balance toward an anti-inflammatory state, alters the levels of enzymes involved in eicosanoid signaling, and possibly disrupts NF-κB signaling, which is associated with histone and non-histone protein hyperacetylation in LPS-stimulated microglia.

Using primary astrocyte cell cultures, we found that LPS (0-25 ng/ml, 4 hr) increased TNF-α and IL-1β in a concentration-dependent manner, which was reduced by treatment with sodium acetate (12 mM). LPS did not alter H3K9 acetylation or IL-6 levels, whereas acetate treatment increased H3K9 acetylation and decreased basal levels of IL-6. Acetate treatment attenuated the LPS-induced increase in TNF-α mRNA, but did not reverse the mRNA levels of other pro-inflammatory cytokines. By contrast, LPS decreased TGF-β1 and IL-4 protein and TGF-β1 mRNA, all of which was reversed with acetate treatment. Further, acetate treatment completely reversed

LPS-induced phosphorylation of MAPK p38 and decreased basal levels of phosphorylated extracellular signal-regulated kinases1/2 (ERK1/2). Acetate treatment also reversed LPS-elevated NF-κB p65 protein level and reduced basal levels of phosphorylated NF-κB p65 at serine 536. Moreover, acetate treatment reversed to control levels the LPS-induced 2-fold increase in $cPLA_2$ phosphorylation and the 1.5-fold increase in Cox-1 protein level, and decreased those of $sPLA_2$ IIA and PLCβ1 below control levels only in the presence of LPS. Acetate treatment decreased basal levels of Cox-2 by 2-fold only in the absence of LPS and had no effect on LPS-induced 3-fold increase in Cox-2 protein levels. The protein levels of total $cPLA_2$, PLCγ1 and PLCδ1 were not altered by either acetate treatment or LPS. Acetate treatment reversed to control levels the LPS-induced 4-fold increase in PGE_2 release. These results suggest that acetate treatment shifts the inflammatory cytokine balance toward an anti-inflammatory state, which is associated with histone hyperacetylation and a disruption in MAPK, eicosanoid and possibly NF-κB signaling in LPS-stimulated primary astrocytes. Overall, these data suggest that acetate treatment has net anti-inflammatory effects *in vivo* and *in vitro* both in LPS-stimulated microglia and astrocyte cultures through neuroglial cell type-specific mechanisms, most notably of which is the reversal of LPS-induced p38 and $cPLA_2$ phosphorylation and PGE_2 release, and reducing basal levels of phosphorylated ERK1/2 in astrocytes.

CHAPTER II

METHODS

Reagent

Antibodies against acetylated H3K9, acetylated H3K14, total histone H3, total histone H4, acetylated histone H4K5, H4K8, H4K12 and H4 K16 were obtained from Upstate Biotechnology (Lake Placid, NY). Antibodies against HDAC1, 2, 3, 4, 5 and 7 were obtained from Cell Signaling Technology Inc. (Danvers, MA). Mouse monoclonal antibody against α-tubulin and goat anti-mouse IgM secondary antibody conjugated with horse radish peroxidase were from Santa Cruz Biotech. Inc. (Santa Cruz, CA). Antibodies against phosphorylated p38 (Thr180/Tyr182), total p38, phosphorylated JNK (Thr183/Tyr185, Thr221/Tyr223), phosphorylated ERK1/2 (Th202/Tyr204, Thr185/Tyr187), and ERK1/2 were from Millipore (Billerica, MA), and anti-JNK and NF-κB p65 antibodies were purchased from Cell Signaling Technology Incorporated (Danvers, MA). Rabbit polyclonal antibodies to IL-1β, IL-6, TNF-α, TGF-β1, IL-4, IL-10 and acetyl-CoA synthetase, and HAT activity assay kit were from Abcam (Cambridge, MA). All Western blot supplies and a goat anti-rabbit horseradish peroxidase-linked antibody were obtained from Bio-Rad Laboratories (Hercules, CA). Glyceryl triacetate was purchased from Sigma (St. Louis, MO). Reverse and forward IL-1β, IL-6, TNF-α , IL-4, IL-10, TGF-β1 and β-actin primers for real-time polymerase chain reaction (qrt-PCR) from SA Biosciences (Frederick, MD),

FastStart Universal SYBR Green Master from Roche Applied Science (Indianapolis, IN), TRIzol® reagent from Life Technologies (Grand Island, NY), the RT² Profiler™ PCR Array was from SABiosceinces (Valencia, CA), nuclease-free water was purchased from Gibco, Life Technologies (Grand Island, NY), and DMEM–F-12 media and fetal bovine serum were from Invitrogen (Grand Island, NY). LPS (Escherichia Coli 055:B5) and proteinase K were purchased from Sigma (St. Louis, MO), antibodies against PLCβ1, γ1, δ1, $cPLA_2$ from Santa Cruz Biotechnology Inc. (Santa Cruz, CA), antibodies against Cox-1, Cox-2 and $sPLA_2$ IIA, and prostaglandin screening EIA kit from Cayman Chemical Company (Ann Arbor, MI), and RNAse A from Invitrogen (Grand Island, NY). Chromatin immunoprecipitation assay kit, antibodies against acetylated H3K9 and normal rabbit IgG, and HDAC activity assay kit were purchased from Millipore (Billerica, MA), QIAquick PCR purification kit from Qiagen (Valencia, CA), protein A and protein G magnetic beads from Invitrogen (Grand Island, NY), complete EDTA-free protease inhibitor cocktail tablets from Roche Applied Science (Indianapolis, IN). All chromatin immunoprecipitation primers (table 1) were ordered from Integrated DNA Technologies (Coraville, IA). All buffering reagents and other chemicals were purchased from EMD Biosciences (Gibbstown, NJ).

Animals

All rats used conformed to the Guide for the Care and Use of Laboratory Animals (NIH publication number 80-23) as approved by the University of North Dakota animal care and use committee. Male Sprague-Dawley rats (220-300 g, Charles River Laboratories, Portage, MI) were allowed to acclimate in our facility for at least

two weeks prior to inclusion in the study and were maintained on a constant 12-hour light cycle and fed a standard lab chow (Purina 2018 Tekled Global) *ad libitum*. Oral glyceryl triacetate (6 g/kg) was used to induce acetate supplementation using feeding tubes (Instech, Solomon, PA) in rats that were starved for at least 12 hours before treatment to normalize circulating levels of glucose and fatty acids (Kargas *et al.* 1990). The rats were divided into six different groups (n = 6 per group). Groups one through five (GTA-treated) were given a single oral dose of glyceryl triacetate while control rats were given a single oral dose of water (6 g/kg).

Induction of Neuroinflammation

In order to induce neuroinflammation, animals were subjected to surgeries by which cannulas (Model 3280PM, Plastics One, Roanoke, VA, USA) connected to subcutaneous osmotic mini-pumps (Model 2004, Durect Corp. Cupertino, CA, USA) were surgically implanted into the fourth ventricle of the rat brain as described in (Reisenauer et al. 2011). The concentration of endotoxin used in these studies (5.0 ng/hr) is based on results showing that this concentration results in significant neuroglia activation and cholinergic cell loss above control treated rats (Reisenauer et al. 2011), and is consistent with previous studies demonstrating a selective increase in arachidonic acid metabolism using this model (Lee *et al.* 2004, Rosenberger et al. 2004). During the infusion period, rats were treated daily with either glyceryl triacetate or water at a dose of 6 g/kg by gastric gavage using feeding tubes (Instech Solomon, Plymouth, PA). The rats used for histone acetylation analysis were divided into four different groups: group one (n = 8) received an aCSF infusion and were treated daily

with water for 28 days (aCSF + H_2O), group two (*n* = 7) received an aCSF infusion and daily treatment with glyceryl triacetate for 28 days (aCSF + GTA), group three (*n* = 8) received a LPS infusion and daily treatment with water for 28 days (LPS + H_2O), and group four (*n* = 5) received a LPS infusion and daily treatment with glyceryl triacetate for 28 days (LPS + GTA). The rats used for IL-1β analysis were divided into three different treatment groups: group one (n = 6) received an aCSF infusion (aCSF), group two (n = 12) received a LPS infusion (LPS), and group three (n = 6) received a LPS infusion and daily treatment with glyceryl triacetate for 28 days (LPS + GTA). On the 28^{th} day of treatment, animals were anesthetized with isoflurane (Butler Animal Health Supply, Dublin, OH) in an induction chamber for 1 min, and then euthanized by decapitation. Brains were immediately removed and flash frozen by immersing in liquid nitrogen. The post-mortem intervals for the brain did not exceed 1 min. All samples were stored at -80º C until used. Total brain homogenate was used for histone, HAT and HDAC isolation. Specific brain regions were not studied because the goal was to determine if acetate had any effect on histone acetylation, HAT and HDAC activity or expression.

Nuclei Isolation

Brain nuclei were isolated by density centrifugation as described (Kim & Shukla 2006). Frozen brain samples were weighed and then transferred to a 50 ml plastic centrifuge tube containing 10 ml of ice cold homogenization buffer (50mM Tris-HCl, pH 6.95 containing 25mM KCl, and 10mM $MgCl_2$ 0.25M sucrose, 1mM sodium orthovanadate, 5mM sodium fluoride, 1mM phenylmethylsulfonyl fluoride (PMSF),

and a protease inhibitor cocktail). The homogenized samples were gravity filtered through 100 µM nylon mesh, then diluted with the addition of another 5 ml of homogenization buffer. The diluted homogenate was then centrifuged at 900 x g for 30 min at 4^{o} C. The pellet was re-suspended in homogenization buffer having a sucrose concentration of 0.8 M sucrose brain by mixing for 30 min at 4^{o} C. The nuclei were isolated by density centrifugation (100,000 x g for 1.5 hr at 4^{o} C) with the lower layer containing homogenization buffer with 1.2 M sucrose brain. Following centrifugation, the supernatant was discarded and the nuclear pellet was washed twice in a hypotonic wash solution (50 mM Tris-HCl, 1 mM KCl, 1.5 mM $MgCl_2$ 6-hydrate, pH 8.0) containing 1mM PMSF using slow intermittent mixing. Using additional samples, the pellets were washed with ammonium sulfate $NH_4(S0_4)_2$ solution (pH 5.5) instead of hypotonic wash and the supernatant was used to compare the yield of HDAC activity as described in Results section #2. The samples were then centrifuged again at 1,000 x g for 20 min at 4^{o} C, the pellet was collected and the supernatant was kept for enzymatic activity and Western blot analysis while the pellets were used to isolate histones as described below.

Acid Extraction of Histones

An acid histone extraction was used to isolate nuclear histones (Shechter *et al.* 2007). The nuclear pellets were re-suspended in 2.0 ml of 0.4 N H_2SO_4 and then incubated with shaking at 4^{o} C overnight. The samples were then centrifuged at 16,000 x g for 10 min at 4^{o} C. The supernatant was transferred to a second test tube and the solution was brought up to 33% trichloroacetic acid (TCA) with the addition of 1.0 ml

100% TCA solution. The samples were incubated at 4^{o} C for 1 hr then centrifuged at 21,000 x g for 5 min at 4^{o} C. The pellets containing the histones were washed with 0.5 ml acetone then allowed to dry at room temperature. The pellets were re-suspended in 2.0 ml of ice cold TKM buffer containing 1 mM PMSF then re-suspended by sonication and mixing. The solution containing the isolated histones was centrifuged again at 12,000 x g for 5 min at 4^{o} C and the supernatant was stored at -80^{o} C. Protein was measured using the Bradford method with bovine serum albumin as standard (Bradford 1976).

Cell Cultures

Primary microglia were derived from C57BL/6 mouse brains as described previously (Dhawan *et al*. 2012). Briefly, cortices were removed and trypsinized. The trypsin was inactivated in microglial growth media (DMEM/F-12 with L-glutamine [Invitrogen]) containing 10% heat-inactivated fetal bovine serum, 5% heat-inactivated horse serum, and antibiotics, penicillin, streptomycin, and neomycin (Gibco, Invitrogen, Carlsbad, CA). The tissue was triturated and plated into tissue culture flasks. After 24 hours all media and cellular debris was replaced with fresh media. After 7 more days, half of the media was replaced and cells were maintained as a mixed glia culture until day 14. At 14 days *in vitro*, microglia were shaken from the mixed glial culture at 200 rpm for 45 minutes and collected for use. The BV2 microglia were obtained from Dr. Colin K. Combs (Grand Forks, ND) and maintained until used as described previously (Rojanathammanee et al. 2011). Cells were plated in 6 well-dishes and allowed to replicate till 90% confluence, (1.1×10^{6} cells/dish). The purity of

the astrocyte cell cultures was found to be 91 + 3% as determined by immunostaining using anti-GFAP antibody (1:1000). Prior to stimulating the cells (3 hr), the media was changed to serum-free media. Plates were divided into 4 different groups; a group treated with 12 mM NaCl as a control group, another group treated with 12 mM sodium acetate, a third group treated with both 6.25 ng/ml LPS and 12 mM NaCl, and a fourth group treated with both 6.25 ng/ml LPS and 12 mM sodium acetate (n = 6 per group for BV-2 cells and primary astrocytes, and n = 5 per group for primary microglia). The concentration of acetate used in this study is based on studies to determine the maximal amount of acetate that did not lead to significant cell death over a 24 hr exposure period, compared to cells grown in serum-fee media. After a single oral gavage of glyceryl triacetate (5.8 g/kg), brain acetate levels rise to 8 µM/g tissue at 1 hr, and then decline to 6 and 2 µM/g tissue at 2 and 4 hr, respectively (Mathew et al. 2005). However, the metabolically active molecule in this process is not acetate, but rather acetyl-CoA which reaches a maximum of 5.7 µg/g brain at 30 min and remains constant out to 4 hr *in vivo* (Reisenauer et al. 2011). The cellular concentration of acetyl-CoA is controlled metabolically by acetyl-CoA synthetases 1 and 2, and not by cellular levels of free acetate (Fujino et al. 2001, Ariyannur et al. 2010). Therefore, our rationale for using the highest tolerable acetate concentration was not to mimic maximal tissue concentrations of acetate but rather to maximize, over a 4 hr-period, cellular levels of acetyl-CoA in an effort to identify metabolic and the inflammatory pathways that are modulated downstream of the formation of acetyl-CoA. For dose-response studies, plates were divided in 6 different groups treated with LPS in the

following concentrations: 25, 12.5, 6.25, 3.125, 1.56, or 0 ng/ml (n = 3). After 4 hr, the media was collected and stored at -20° C, and the cells were lysed in either TRIzol® reagent for qrt-PCR analysis or ice cold RIPA lysis buffer (150 mM sodium chloride, Triton X-100, 0.5% sodium deoxycholate, 0.1% sodium dodecyl sulphate, 50 mM Tris, pH 8.0) for Western blot analysis and stored at -80° C until used.

Western Blot Analysis

Equal amounts of protein were prepared by boiling samples in loading buffer composed of 95% Laemmli sample buffer and 5% 2-mercaptoethanol (Sigma, St. Louis, MO). The separation of proteins was performed using a 10-20% Tris-HCl gel with an electrophoresis separation of 100 volts for 2 hr. The electrophoretic transfer of proteins onto a 0.45 μm nitrocellulose membrane was performed at 100 volts for 90 min in ice. Primary antibodies were prepared at the following concentrations in 20 mM Tris buffer, pH 7.4 containing 150 mM NaCl and 0.05 % Tween 20 (TTBS) containing 5 % non-fat dried milk. The antibody concentration used were total histone H4 (1:1000), acetylated histone H4K5 (1:800), acetylated histone H4K8 (1:2000), acetylated histone H4K12 (1:800), acetylated histone H4K16 (1:1000), total histone H3 (1:500), acetylated histone H3K9 (1:1000), acetylated histone H3K14 (1:1000), HDAC 1, 2, 3, 4, 5 and 7 (1:1000), acetyl-CoA synthetase (1:500), IL-1β, IL-6, TNF-α, TGF-β1, IL-4, IL-10, total p38, phosphorylated p38, total JNK, phosphorylated JNK, total ERK1/2, phosphorylated ERK1/2, all NF-κB antibodies (1:1000), phosphorylated $cPLA_2$ (1:250), total $cPLA_2$ (1:500), $sPLA_2$ IIA (1:500), PLCβ1 (1:250), PLCγ1 (1:350), PLCδ1 (1:350), Cox-1 (1:1000) and Cox- 2 (1:1000), and α-tubulin (1:3000).

All primary antibodies were incubated with the nitrocellulose membranes overnight at 4^{o} C. The blots were incubated with the appropriate secondary antibody conjugated with a horse radish peroxidase at a dilution of 1:3000 in TTBS. The blots probed with α-tubulin antibody were conjugated with a horse radish peroxidase-linked goat anti-mouse IgM secondary antibody at a dilution of 1:4000 in TTBS. Protein bands were visualized with a SuperSignal® West Pico or Femto Chemiluminescent Substrate (Pierce, Rockford, IL) using a UVP Bioimaging System (Upland, CA). Image capturing and analysis was performed with LabWorks™ imaging software (version 4.5, Upland, CA). Western blot data of acetylated histones is expressed as of the ratio of the optical density of acetylated histone residues to the optical density of total histone. Phosphorylated MAPK p38, JNK, ERK1/2, and phosphorylated $cPLA_2$ are normalized to total MAPK p38, JNK, ERK1/2, and $cPLA_2$, respectively. Western blot data of all other proteins is expressed as the ratio of the optical density of the respective protein to the optical density of the loading control α-tubulin.

HDAC and HAT Enzyme Activity Assays

HDAC activity was measured using the colorimetric HDAC activity assay kit (Millipore, Billerica, MA) according to the manufacturer's instructions. The colorimetric HDAC assay measures the total HDAC activity in a two-step procedure performed in a 96-well plate. In the first step, samples are incubated with the HDAC assay substrate, allowing deacetylation of the substrate. Next, the addition of an "Activator Solution" releases p-nitroanilide from the deacetylated substrate or standard which is monitored by spectrophotometric analysis. Nuclear extracts were added to the

assay buffer with HDAC substrate and mixed thoroughly. The samples were then incubated at 37° C for 75 min. At 75 min, an aliquot of the activator solution was added to each well, then following a 15 min room temperature incubation, the absorbance was measured at 405 nm. Nuclear extract provided by the manufacturers was used as a positive control and water was used as a negative control. The HAT activity was measured using the colorimetric HAT activity assay kit (Abcam, Cambridge, MA) according to the manufacturer's instructions. The colorimetric HAT activity assay depends on the acetylation of a peptide substrate by the active HAT; a process associated with the release of the free form of co-enzyme A. Co-enzyme A serves as an essential co-enzyme for the production of NADH which is measured using spectrophotometric analysis upon its reaction with a soluble tetrazolium dye. Briefly, 40 µl of nuclear extract was incubated with HAT substrate I and II and NADH generating enzyme in 2 x HAT assay buffer for 4 hr at 37° C and absorbance was measured at 450 nm using a Labsystems Multiskan plate reader (Helsinki, Finland). Nuclear extracts provided by the manufacturer were used as positive control and water was used as negative control. HAT activity is expressed as the ratio of the absorbance at 450 nm to the amount of nuclear extract as outlined by the manufacturer.

Quantitative Real-time Polymerase Chain Reaction (qrt-PCR)

Brain cortex samples (50-100 mg each) were homogenized in 1 ml TRIzol® reagent, using a Polytron homogenizer. Homogenized samples were incubated at room temperature for 5 min to permit dissociation of nucleoprotein complexes before adding 0.2 ml of chloroform, shaking the tubes vigorously by hand, and incubating again at

room temperature for 3 min. The samples were then centrifuged at 12,000 x g for 10 min at 4° C. Following centrifugation, the upper clear aqueous phase containing RNA was transferred to fresh tubes where RNA was precipitated from the aqueous phase by mixing with 0.5 ml of isopropyl alcohol. The mix was incubated at room temperature for 10 min then centrifuged at 12,000 x g for 10 min at 4° C. The RNA pellet was washed once with 1 ml of 75 % ethanol and centrifuged at 7,500 x g for 5 min at 4° C. At the end of the RNA extraction, ethanol was decanted and the RNA pellet was allowed to air-dry at room temperature for 5 min before re-dissolving in 200 µl of nuclease-free water. One µg of RNA per sample was used for cDNA synthesis using iScript cDNA synthesis kit (Bio-Rad, Hercules, CA) according to the manufacturer's instructions. Amplification was performed using 500 ng cDNA, 500 nM of each of the reverse and forward primers, and FastStart Universal SYBR Green Master (Roche Applied Science, Indianapolis, IN) in a final reaction volume of 50 µl, using a two-step cycling program of 1 cycle of 95° C for 10 min followed by 40 repeats of 95° C for 15 sec and 60° C for 60 sec in iCycler iQ Multicolor Real-Time PCR Detection System (Bio-Rad, Hercules, CA). The expression of all transcripts amplified was normalized to the expression of β-actin. PCR quantification was performed using the Livak formula $2^{-\Delta\Delta Ct}$ (Livak & Schmittgen 2001). The amplicon was mixed with DNA gel loading buffer 10 x (5 Prime, Gaithersburg, MD), and run on 1 % agarose gel at 100 volts for 1 hr. TrackIt™ DNA ladder (Invitrogen, Grand Island, NY) was used.

Quantitative Real-time Polymerase Chain Reaction (qrt-PCR) Array

Brain cortex samples (50-100 mg each) were used for mRNA extraction, cDNA synthesis and amplification as described in detail in the previous section. The RT² Profiler™ PCR Array PARN 052 (SABiosceinces) has built-in primers in the 96-well plate, and was used according to the manufacturer's instructions. Data analysis was performed using the SABiosceinces website data analysis tool.

Lactate Dehydrogenase Assay

Cellular release of lactate dehydrogenase (LDH) used to measure cell viability was measured using a commercial nonradioactive assay kit (Clontech Inc.), according to the manufacturer's guidelines. Absorbance measurements were taken at 490 nm.

Chromatin Immunoprecipitation

After treating the BV-2 cells for 4 hr, cross linking was done using 1% paraformaldehyde at room temperature for 10 min, then stopped by 0.125 M glycine at room temperature for 5 min. The cells were then washed once with phosphate-buffered saline ((PBS) 137 mM NaCl, 2.7 mM KCl, 10 mM Na_2HPO_4, 2 mM KH_2PO_4, and pH 7.4) before adding 0.2% trypsin and incubating at 37° C for 5 min in 5% carbon dioxide. Trypsin was neutralized by twice the volume of fetal bovine serum. One million cells per chromatin immunoprecipitation per antibody were suspended in SDS lysis buffer (1% SDS, 10 mM EDTA, 50 mM Tris, pH 8.1) containing protease inhibitor cocktail and sonicated for 7 cycles of 12 pulses with 3-sec intervals on ice between cycles. The sonicated cells were centrifuged at 15000 g to remove the debris out of the lysates. Seven µg of acetylated H3K9 antibody and normal rabbit IgG,

protein A and protein G magnetic beads were used for immunoprecipitation for 3 hr at 4° C. The magnetic beads were washed 4 times with low-salt wash buffer (0.1% SDS, 1% Triton X-100, 2 mM EDTA, 20 mM Tris-HCl, pH 8.1, 150 mM NaCl), once with high-salt wash buffer (0.1% SDS, 1% Triton X-100, 2 mM EDTA, 20 mM Tris-HCl, pH 8.1, 500 mM NaCl), and once with TE buffer (10 mM Tris-HCl, 1 mM EDTA, pH 8.0). The samples were then eluted at 65° C for 15 min using elution buffer (50 mM Tris-HCl, 10 mM EDTA, 1% SDS, pH 8.0). Samples were incubated at 65° C overnight to reverse the crosslinks, then incubated with RNAse A (0.2 µg/ml) for 2 hr at 37° C, and with proteinase K (0.2 µg/ml) for 2 hr at 55° C. One µg of the Chromatin immunoprecipitation end product, with 1 µg of forward and reverse primers, 10 µl SYBR green, and 8 µl of nuclease-free water were used for quantitative real-time polymerase chain reaction (qrt-PCR).

Prostaglandin E_2 Quantification using Enzyme Immunoassay

PGE_2 release was measured in the media of BV-2 microglia and primary astrocyte cell cultures using prostaglandin screening enzyme immunoassay (EIA) kit according the manufacturer's instructions. The test depends on the competition between PGs and PG-acetyl choline esterase conjugate for a limited amount on PG antiserum. Absorbance was read at 405 nm.

Statistical Analysis

To compare between more than two groups, parametric or nonparametric One Way Analysis of Variance (ANOVA) was used when appropriate, followed by Tukey's or Dunn's post-hoc test, respectively. When comparison was made between only two

groups, two-tailed unpaired t-test was used to calculate statistical differences using GraphPad InStat statistical software (Version 3.10, San Diego, CA). All results are expressed as means ± SD and significance was set at $p \leq 0.05$. Figures were prepared using SigmaPlot for Windows, version 10.0, Build 10.0.1.25.

CHAPTER III

RESULTS

Method Optimization for Western Blot Analysis

Saturation of the Western blot image occurs when too much protein is loaded or as a result of increasing the exposure time of the Western blot during chemiluminescence detection using the imaging system. To demonstrate that, the same Western blot was probed for the loading control histone H4 (primary antibody concentration 1:1000) and exposed during chemiluminescence detection for 5 min (Figure 1A) and 30 sec (Figure 1B). The analysis of the blot in Figure 1A using Visionwoks® software demonstrated a flat-topped peak with maximum intensity of around 3000 (Figure 1C). The analysis of the blot in Figure 1B using Visionwoks® software demonstrated a pointed peak with maximum intensity of around 2500 (Figure 1D). That is, the intensity of the peak in Figure 1C was 1.2 times greater than that of Figure 1D even though the exposure time of the blot in figure 1A was 10 times that of the blot in figure 1B. Therefore, the increase in exposure time during chemiluminescence detection was not matched by an equal increase in the intensity of the optical density indicating saturation which prevents accurate quantification of protein based on the optical density. In the light of that, before embarking on Western blot analysis for the histone acetylation studies, we performed experiments to optimize

the protein amount and exposure duration during chemiluminescent detection to avoid saturation with Western blot analysis.

Optimizing the amount of protein for Western blot analysis.

In order to determine the optimal amount of protein to use for Western blot analysis, we loaded a serial dilution of histone extract (41-0.08 µg/lane), probed for the loading control histone H4 (1:1000), and exposed the blot for 2 min (Figure 2A). We found that optical density leveled off with protein amounts greater than 3 µg/lane (Figure 2B). These data demonstrate that the linear range of protein amount under (A)
these experimental conditions is 1-3 µg (Figure 3C). The correlation coefficient is close to 1 ($r^2 = 0.993$), which means that the amount of protein can be quantified based on the optical density without saturation because increasing the protein load within this range is matched by proportionate increases in intensity of optical density.

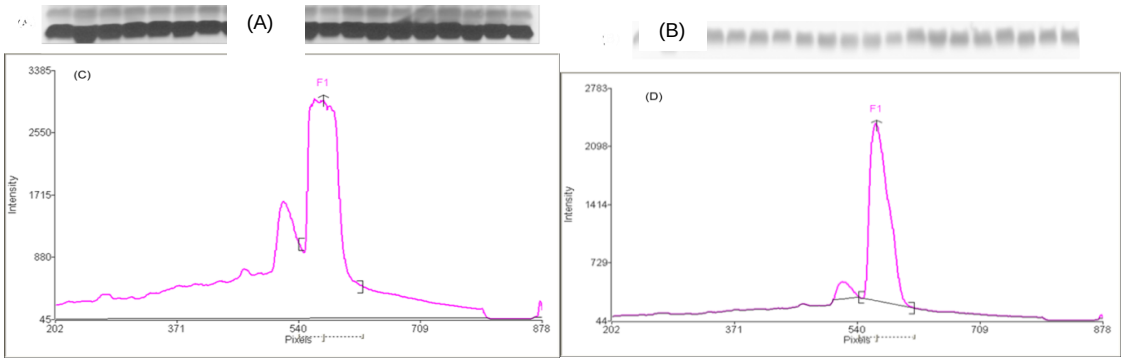

Figure 1. Demonstration of saturation in Western blot analysis.

Images obtained by Visionworks® software of the loading control histone H4 (primary antibody concentration 1:1000) representing the intensity of the optical density on the y-axis. Panel (A) demonstrates a saturated Western blot image exposed during chemiluminescence detection for 5 min. Panel (B) demonstrates the same

Western blot image after 30 sec of exposure. Panel (C) shows the optical density analysis of the image in panel (A) using Visionworks® software and demonstrates saturation. Panel (D) demonstrates the optical density analysis of image in panel (B) and represents a quantifiable image with no saturation.

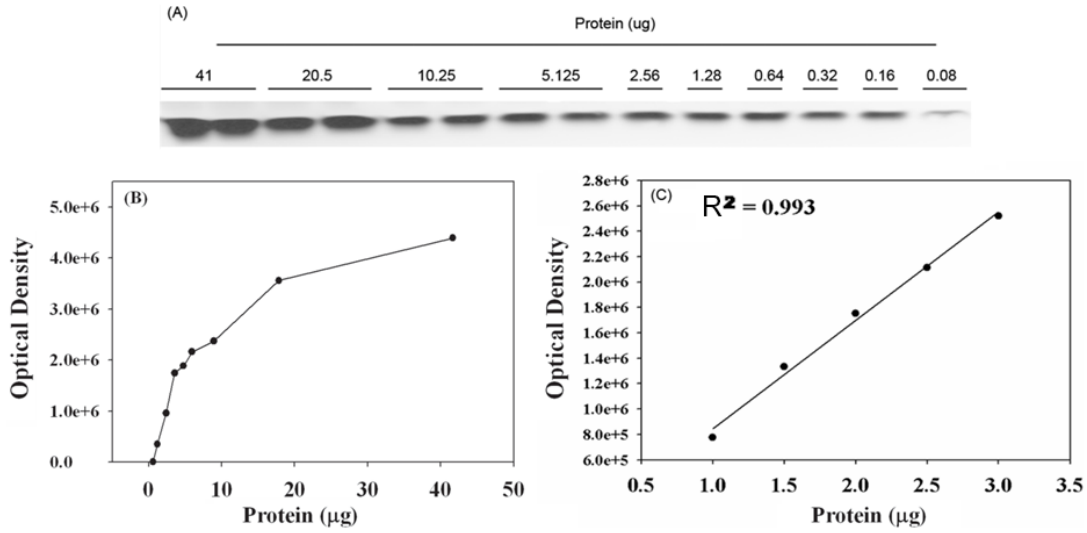

Figure 2. Demonstration of the quantifiable range of protein content for Western blot analysis.

Optical density was plotted on the y-axis versus protein (µg) on the x-axis. Panel (A) shows the Western blot image of the serial dilution of histone extract (41-0.08 µg/lane), probed for with anti-histone H4 (1:1000), and exposed during chemiluminescence detection for 2 min. Panel (B) represents the quantification of the optical density of the protein concentrations (41-0.08 µg/lane) and demonstrates leveling off of the optical dentistry with protein amounts greater than 3 µg/lane. Panel (C) demonstrates the linear range of protein (1-3 µg/lane) prepared to represent a quantifiable range of protein. Blotting histone in this range allows the quantification of histone acetylation state based on the optical density without saturation.

Optimizing the duration of exposure during chemiluminescene detection for Western blot analysis.

Because saturation develops with increasing the exposure time during the chemiluminescence detection, we proceeded to determine the optimal duration for Western blot exposure. A Western blot analysis was performed with loading histone extract (3 µg), probing for the loading control histone H4 (1:1000), and the blot was exposed for a range of durations between 15 sec and 30 min (Figure 3A). The optical density increased with increasing the exposure time from 15 sec to 4 min before leveling off (Figure 3A and B). These data demonstrate that the linear range for Western blot exposure under these experimental conditions is between 15 sec and 4 min. The correlation coefficient is close to 1 ($r^2 = 0.998$), which means that increasing the Western blot exposure within this range is matched by proportionate increases in optical density without saturation.

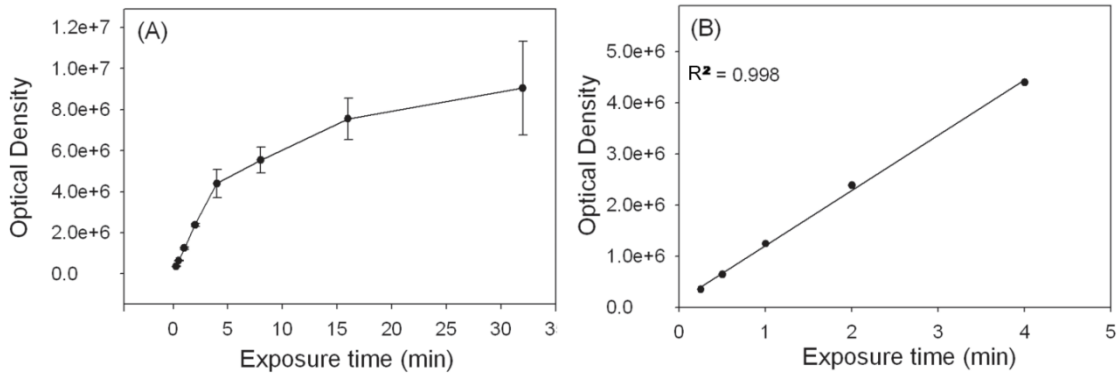

Figure 3. Demonstration of the optimal exposure duration for Western blot during the chemiluminescence detection.

The optical density is plotted on the y-axis verses the exposure time (min) on the x-axis. Panel (A) shows leveling off of the optical density with exposure for more than 4 min. Panel (B) shows the linear part of the curve from 30 sec to 4 min.

The rationale for using histone extract for these optimization studies is that it is purer and more concentrated than whole cell lysates and brain homogenates. Therefore, saturating amounts of protein in histone extract are unlikely to be saturating when used to probe for less concentrated targets; for example, MAPK p38 or $cPLA_2$ in using whole cell lysates or brain homogenate. Likewise, the antibody against total histone H4 detects all acetylated and non-acetylated histones H4, and therefore saturating protein amounts detected by total histone H4 antibody are unlikely to be saturating when probing for the acetylated histones. For Western blot analyses other than histone acetylation studies, we avoided saturation by capturing the images of each blot at several exposure times and depended on the shape of the peak on the image generated by Visionworks® software to exclude saturation.

Determining the Distribution of HDAC Activity in Different Cellular Fractions

We measured the levels of HDAC activity in the different cellular fractions obtained during the procedures of nuclei isolations. In addition to washing the nuclear pellet with hypotonic wash, we used additional samples to wash the nuclear pellet with $NH_4(S0_4)_2$ solution to compare the HDAC activity yielded by the two methods (Method section under "nuclei isolation"). We found that each of the hypotonic wash 1 and 2 had 2-3 times more HDAC activity than any of the other

fractions including the cytosol (Figure 4). Therefore, hypotonic wash 1 and 2 were combined and used for measuring the enzymatic activities of HAT and HDAC.

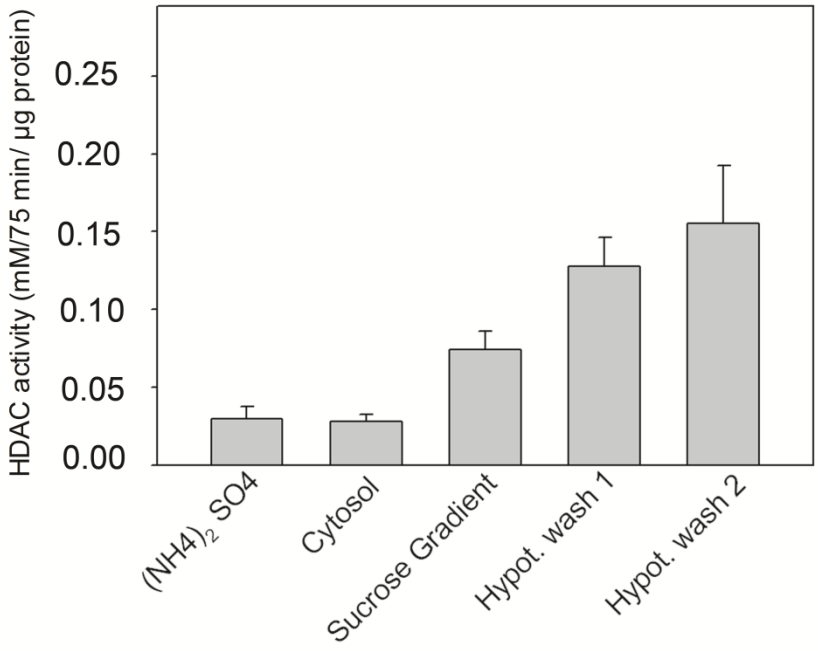

Figure 4. Comparison between the levels of HDAC activity in the cellular fractions obtained during the procedure of isolation of nuclei and with $NH_4(S0_4)_2$ wash.

Hypotonic wash 1 and 2 had considerably higher HDAC activity than the other fractions and the $NH_4(S0_4)_2$ wash, so they were used for the measurement of HAT and HDAC enzymatic activities. The composition of the hypotonic washes, sucrose gradient and $NH_4(S0_4)_2$ are described in the Method section under "Nuclei isolation".

A Single Oral Dose of Acetate Supplementation and Brain Histone Acetylation in Normal Rats

The proportion of acetylated H3 and H4 to total histone was measured at differing time points following a single oral gavage with glyceryl triacetate (6 g/kg) using Western blot analysis. Specific antibodies against acetylated histones H4K5, H4K8, H4K12, H4K16, H3K9, and H3K14 as well as specific antibodies towards total

histone H3 and total histone H4 were used to measure brain histone acetylation state. Total histone H3, H3K9, and H3K14 were detected as protein bands at 17 kDa which correspond to the molecular weight of these types of histones (Figure 5A). Similarly, H4K5, H4K8, H4K12, H4K16 and total histone H4 were detected as protein bands at 10 kDa which correspond to the molecular weight of these types of histones. Optical density analysis of the Western blots showed that acetate supplementation significantly increased the acetylation state of brain histone H3K9 by 1.5-fold at 4 hr following treatment compared to controls (Figure 5B). No changes in the acetylation of brain histone H3K14 were detected at any of the time points examined (Figure 5C). Optical density analysis of acetylated histone H4 showed that the acetylation state of brain histone H4K8 was increased 1.7-fold at 2 and 4 hr and brain histone H4K16 was increased 1.7- and 1.8-fold at 4 and 24 hr following treatment (Figure 5E and G). Acetate supplementation did not change the acetylation state of brain histone H4K5 and H4K12 at any of the time points examined (Figure 5D and F). These data suggest that a single oral dose of acetate treatment can induce site- and time-specific histone acetylation changes.

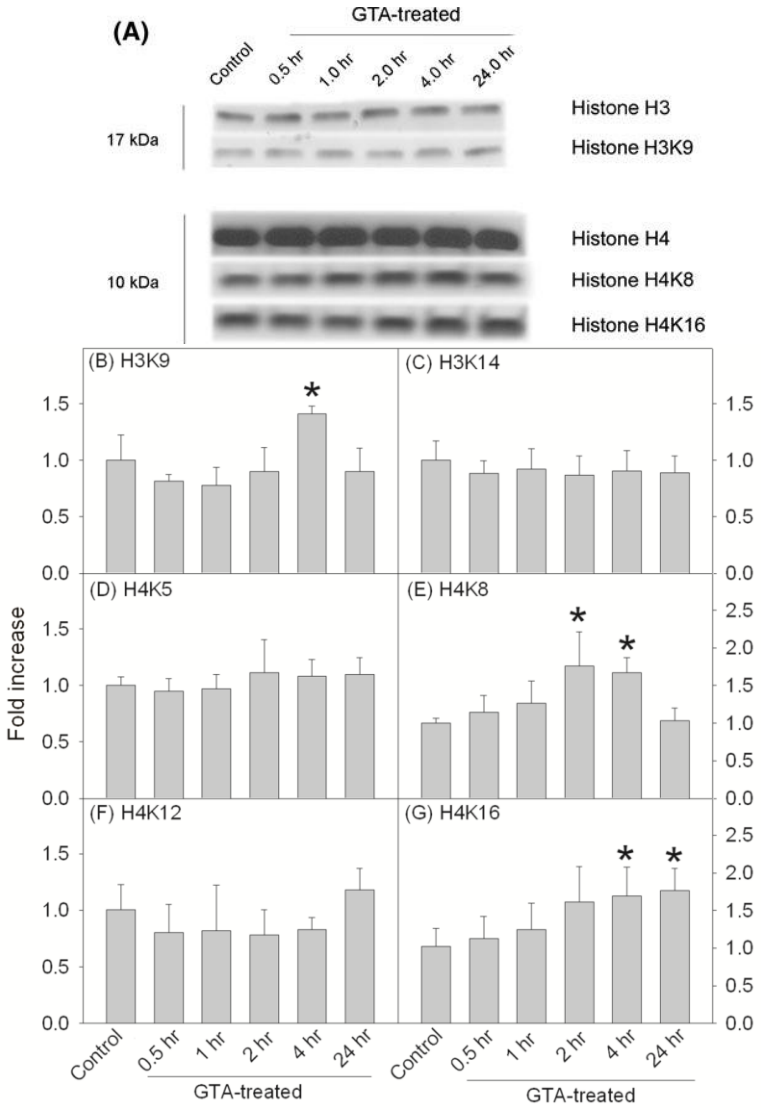

Figure 5. A single oral dose of acetate supplementation and brain histone acetylation in normal rats.

The effect of a single oral dose of acetate supplementation on the histone acetylation state of brain histones H3K9, H4K8, and H4K16 at 0.5, 1, 2, 4 and 24 h following treatment with 6 g/kg glyceryl triacetate (GTA). Panel A shows representative images of the Western blots while panels B-G show the quantification of the optical densities of acetylated histone. The different panels represent the

acetylation ratio of H3K9, H3K14, H4K5, H4K8, H4K12 and H4K16 normalized to total H3 or total H4, respectively. Bars represent the means ± SD of optical density analysis where statistical significance (*) was set at $p \leq 0.05$ as determined by One Way ANOVA followed by Tukey's post-hoc test (n = 6 animals per group).

A Single Oral Dose of Acetate Supplementation and Brain HDAC and HAT Activity

Having observed an increase in brain histone H3 and H4 acetylation state following acetate supplementation, we proceeded to determine the effect that a single oral dose of glyceryl triacetate has on the temporal activity of brain HDAC and HAT. Using commercially available HDAC and HAT assay kits, we observed a significant 2.3- and 2.8-fold decrease in the brain HDAC activity at 2 and 4 hr following treatment, respectively (Figure 6A). The HDAC activity in the control sample was 0.198 ± 0.06 mM/75 min/μg protein while the HDAC activities at 2 and 4 hr were 0.085 ± 0.03 and 0.07 ± 0.02 mM/75 min/μg protein, respectively. In parallel experiments, we did not observe significant changes in brain HAT activity at any of the time points examined when compared to controls (Figure 6B).

A Single Oral Dose of Acetate Supplementation and Brain HDAC Expression

HDAC enzymes are classified into three different classes (de Ruijter et al. 2003). Class I (1, 2, 3, and 8) and class II (4, 5, 6, 7, and 9) are localized in the nucleus or shuttle between the cytoplasm and the nucleus following stimulation, respectively. Class III, the sirtuins, found primarily in the cytoplasm and mitochondria are inhibited by nicotinamide unlike conventional HDAC inhibitors (Avalos et al. 2005, Sanders *et al.* 2007). Therefore, based on the nuclear localization and to explain the decrease in

nuclear HDAC activity, we measured the expression of class I and II HDAC using Western blot analysis. Specific antibodies against HDAC1, 2, 3, 4, 5 and 7 were used to measure brain HDAC expression levels as compared to control animals. The proportion of HDAC to α-tubulin was calculated at 4 hr following a single oral gavage with glyceryl triacetate (6 g/kg) (Figure 7A).

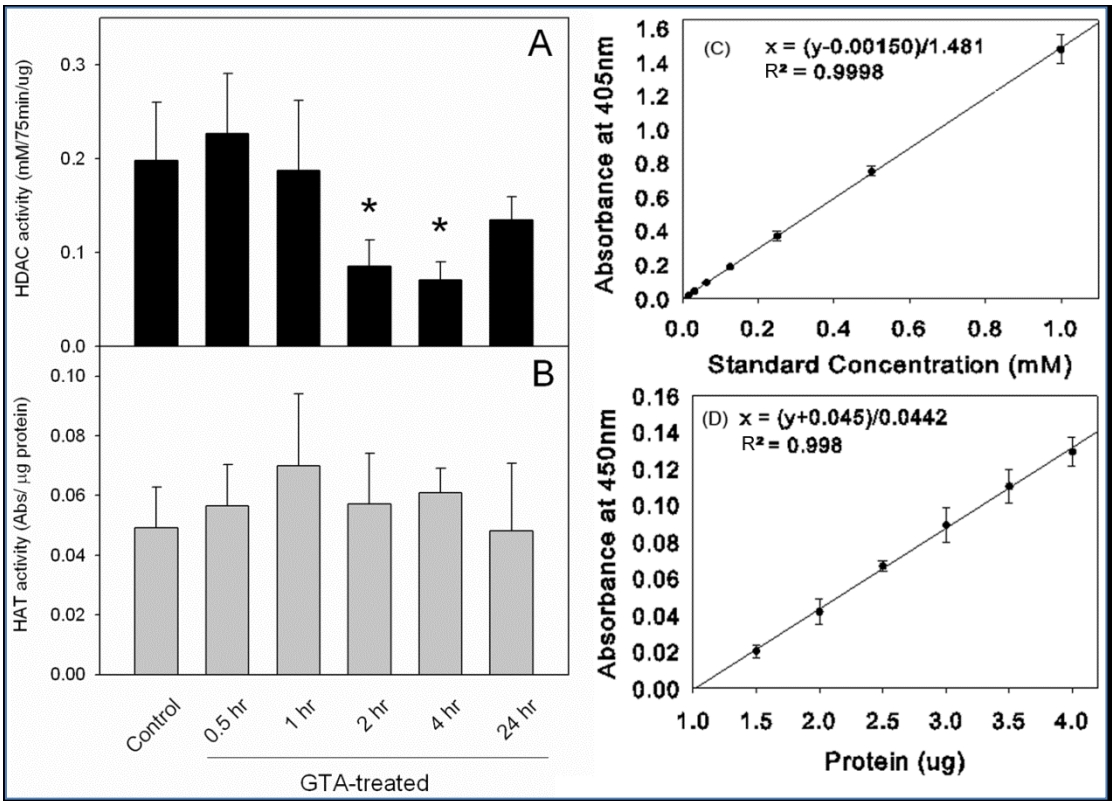

Figure 6. A single oral dose of acetate supplementation and brain HDAC and HAT activity.

The effect of a single oral dose of acetate supplementation on histone deacetylases (HDAC, panel A) and histone acyltransferases (HAT, panel B) activity in different rat groups euthanized at 0.5, 1, 2, 4, and 24 h following treatment with 6 g/kg

glyceryl triacetate (GTA). Panel C shows the standard curve for colorimetric HDAC assay. The linear part of the curve lies between standard concentrations 1 mM and 0.016 mM and the absorbance value is read at 405 nm. Panel D shows the standard curve for colorimetric HAT assay set up using different dilutions of the sample with the highest protein concentration. The graph shows steady increase in the absorbance at 450 nm with increasing the protein content from 1.5 to 4 μg. All our samples fell within this range. Bars represent the means ± SD of absorbance reading at 405 nm after 75 min of incubation at 37° C normalized to the protein assayed (μg). Statistical significance (*) was set at $p \leq 0.05$ as determined by One Way ANOVA followed by Tukey's post-hoc test (n = 6 animals per group).

The analysis detected protein bands at 62, 60, 49, 140, 124, 105 and 50 kDa corresponding to the molecular weights of HDAC1, 2, 3, 4, 5, 7 and α-tubulin, respectively (Figure 7A). Optical density analysis of these Western blots showed that acetate significantly decreased brain HDAC2 levels by 50% below control values at 4 hr following treatment (Figure 7B). Acetate supplementation did not decrease the expression of the other brain HDAC measured. These results suggest that the increase in histone acetylation following acetate supplementation may be due to a decrease in the protein levels of HDAC2.

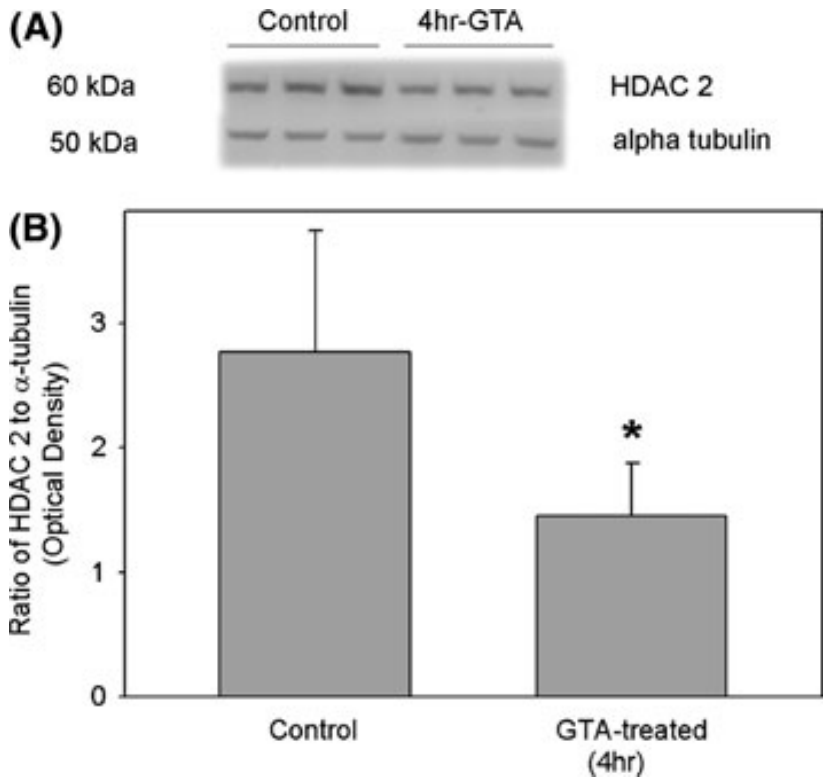

Figure 7. A single oral dose of acetate supplementation and brain HDAC expression.

The effect of a single oral dose of acetate supplementation on the brain HDAC2 levels at 4hr, in control and glyceryl triacetate (GTA)-treated rats. Figure 7A shows representative images of Western blots of HDAC2 and α-tubulin. Figure 7B shows the ratio of brain HDAC2 normalized to α-tubulin. Bars represent the means $\pm$ SD of optical density analysis where statistical significance (*) was set at $p \leq 0.05$ as determined using a two-tailed unpaired t-test (n = 6 animals per group).

Long-term Acetate Supplementation and Brain Histone H3 and Histone H4 Acetylation in a Rat Model of Neuroinflammation

The proportions of acetylated histone H3 and H4 were measured using Western blot analysis. Total H3, acetylated H3K9, and acetylated H3K14 were detected as

protein bands corresponding to a molecular weight of 17 kDa (Figure 8A). Optical density analysis of acetylated H3 showed a 1.6-fold increase in the proportion of H3K9 in the two groups of rats subjected to acetate supplementation (aCSF + GTA) and (LPS + GTA), compared to controls (aCSF + H_2O) (Figure 8B). Interestingly, the proportion of acetylated H3K9 was decreased by 2-fold in rats subjected to neuroinflammation and treated with water (LPS + H_2O) and 3-fold when compared to rats that received acetate (aCSF + GTA) and (LPS + GTA). Neither acetate supplementation nor neuroinflammation altered the acetylation state of brain H3K14.

Total H4 and acetylated H4K5, H4K8, H4K12, and H4K16 were detected as a protein bands at 10 kDa which correspond to the molecular weight of these histones (Figure 9A). Similar to the proportional increases in acetylated H3K9, the proportions of acetylated H4K8 and H4K16 were significantly increased by 2-fold in rats subjected to acetate supplementation (aCSF + GTA) and (LPS + GTA) (Figure 9B). However, unlike the proportion of acetylated H3K9, the proportion of acetylated H4K8 and H4K16 were not decreased in the rats subjected to neuroinflammation and treated with water (LPS + H_2O) when compared to controls (aCSF + H_2O). Neither acetate supplementation nor neuroinflammation altered the acetylation state of H4K5 or H4K12. These results suggest that acetate supplementation can selectively and positively regulate the acetylation of both histone H3 and H4 at specific acetylation sites. However, LPS-induced neuroinflammation only decreased the acetylation state of H3K9, which was effectively reversed with acetate supplementation.

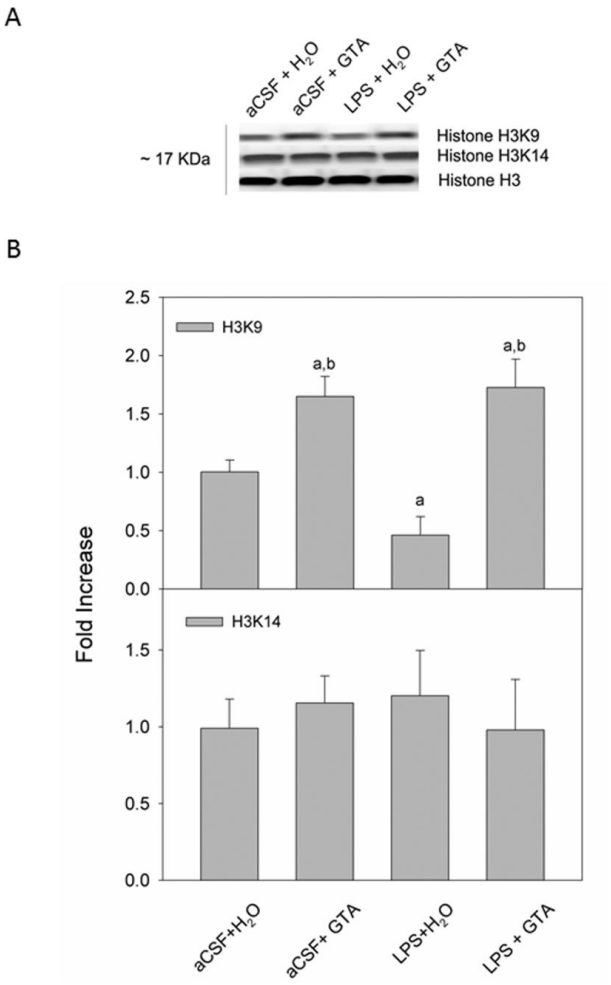

Figure 8. Long-term acetate supplementation and brain histone H3 acetylation in a rat model of neuroinflammation.

.

Changes in the acetylation state of brain H3K9, and H3K14 in control rats (aCSF), rats subjected to neuroinflammation (LPS), and rats treated with either water (H2O) or glyceryl triacetate (GTA). Panel A shows representative images of the Western blots, and panel B shows the averaged proportion of brain H3K9 and H3K14, normalized to total H3. The data represent the means ± SD where statistical significance (a = compared to aCSF + H2O, and b = compared to LPS + H2O) was set at $p \leq 0.05$, as determined by One Way ANOVA followed by Tukey's post-hoc test.

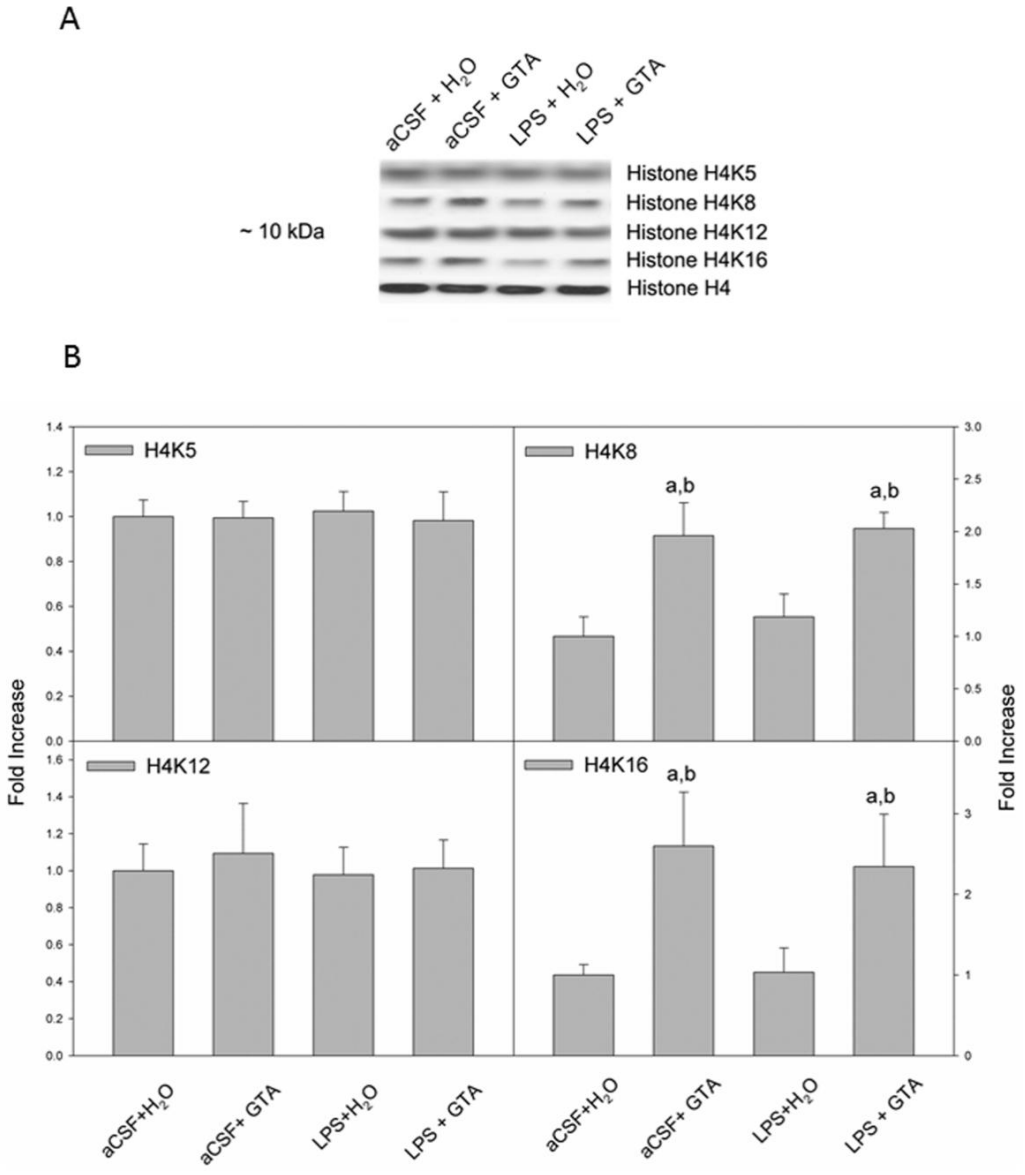

Figure 9. Long-term acetate supplementation and brain histone H4 acetylation in a rat model of neuroinflammation.

Changes in the acetylation state of brain H4K5, H4K8, H4K12, and H4K16 in control rats (aCSF) and rats subjected to neuroinflammation (LPS), and rats treated with either water (H2O) or glyceryl triacetate (GTA). Panel A shows representative

images of the Western blots, while panel B shows the averaged proportion of brain H4K5, H4K8, H4K12, andH4K16, normalized to total H4. The data represent the means ± SD where statistical significance (a = compared to aCSF + H2O, and b = compared to LPS + H2O) was set at $p \leq 0.05$, as determined by One Way ANOVA followed by Tukey's post-hoc test.

Long-term Acetate Supplementation and Brain HDAC and HAT Activities in a Rat Model of Neuroinflammation

Because the brain histone acetylation state is controlled by the activities of HAT and HDAC, we examined the effect that acetate supplementation had on brain HAT and HDAC activities in different test groups. Using commercially available HDAC and HAT assay kits, we found that acetate supplementation significantly increased by 1.8- and 1.6-fold the activity of brain HAT in (aCSF + GTA) and (LPS + GTA) groups, respectively, compared to controls (aCSF + H_2O) (Figure 10). No changes in HAT activity were observed in rats subjected to neuroinflammation and treated with water (LPS + H_2O). The HAT activity in the control sample was 35 ± 12 absorbance units at 450 nm/µg protein, while the HAT activities in the (aCSF + GTA) and the (LPS + GTA) groups were 62 ± 14 and 56 ± 10 absorbance units at 450 nm/µg protein, respectively. In parallel experiments, we did not find any changes in brain HDAC activity in any of the groups tested. These results suggest that long-term acetate supplementation, and not LPS-induced neuroinflammation, positively regulates brain HAT activity with no apparent effect on brain HDAC activity.

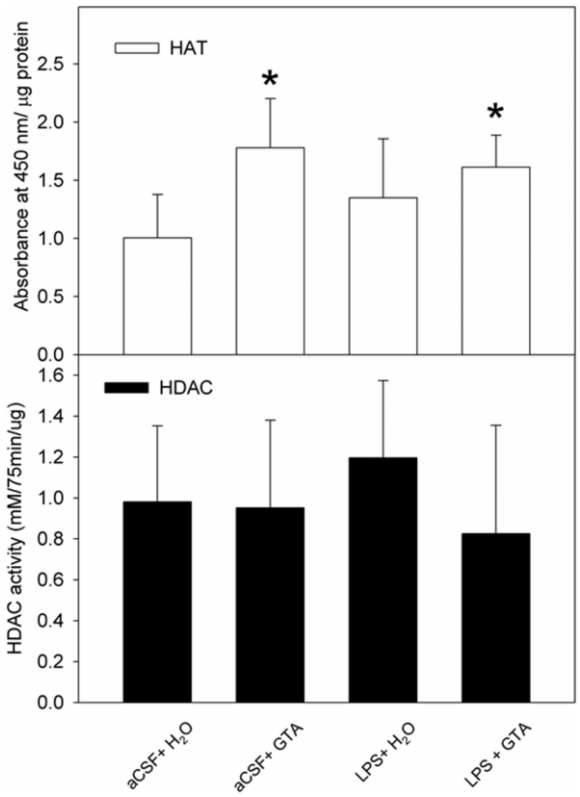

Figure 10. Long-term acetate supplementation and brain HDAC and HAT activities in a rat model of neuroinflammation.

The effect of long-term acetate supplementation on brain HAT and HDAC activities in control rats (aCSF) and rats subjected to neuroinflammation (LPS), and rats treated with either water (H_2O) or glyceryl triacetate (GTA). Panel (A) represents changes in brain histone acyltransferases (HAT), and panel (B) represents changes in histone deacetylases (HDAC) activities. HAT enzyme activity is expressed as the means ± SD of absorbance reading at 450 nm after 4 hr of incubation at 37° C, normalized to the protein assayed (µg). HDAC enzyme activity is expressed as the means ± SD of absorbance at 405 nm after 75 min of incubation at 37° C, normalized to the protein assayed (µg). Statistical significance (* = compared to aCSF + H_2O

controls) was set at $p \leq 0.05$, as determined by nonparametric One Way ANOVA followed by Dunn's post-hoc test.

Long-term Acetate Supplementation and Brain HDAC Expression in a Rat Model of Neuroinflammation

We found earlier that a single oral dose of glyceryl triacetate decreases HDAC activity and reduces the expression of HDAC2 (Soliman & Rosenberger 2011). We did not observe changes in HDAC activity suggesting that the effects of long-term treatment differ substantially from a single oral dose. In order to further understand the effect that long-term acetate supplementation has on HDAC expression, we measured changes in the individual HDAC levels using Western blot analysis. Optical density analysis showed that HDAC1 expression was significantly elevated by 2.4- and 1.7-fold in rats treated with glyceryl triacetate; (aCSF + GTA) and (LPS + GTA) (Figure 11B). A similar effect was found in HDAC2 expression where the level was significantly increased by 1.7-fold in rats treated with acetate (aCSF + GTA), but not in rats subjected to neuroinflammation (LPS + GTA). The expression levels of HDAC1 and HDAC2 were not altered by LPS-induced neuroinflammation treated with water (LPS + H_2O). On the contrary, the levels of HDAC3 were significantly decreased by 40% in rats treated with acetate; (aCSF + GTA) and (LPS + GTA) as compared to control rats (aCSF + H_2O). The HDAC3 expression level was not altered in rats subjected to neuroinflammation treated with water (LPS + H_2O) as compared to control rats (aCSF + H_2O). Most interestingly, the expression of HDAC7 was increased by 1.7-fold in rats subjected to neuroinflammation and treated with water (LPS + H_2O) which was effectively reversed with acetate supplementation (aCSF + GTA) and (LPS

+ GTA). No changes were found in the expression levels of HDAC4 and 5 in any of the groups tested. These results suggest the HDAC7 may play a positive role in the inflammatory process evoked by long-term LPS infusion that does respond to long-term acetate supplementation.

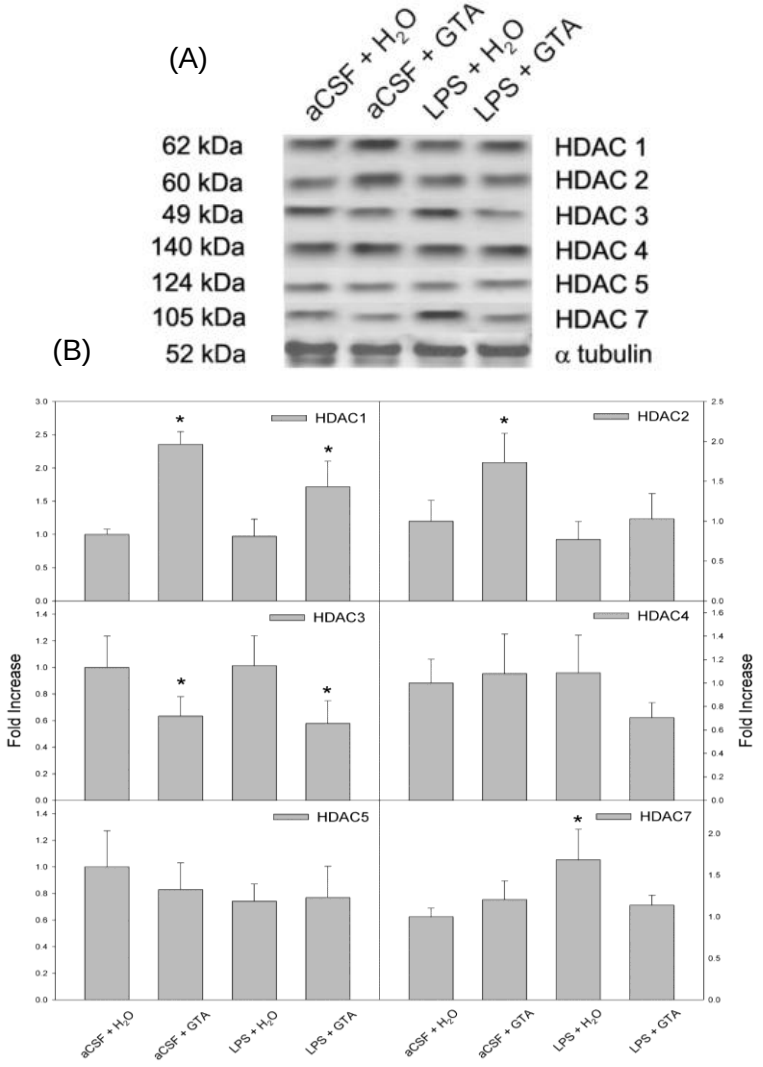

Figure 11. Long-term acetate supplementation and brain HDAC expression in a rat model of neuroinflammation.

The effect of long-term acetate supplementation on the expression of individual brain HDAC in control rats (aCSF) and rats subjected to neuroinflammation (LPS), and rats treated with either water (H_2O) or glyceryl triacetate (GTA). Panel A shows representative images of the Western blots, while panel B shows the quantifications of HDAC1, 2, 3, 4, 5 and 7. Data in panel B represent means ± SD of the optical densities of HDAC1, 2, 3, 4, 5 & 7, normalized to α-tubulin. Statistical significance (* = compared to aCSF + H_2O controls) was set at $p \leq 0.05$, as determined by One Way ANOVA followed by Tukey's post-hoc test for HDAC2, 3, 4 & 5, and nonparametric One Way ANOVA followed by Dunn's post-hoc test for HDAC1 & 7.

Long-term Acetate Supplementation and Brain IL-1β Expression in a Rat Model of Neuroinflammation

To test whether acetate supplementation can reduce the expression of pro-inflammatory cytokines *in vivo*, and to provide insight into the anti-inflammatory mechanism by which acetate supplementation is effective in this model of neuroinflammation, we measured the effect that acetate treatment has on the protein and mRNA levels of brain pro-inflammatory cytokine IL-1β. In these experiments, we found protein bands corresponding to a molecular weight of 17 kDa corresponding to IL-1β (Figure 12A), and cDNA bands corresponding to 209 and 131 base pairs which correspond to the expected base pair size of IL-1β and β-actin, respectively (Figure 12C). In rats subjected to neuroinflammation (LPS + H_2O), IL-1β protein and mRNA levels were significantly elevated by 1.3- and 10-fold, respectively, (Figure 12B and D). Further, the long-term acetate supplementation significantly reduced the expression

level of IL-1β below that found in rats subjected to neuroinflammation (LPS), and equal to the control levels (aCSF).

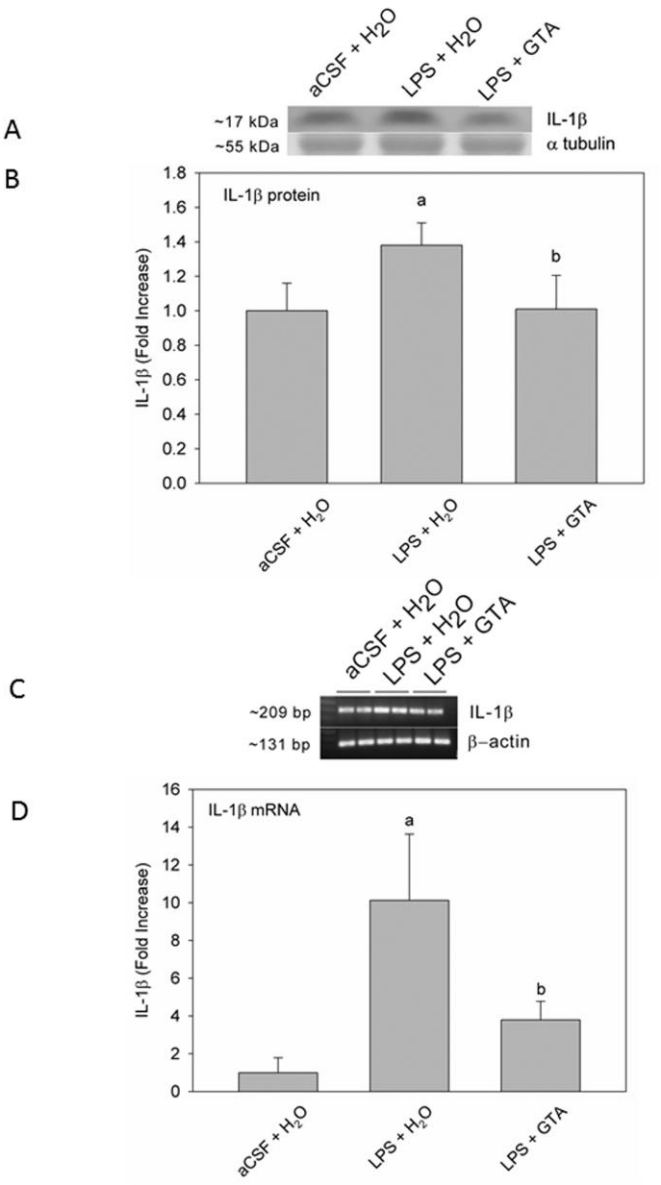

Figure 12. Long-term acetate supplementation and brain IL-1β expression in a rat model of neuroinflammation.

The effect of long-term acetate supplementation on the expression of brain IL-1β in control rats (aCSF) and rats subjected to neuroinflammation (LPS), and rats treated with either water (H_2O) or glyceryl triacetate (GTA) as determined by Western blot analysis and quantitative real-time PCR. Panel A shows Western blot representative images of bands for IL-1β and α-tubulin and panel B shows the means ± SD of the normalized optical density of IL-1β protein. Panel C shows representative images of the bands for IL-1β and β-actin cDNA and panel D shows the means ± SD of the normalized amplified IL-1β cDNA. Statistical significance (a = compared to aCSF + H_2O, and b = compared to LPS + H_2O) was set at $p \leq 0.05$ (n = 6, per group), as determined by One Way ANOVA followed by Tukey's post-hoc test.

Optimizing the Duration of Acetate Treatment and LPS Concentration in BV-2 Microglia

In rat brain, H3K9 acetylation is reduced by 50% in a model of neuroinflammation and is returned to control levels with acetate supplementation. To determine the duration of acetate treatment required to achieve a similar H3K9 hyperacetylation pattern *in vitro*, we treated BV-2 microglia with 12 mM sodium acetate for 1, 2 and 4 hr (Figures 13A and B). Cell lysates were used for Western blot analysis to measure acetylated H3K9, total histone H3 (Figure 13A). We found that acetate treatment increased H3K9 acetylation by 2 hr which remained elevated out to 4 hr (Figure 13B). To insure protein expression following treatment, we used 4 hr as the treatment duration for all the experiments with the exception of change in MAPK phosphorylation where additional time points were used. To determine the optimal LPS concentration required to produce the same percentage of H3K9 hypoacetylation

found *in vivo*, we treated BV-2 microglia for 4 hr using a serial dilution of LPS ranging between 0 and 25 ng/ml (Figures 13C and D-G). Cell lysates were used for Western blot analysis to measure acetylated H3K9, total histone H3 and the pro-inflammatory cytokines pro-IL-1β, IL-6, and TNF-α, which were detected as protein bands corresponding to the molecular weights of 17, 17, 32, 25 and 23, respectively (Figure 13C). LPS reduced H3K9 acetylation and increased the pro-inflammatory cytokine levels in a concentration-dependent manner (Figures 13D-G). Based on these data, we used the LPS concentration 6.25 ng/ml because this concentration resulted in a 50% reduction in H3K9 acetylation, similar to that found *in vivo* (Soliman et al. 2012b), and also increased protein levels of all the pro-inflammatory cytokines measured.

In figure 13 below, time-dependent acetate-induced H3K9 hyperacetylation and dose-response study showing the effects of different LPS concentrations (0-25 ng/ml, 4 hr) on H3K9 acetylation and the expression of pro-inflammatory cytokines in BV-2 microglia. Panels A and C show representative images of the Western blots. Panel B shows the averaged proportion of H3K9 normalized to total H3 (n = 3) after 1, 2 and 4 hr of treatment with 12 mM sodium acetate. Panels D, E, F and G show the optical densities of H3K9 normalized to total H3 and the pro-inflammatory cytokines pro-IL-1β, IL-6, and TNF-α normalized to the loading control α-tubulin (n = 3). The graphs represent the means ± SD where statistical significance (* = compared to control in panel B and compared to LPS 0 ng/ml in panels D-G) was set at $p \leq 0.05$, as determined by One Way ANOVA followed by Tukey's post-hoc test.

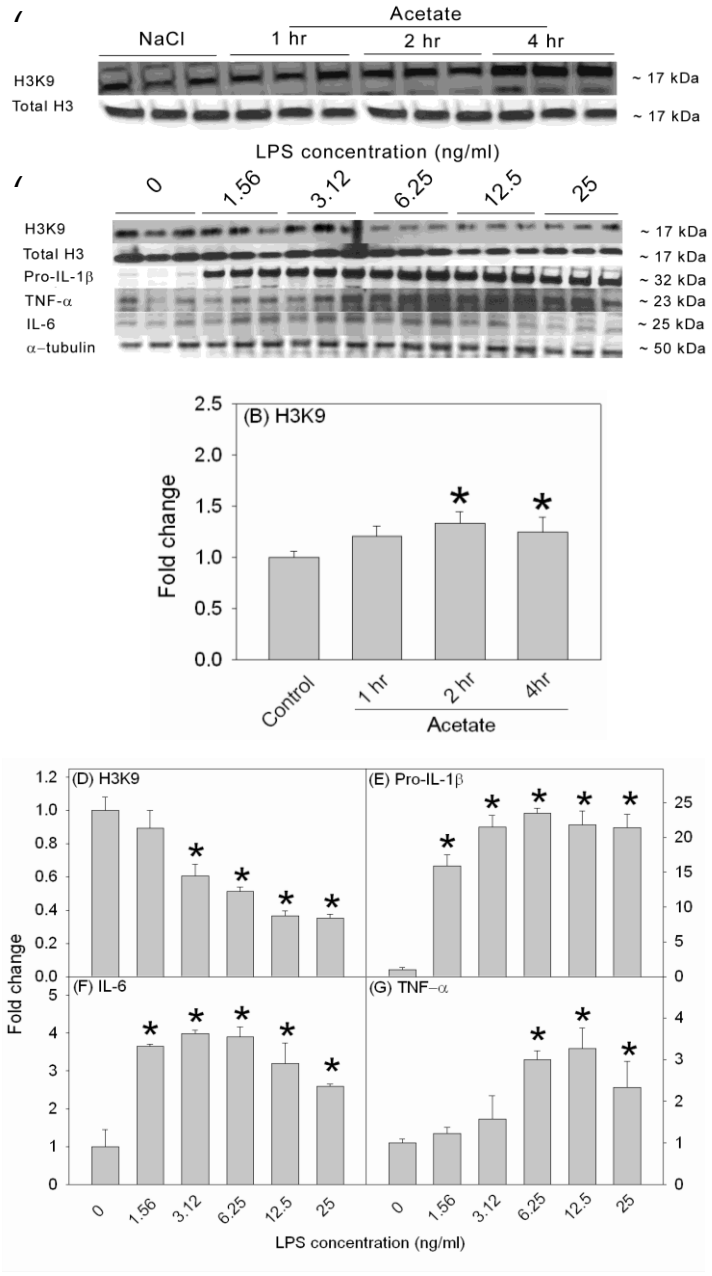

Figure 13. Optimizing the duration of acetate treatment and LPS concentration in BV-2 microglia.

Acetate Treatment Reverses LPS-induced H3K9 Hypoacetylation without Inducing Cytotoxicity in Primary Microglia

To determine the ability of acetate treatment to reverse LPS-induced H3K9 hypoacetylation in microglia similar to that found in the rat (Soliman et al. 2012b), we treated primary mouse microglia with LPS 6.25 ng/ml for 4 hr in the presence and absence of 12 mM sodium acetate, with 12 mM NaCl treatment as control. Using whole cell lysates for Western blot analysis, we found that primary microglia express the enzyme acetyl-CoA synthetase which converts acetate to acetyl-CoA, as protein bands corresponding to the molecular weight of 79 kDa (Figure 14A). The expression level of ACS was not different between groups (Figure 14B). Further, acetate treatment increased H3K9 acetylation by 1.7-fold, whereas LPS reduced H3K9 acetylation by 50% (Figure 14C). Acetate treatment, similar to that found *in vivo*, effectively increased H3K9 acetylation to control levels in the presence of LPS (Figure 14C). Cell viability assays showed no difference in cell survival between groups (Figure 14D). These data indicate that acetate treatment *in vitro* reverses LPS-induced H3K9 hypoacetylation in microglia similar to that found *in vivo* (Soliman et al. 2012b).

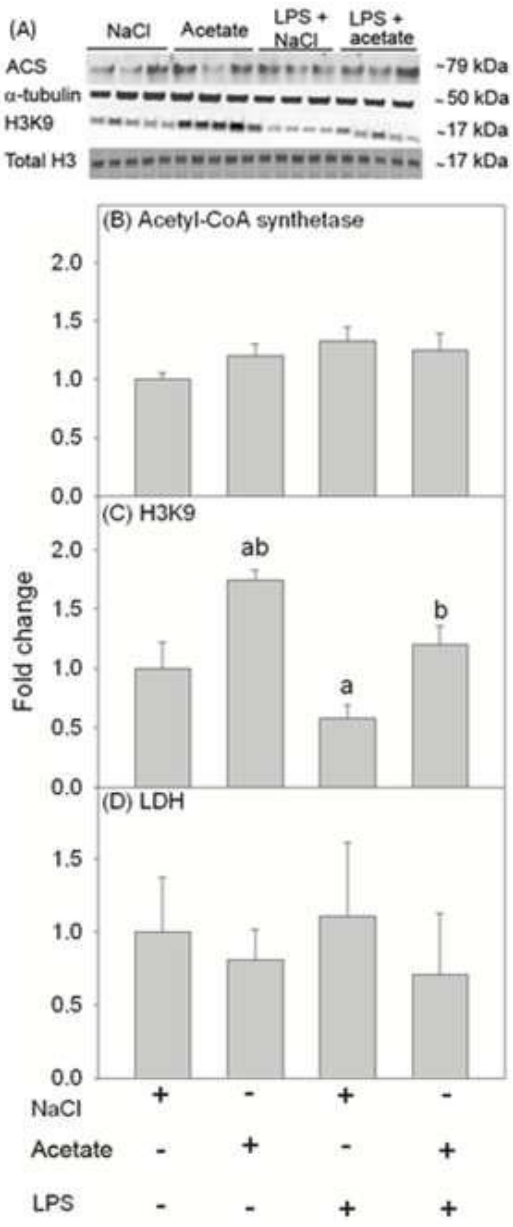

Figure 14. Acetate treatment and H3K9 acetylation in LPS-stimulated primary microglia.

Changes in histone acetylation in primary mouse microglial cell culture stimulated for 4 hr with LPS 6.25 ng/ml, and the reversal of these effects upon treatment with 12 mM sodium acetate. Panel A shows representative images of the

Western blots. Panels B and C show the optical densities of acetyl-CoA synthetase enzyme normalized to the loading control α-tubulin (n = 3) and H3K9 normalized to total H3 (n = 5), respectively. Panel D shows the quantification of the ratio of secreted LDH in the media to total cellular LDH (n = 5). Bars represent means $\pm$ SD where statistical significance (a = compared to NaCl, and b = compared to LPS) was set at $p \leq 0.05$, as determined by a one way ANOVA followed by Tukey's post-hoc test.

Acetate Treatment Reverses LPS-induced Increases in the Pro-inflammatory Cytokine Proteins, but not mRNA, in Primary Microglia

To determine the ability of acetate treatment to reverse pro-inflammatory cytokine production *in vitro* similar to that found *in vivo* (Soliman et al. 2012b), cell lysates were analyzed using Western blot to probe for IL-1β, IL-6 and TNF-α (Figure 15A). We found that LPS increased pro-IL-1β, IL-6 and TNF-α by about 4, 1.5 and 2.5-fold, respectively which were returned to control levels with acetate treatment (Figures 15B, D and F). In parallel studies, we found that LPS increased the mRNA levels of all the pro-inflammatory cytokines measured but were not altered by acetate treatment (Figures 15C and G) with the exception of IL-6 mRNA which was attenuated 3-fold (Figure 15E). These data demonstrate that this *in vitro* system reproduces the findings from the animal model, and that acetate treatment decreases pro-inflammatory cytokine levels possibly by disrupting mRNA translation or by increasing protein turnover.

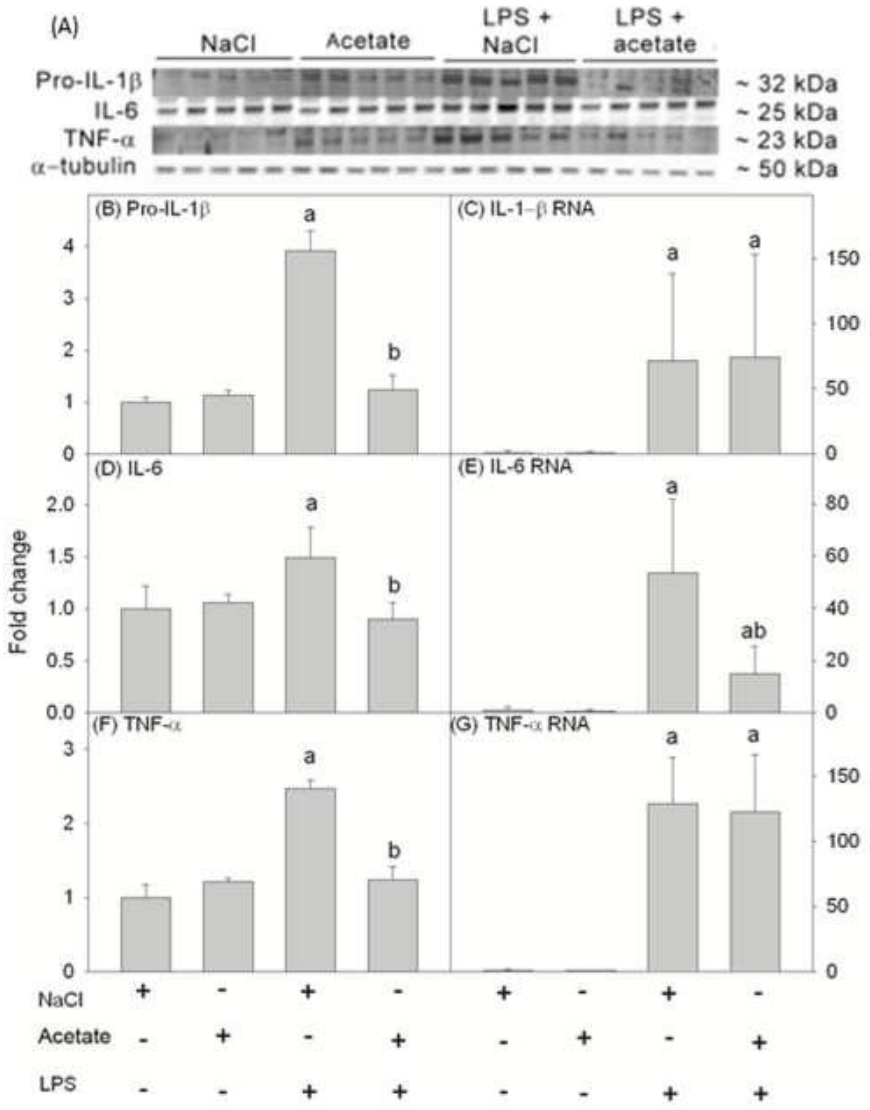

Figure 15. Acetate treatment and the expression of pro-inflammatory cytokines in LPS-stimulated primary microglia.

Changes in the pro-inflammatory cytokines IL-1β, IL-6, and TNF-α in primary mouse microglial cell culture stimulated for 4 hr with LPS 6.25 ng/ml with and without 12 mM sodium acetate. Panel A shows representative images of the Western blots. Panels B, D and F show the optical densities of the pro-inflammatory cytokines pro-IL-1β, IL-6 and TNF-α, respectively, normalized to the loading control α-tubulin (n = 5).

Panels C, E and G show the changes in the mRNA levels of the pro-inflammatory cytokines IL-1β, IL-6 and TNF-α, quantified by qrt-PCR and normalized to β-actin (n = 5). Bars represent means ± SD where statistical significance (a = compared to NaCl, and b = compared to LPS) was set at $p \leq 0.05$, as determined by a one way ANOVA followed by Tukey's post-hoc test.

Acetate Treatment Reverses LPS-induced H3K9 Hypoacetylation in BV-2 Microglia without Inducing Cell Death

We examined H3K9 acetylation in BV-2 microglia (Figure 16A) under the same experimental conditions used with primary mouse microglia to confirm that both cell types respond similarly. First, we confirmed that BV-2 microglia express acetyl-CoA synthetase; which was not different between groups (Figure 16B). Further, we found that acetate treatment increased H3K9 acetylation by 1.8-fold, and reversed the LPS-induced 50% reduction in H3K9 acetylation (Figure 16C) similar to that found in primary microglia cultures. Further, like the primary microglia cultures, treatment did not alter cell viability (Figure 16D).

Acetate Treatment Reverses the LPS-induced Increases in Pro-inflammatory Cytokine Protein, but not mRNA, in BV-2 Microglia

We proceeded to determine the effect of acetate treatment and LPS on pro-inflammatory cytokine proteins (Figure 17A) and mRNA levels in BV-2 microglia under the same experimental conditions used with primary microglia to confirm that both cell types respond similarly in this regard. We found that LPS increased pro-IL-1β, IL-6 and TNF-α production by 25-, 1.5-, and 8-fold respectively which were returned to control levels with acetate treatment (Figures 17B, D, and F).

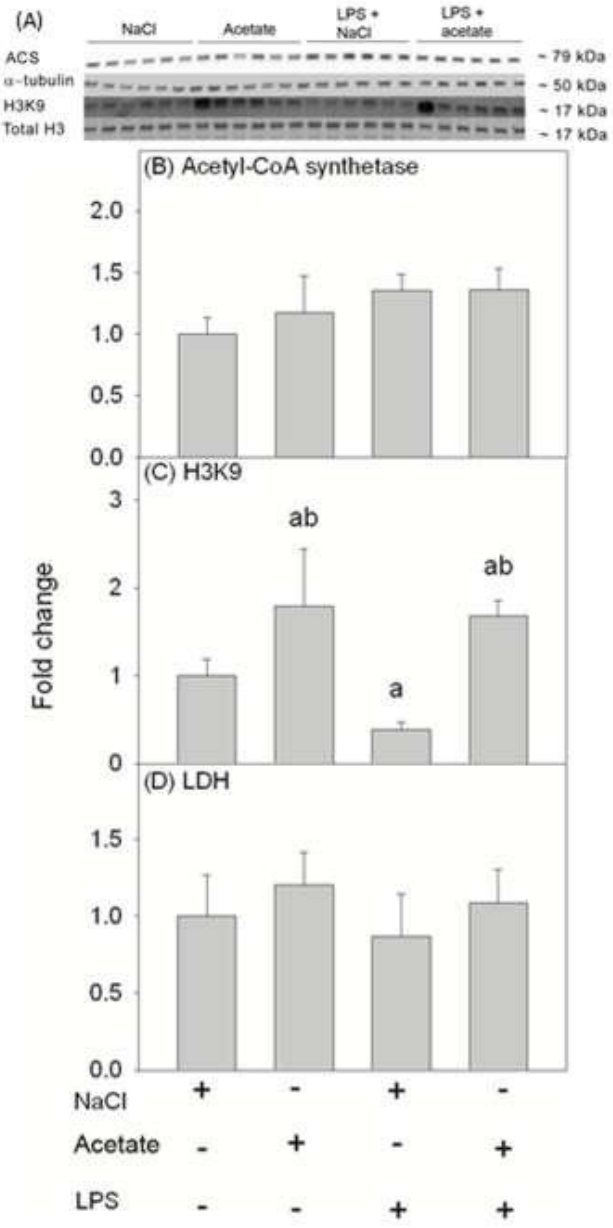

Figure 16. Acetate treatment and H3K9 acetylation in LPS-stimulated BV-2 microglia.

Changes in histone acetylation in BV-2 microglial cell culture stimulated for 4 hr with LPS 6.25 ng/ml, and the reversal of these effects upon treatment with 12 mM sodium acetate. Panel A shows representative images of the Western blots. Panels B and C show the optical densities of acetyl-CoA synthetase enzyme normalized to the

loading control α-tubulin and H3K9 normalized to total H3, respectively (n = 6). Panel D shows the quantification of the ratio of secreted LDH in the media to total cellular LDH (n = 6). Bars represent means ± SD where statistical significance (a = compared to NaCl, and b = compared to LPS) was set at $p \leq 0.05$ (n = 6, per group), as determined by a one way ANOVA followed by Tukey's post-hoc test.

In parallel, we found that LPS increased the mRNA levels of the same pro-inflammatory cytokines similar to that found with the primary microglia cultures and were not altered by acetate treatment (Figures 17C and G) with the exception of IL-6 which was attenuated 2-fold (Figure 17E). Therefore, the inflammatory response of BV-2 microglia towards LPS and acetate treatment is similar to that of primary microglia.

Acetate Treatment Increases the Expression of Anti-inflammatory Cytokines in BV-2 Microglia

Anti-inflammatory cytokines are an integral part of the inflammatory response to minimize the potential of the pro-inflammatory cytokines to produce neuronal damage. We determined the effect of acetate treatment on expression levels of the anti-inflammatory cytokine proteins TGF-β1, IL-4, and IL-10 (Figure 18A). Acetate treatment did not alter the protein levels of TGF-β1 or IL-10 (Figures 18B and F); however, IL-4 was increased by 1.3-fold (Figure 18D). In parallel, we found that acetate treatment increased TGF-β1 mRNA by 2-fold (Figure 18C) and IL-4 mRNA by 11- and 4-fold, depending on the group (Figure 18E). Conversely, LPS increased IL-10 protein and mRNA by 1.4- and 16-fold, respectively. Acetate treatment returned IL-10 protein to control levels and attenuated IL-10 mRNA by 8-fold (Figures 18F and G).

The possible reasons why increases in mRNA levels are not paralleled by increased protein levels may involve mRNA stability or reflect the short treatment duration. Regardless, these data suggest that acetate treatment modulates pro- and anti-inflammatory cytokine release in BV-2 microglia towards a more anti-inflammatory state.

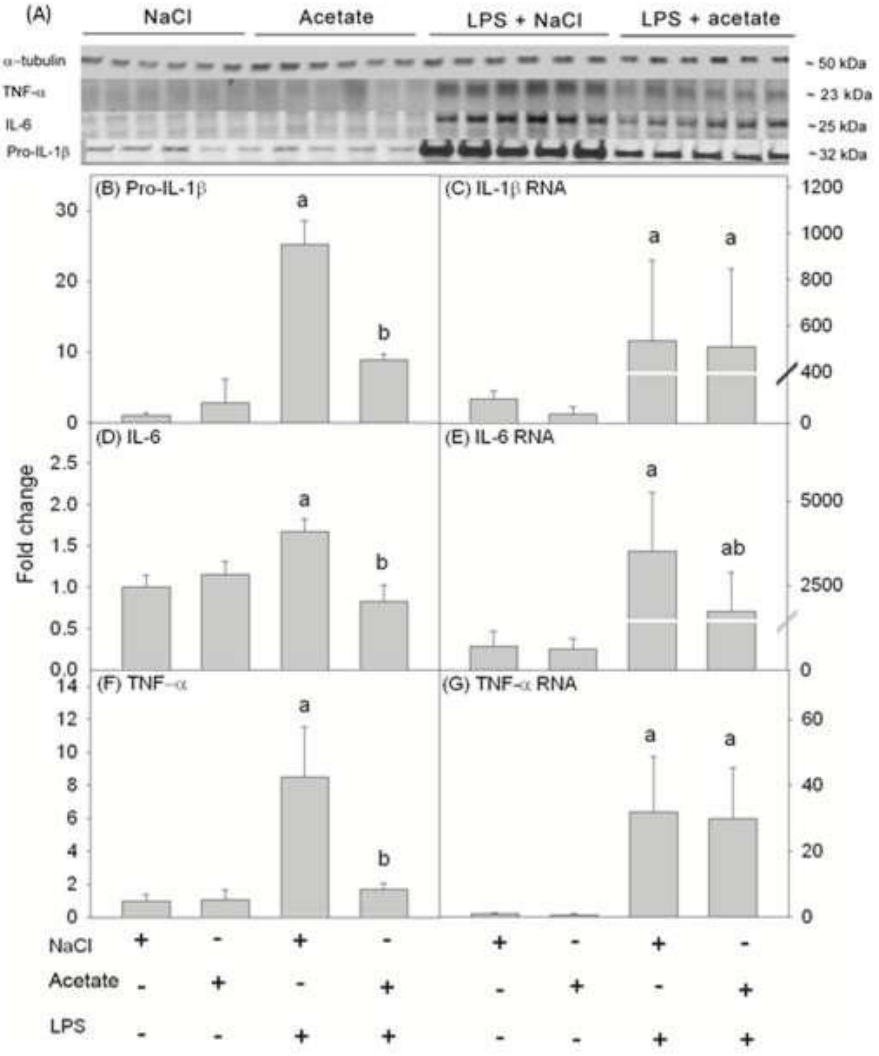

Figure 17. Acetate treatment and the expression of pro-inflammatory cytokines in LPS-stimulated BV-2 microglia.

Changes in the pro-inflammatory cytokines IL-1β, IL-6, and TNF-α in BV-2 microglial cell culture stimulated for 4 hr with LPS 6.25 ng/ml with and without 12 mM sodium acetate. Panel A shows representative images of the Western blots. Panels B, D and F show the optical densities of the pro-inflammatory cytokines pro-IL-1β, IL-6 and TNF-α, respectively, normalized to the loading control α-tubulin. Panels C, E and G show the changes in the mRNA levels of the pro-inflammatory cytokines IL-1β, IL-6 and TNF-α, quantified by qrt-PCR and normalized to β-actin. Bars represent means ± SD where statistical significance (a = compared to NaCl, and b = compared to LPS) was set at $p \leq 0.05$ (n = 6, except pro-IL-1β where n = 5), as determined by a one way ANOVA followed by Tukey's post-hoc test.

In Figure 18 below, changes in the anti-inflammatory cytokines TGF-β1, IL-4, and IL-10 in BV-2 microglial cell culture stimulated for 4 hr with LPS 6.25 ng/ml with and without treatment with 12 mM sodium acetate. Panel A shows representative images of the Western blots. Panels B, D and F show the optical densities of the anti-inflammatory cytokines TGF-β1, IL-4, and IL-10, respectively, normalized to the loading control α-tubulin (n = 6). Panels C, E and G show the changes in the mRNA levels of the anti-inflammatory cytokines TGF-β1, IL-4, and IL-10, quantified by qrt-PCR and normalized to β-actin (n = 6). Bars represent means $\pm$ SD where statistical significance (a = compared to NaCl, and b = compared to LPS) was set at $p \leq 0.05$, as determined by a one way ANOVA followed by Tukey's post-hoc test.

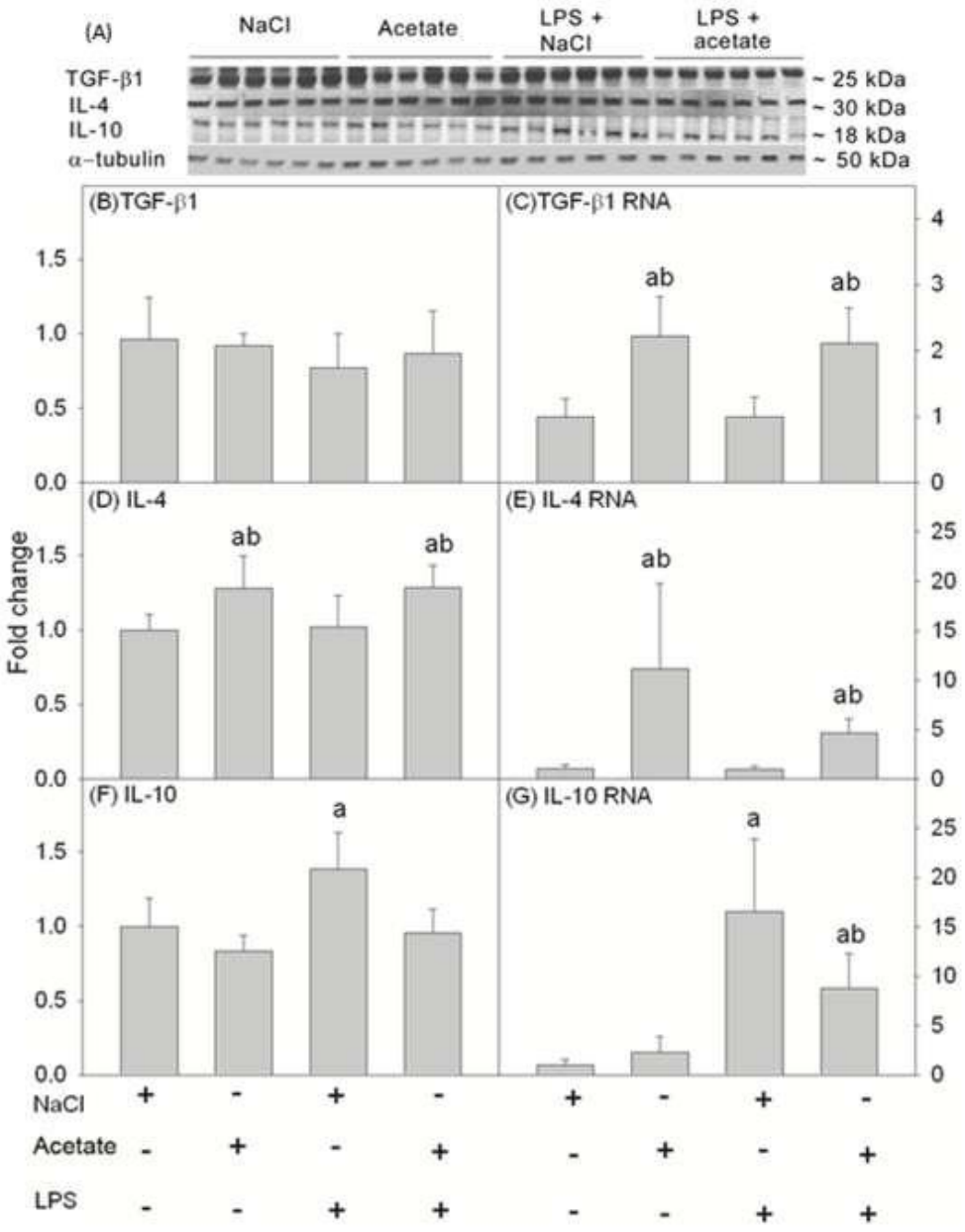

Figure 18. Acetate treatment and the expression of anti-inflammatory cytokines in LPS-stimulated BV-2 microglia.

Acetate Treatment and LPS Alter MAPK Phosphorylation in a Time-dependent Manner in BV-2 Microglia

Because MAPK signaling can be inhibited by the acetylation of MAPK phosphatase-1 which induces deacetylation and deactivation of MAPK (Cao et al. 2008), we measured the effects of acetate treatment on LPS-induced MAPK phosphorylation at 0.5, 1, 2, and 4 hr. The rationale for including multiple time points is that other studies reported MAPK activation by LPS at much earlier time points than 4 hr (Schumann *et al.* 1996, Kraatz *et al.* 1998). Whole cell lysates were used for Western blot analysis, and phosphorylated p38, p38, phosphorylated JNK, JNK, phosphorylated ERK1/2 and ERK1/2 were detected as protein bands corresponding to the molecular weights of 38, 38, 46, 54 and 46, and 42 and 46 kDa, respectively (Figure 19A). At 0.5 and 1 hr, neither LPS nor acetate treatment had an effect on the levels of phosphorylated MAPK (Figures 19B-D). At 2 hr, acetate treatment reduced the level of phosphorylated p38 as compared to LPS, and LPS increased JNK phosphorylation by 5-fold, which was attenuated 2.5-fold with acetate treatment (Figures 19B and C). At 4 hr, LPS increased phosphorylated p38 and phosphorylated JNK by 2-fold and was not altered upon acetate treatment; however treatment did increase the level of phosphorylated ERK1/2 by 2-fold only in the presence of LPS (Figures 19B-D).

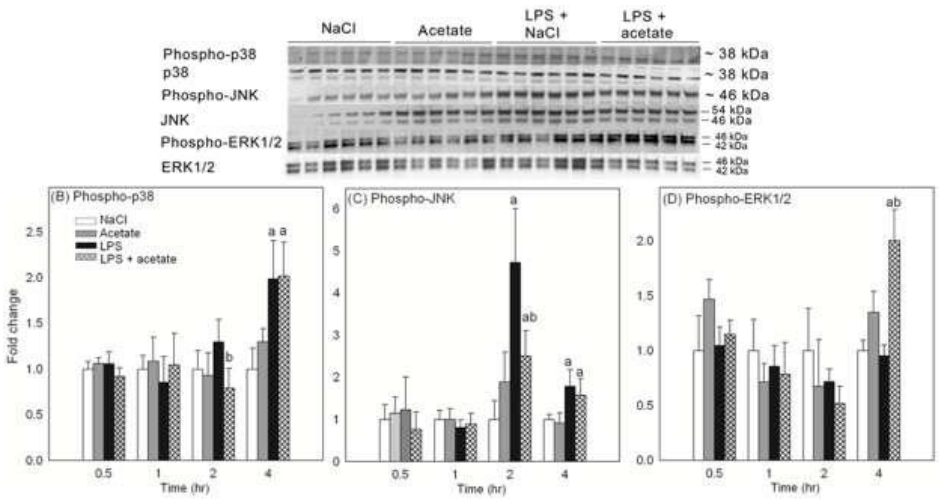

Figure 19. Acetate treatment and MAPK phosphorylation in LPS-stimulated BV-2 microglia.

Changes in the phosphorylation state of MAPK p38, JNK and ERK1/2 in BV-2 microglia stimulated for 0.5, 1, 2 and 4 hr with LPS 6.25 ng/ml with and without 12 mM sodium acetate. Panel A shows representative images of the Western blots from the 4 hr experiment. Panels B, C and D show the optical densities of phosphorylated MAPK p38, JNK and ERK1/2 normalized to the loading controls MAPK p38, JNK and ERK1/2, respectively (n = 6). The data represent the means ± SD where statistical significance (a = compared to NaCl, b = compared to LPS) was set at $p \leq 0.05$, as determined by One Way ANOVA followed by Tukey's post-hoc test.

Acetate Treatment Alters LPS-induced Increases in NF-κB p65 Protein Levels and Phosphorylation at Serine 468 in BV-2 Microglia

Because NF-κB signaling is altered by acetylation of p65 (Kiernan et al. 2003, Chen et al. 2001, Huang et al. 2010a) and has a prominent role in the regulation of inflammatory and immune responses, we tested the effect of acetate treatment on LPS-induced changes in p65 protein levels, phosphorylation and acetylation after 4 hr of

treatment. Whole cell lysates were used for Western blot analysis, and total p65, phosphorylated p65 at serine 536, phosphorylated p65 at serine 468, and acetylated p65 at lysine 310 were detected as protein bands corresponding to the molecular weight of 65 kDa (Figure 20A). LPS increased the total protein level of p65 by 1.5-fold which returned to control levels with acetate treatment (Figure 20B). While neither acetate treatment nor LPS altered the level of phosphorylated p65 at serine 536, LPS did increase the levels of phosphorylated p65 at serine 468 by 2-fold which was reduced to control levels with acetate treatment (Figures 20C and D). In addition, acetate treatment induced p65 hyperacetylation at lysine 310 by 3.5 and 4-fold depending on the group (Figure 20E). These data suggest that acetate metabolism alters the LPS-induced p65 response in microglia, and that the anti-inflammatory effect of acetate treatment can potentially be attributed to acetylation of non-histone targets.

In Figure 20, changes in the protein level, phosphorylation and acetylation states of NF-κB p65 in BV-2 microglia cell culture stimulated for 4 hr with LPS 6.25 ng/ml with and without 12 mM sodium acetate. Panel A shows representative images of the Western blots. Panel B shows the optical density of total NF-κB p65 normalized to the loading control α-tubulin. Panels C, D and E show the optical densities of phosphorylated p65 at S536, phosphorylated p65 at serine 468 and acetylFated p65 at lysine 310 normalized to total p65, respectively (n = 6). The data represent the means ± SD where statistical significance (a = compared to NaCl and b = compared to LPS) was set at $p \leq 0.05$, as determined by One Way ANOVA followed by Tukey's post-hoc test. Abbreviations are: S536, serine 536; S468; serine 468: and K310, lysine 310.

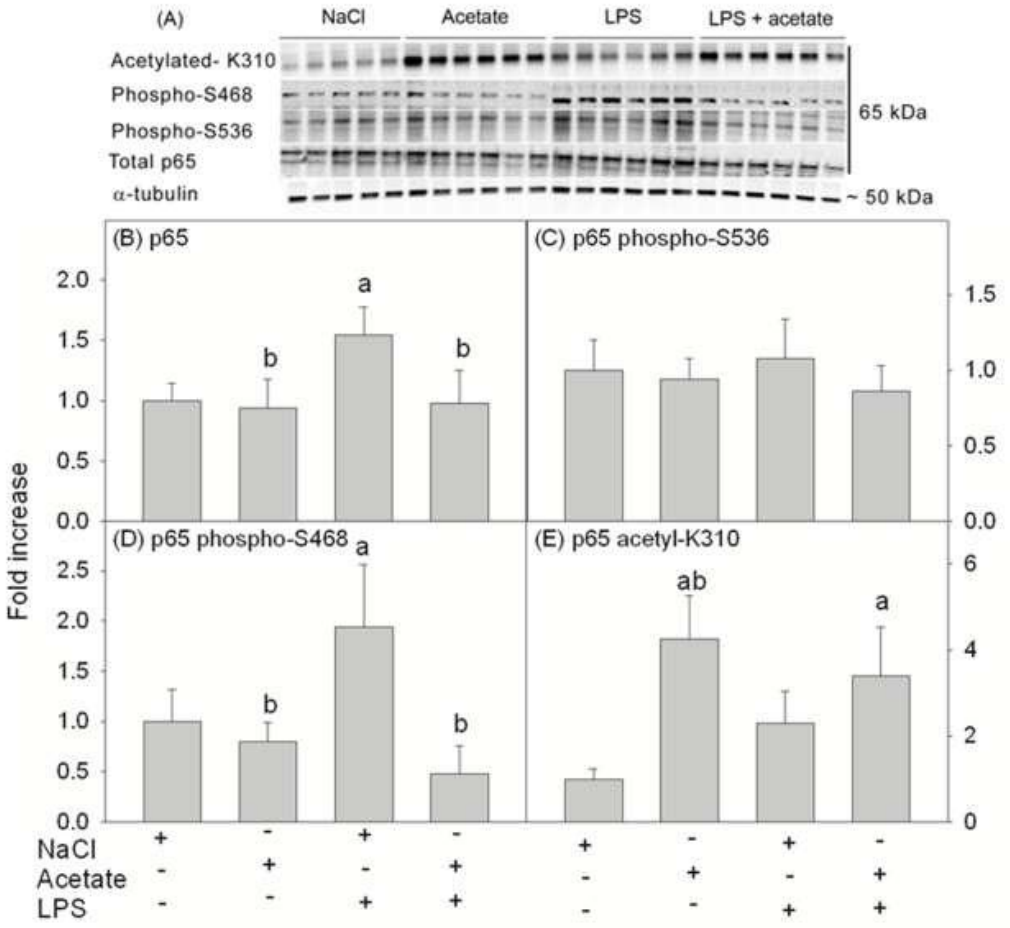

Figure 20. Acetate treatment and NF-κB p65 protein levels and modifications in LPS-stimulated BV-2 microglia.

Optimizing the Duration of Acetate Treatment and LPS Concentration in Primary Astroglial Cultures

To determine the duration of acetate treatment required to achieve H3K9 hyperacetylation pattern *in vitro* similar to that found *in vivo* (Soliman et al. 2012b), we treated primary astrocytes with 12 mM sodium acetate for 1, 2 and 4 hr (Figures 21A and B). Cell lysates were used for Western blot analysis to measure acetylated H3K9, total histone H3 (Figure 21A). We found that acetate increased H3K9 acetylation at 1

hr which remained increased out to 4 hr (Figure 21B). To insure protein expression following treatment, we used 4 hr as the treatment duration for all the experiments. To determine the optimal LPS concentration required to produce the same percentage of H3K9 hypoacetylation *in vitro* similar to that found *in vivo* and in LPS-stimulated microglia *in vitro,* using a serial dilution of LPS (0-25 ng/ml), we treated primary astrocytes for 4 hr (Figures 21C and D-G). Cell lysates were used for Western blot analysis to measure acetylated H3K9, total histone H3 and the pro-inflammatory cytokines pro-IL-1β, IL-6, and TNF-α, which were detected as protein bands corresponding to the molecular weights of 17, 17, 32, 25 and 17 kDa, respectively (Figure 21C). Interestingly, LPS did not alter H3K9 acetylation or IL-6 protein levels and increased pro-IL-1β and TNF-α protein levels in a concentration-dependent manner (Figures 21D-G). Based on these data, we decided to use the LPS concentration 6.25 ng/ml because this concentration increased both pro-IL-1β and TNF-α protein levels, and also to conform to the concentration used for the treatment of primary and BV-2 microglia.

In Figure 21, time-dependent acetate treatment-induced H3K9 hyperacetylation and dose-response study showing the effects of different LPS concentrations (0-25 ng/ml, 4 hr) on H3K9 acetylation and the expression of pro-inflammatory cytokines in primary mouse astrocyte cell culture. Panels A and C show representative images of the Western blots. Panel B shows the averaged proportion of H3K9 normalized to total H3 (n = 3) after 1, 2 and 4 hr of treatment with 12 mM sodium acetate. Panels D, E, F and G show the optical densities of H3K9 normalized to total H3 and the pro-

inflammatory cytokines pro-IL-1β, IL-6, and TNF-α normalized to the loading control α-tubulin (n = 3). The graphs represent the means ± SD where statistical significance (* = compared to control in panel B, and compared to LPS 0 ng/ml in panels D-G) was set at $p \leq 0.05$, as determined by One Way ANOVA followed by Tukey's post-hoc test.

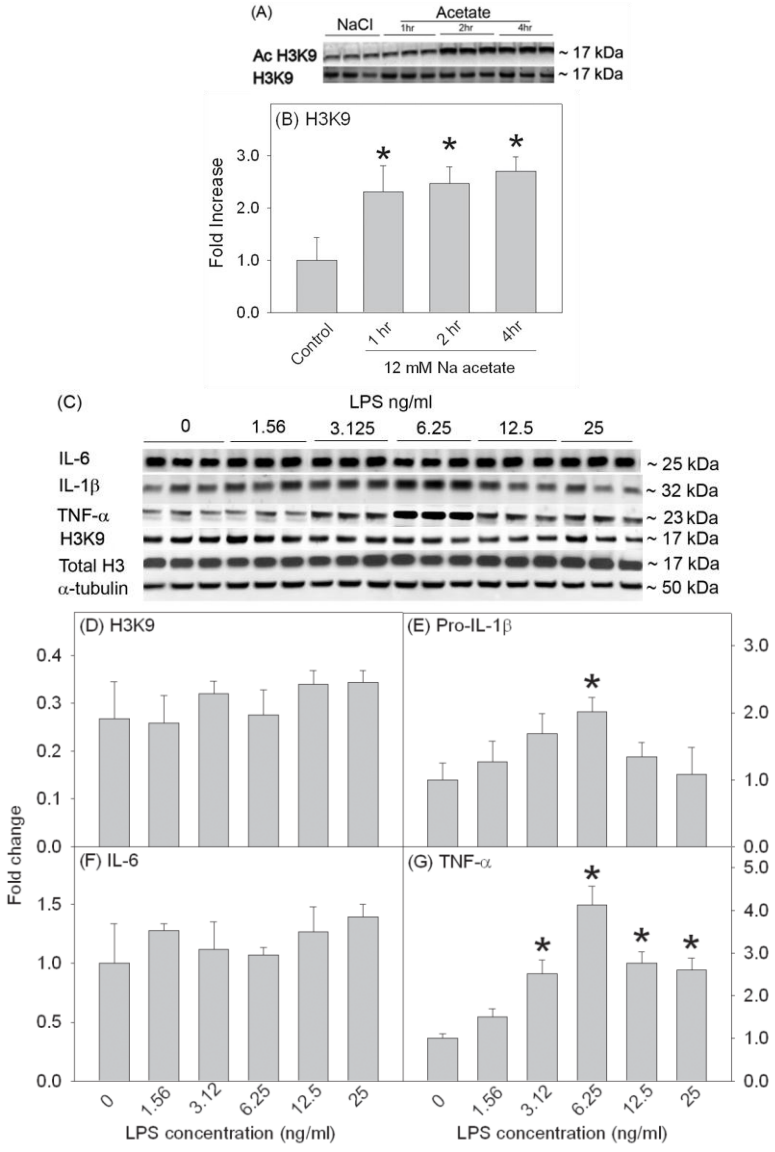

Figure 21. Optimizing the duration of acetate treatment and LPS concentration in primary astroglial cultures.

Acetate Treatment causes H3K9 Hyperacetylation without Inducing Cytotoxicity in LPS-stimulated Primary Astrocytes

In order to determine the effect of acetate on H3K9 acetylation in LPS-challenged astrocytes, we treated primary astrocyte cultures with 6.25 ng/ml LPS in the presence and absence of 12 mM sodium acetate, and compared the results to cells treated with 12 mM NaCl as a control group. Using whole cell lysates for Western blot analysis, we found that primary astrocytes express acetyl-CoA synthetase; the enzyme which converts acetate to acetyl-CoA, as protein bands corresponding to the molecular weight of 79 kDa (Figure 22A). The expression levels of ACS were not different between groups (Figure 22B). In addition, while LPS did not alter H3K9 acetylation, acetate supplementation increased H3K9 acetylation by 2-fold in the presence and absence of LPS challenge (Figure 22D). This finding is different than microglia where the same concentration of LPS reduces H3K9 acetylation by about 50%. Measuring cellular release of LDH as an index of cell death showed no difference in cell survival between groups (Figure 22C). These data indicate that acetate treatment *in vitro* induces H3K9 hyperacetylation in astrocytes similar to that found *in vivo* using oral glyceryl triacetate in a rat model of neuroinflammation (Soliman et al. 2012b) and in LPS-stimulated microglia *in vitro* (Soliman et al. 2012a), without altering acetyl-CoA synthetase protein levels or inducing cell death.

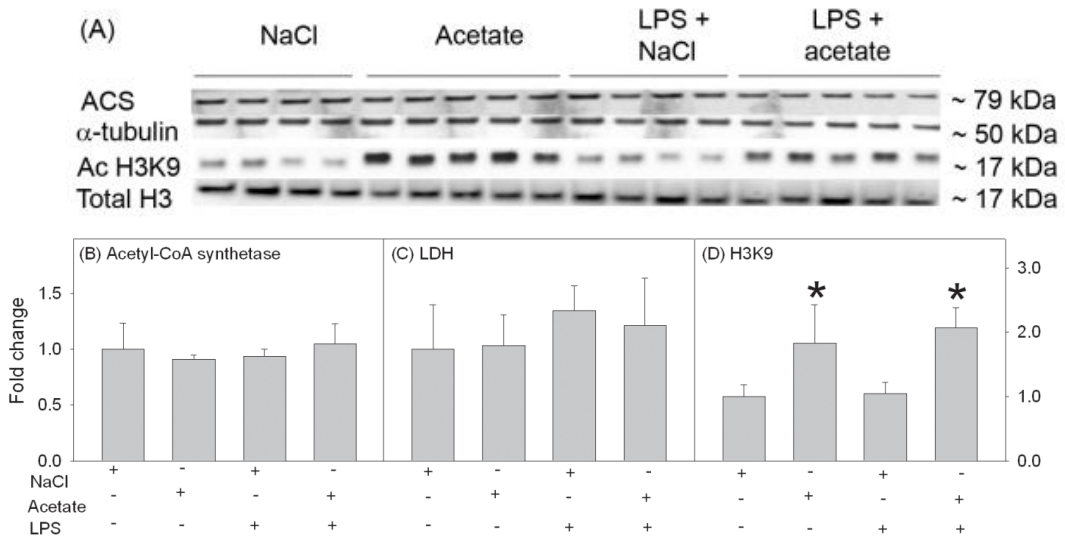

Figure 22. Acetate treatment and H3K9 acetylation in LPS-stimulated primary astrocytes.

Changes in histone acetylation in primary mouse astrocyte cell culture stimulated for 4 hr with LPS 6.25 ng/ml and/or 12 mM sodium acetate, with 12 mM NaCl as control. Panel A shows representative images of the Western blots. Panels B and D show the optical densities of acetyl-CoA synthetase enzyme normalized to the loading control α-tubulin, and H3K9 normalized to total H3, respectively. Panel C shows the quantification of the ratio of secreted LDH in the media to total cellular LDH. Bars represent means $\pm$ SD where statistical significance (* = compared to NaCl, n = 4, 5, 4, and 5) was set at $p \leq 0.05$, as determined by One Way ANOVA followed by Tukey's post-hoc test.

Acetate Reverses LPS-induced Increases in the Pro-inflammatory Cytokine Proteins, but not mRNA, in Primary Astrocytes

To determine the ability of acetate to reverse pro-inflammatory cytokine production *in vitro* similar to that found in whole brain *in vivo* (Soliman et al. 2012b) and in LPS-stimulated microglia *in vitro* (Soliman et al. 2012a), cell lysates were analyzed using Western blot to probe for IL-1β, IL-6 and TNF-α (Figure 23A). We found that LPS increased pro-IL-1β, TNF-α production, but not IL-6, by about 3.5 and 2.5-fold, respectively (Figure 23 B and F). Acetate treatment only partially attenuated LPS-induced increases in pro-IL-1β (Figure 23B), completely reversed TNF-α (Figure 23F), and decreased IL-6 basal levels by about 40% (Figure 23D). Quantifying mRNA using qrt-PCR showed that LPS increased the mRNA levels of the 3 pro-inflammatory cytokines measured that were not altered by acetate treatment (Figures 23C and E) with the exception of TNF-α mRNA which was only partially attenuated (Figure 23G).

Acetate Modulates the Expression of the Anti-inflammatory Cytokines in LPS-challenged Primary Astrocytes

Anti-inflammatory cytokines are produced during the inflammatory response as a part of self-checking mechanisms, to mitigate the destructive effects of unopposed pro-inflammatory mediators. We determined the effect of acetate treatment on expression levels of the anti-inflammatory cytokine proteins TGF-β1, IL-4, and IL-10 in LPS-stimulated primary astrocytes (Figure 24A), that were detected as protein bands corresponding to the molecular weights of around 25, 30 and 18 kDa, respectively. Acetate treatment reversed the LPS-induced reduction in the TGF-β1 mRNA and protein, and IL-4 protein (Figure 24B, C and D) and upregulated IL-4 mRNA by 3-fold

and protein by 1.3-fold (Figure 24D and E). Interestingly, IL-10 mRNA was increased by about 4-fold with acetate treatment, while the protein levels were decreased by 2-fold. IL-10 protein and mRNA were not altered by LPS (Figure 24F and G). We speculate that this could be due to either interference with mRNA translation, increased protein turnover, or enhanced secretion into the extracellular milieu. Regardless, these data suggest that acetate modulates pro- and anti-inflammatory cytokine in primary astrocytes towards a more anti-inflammatory state similar to that found in LPS-stimulated microglia (Soliman et al. 2012a).

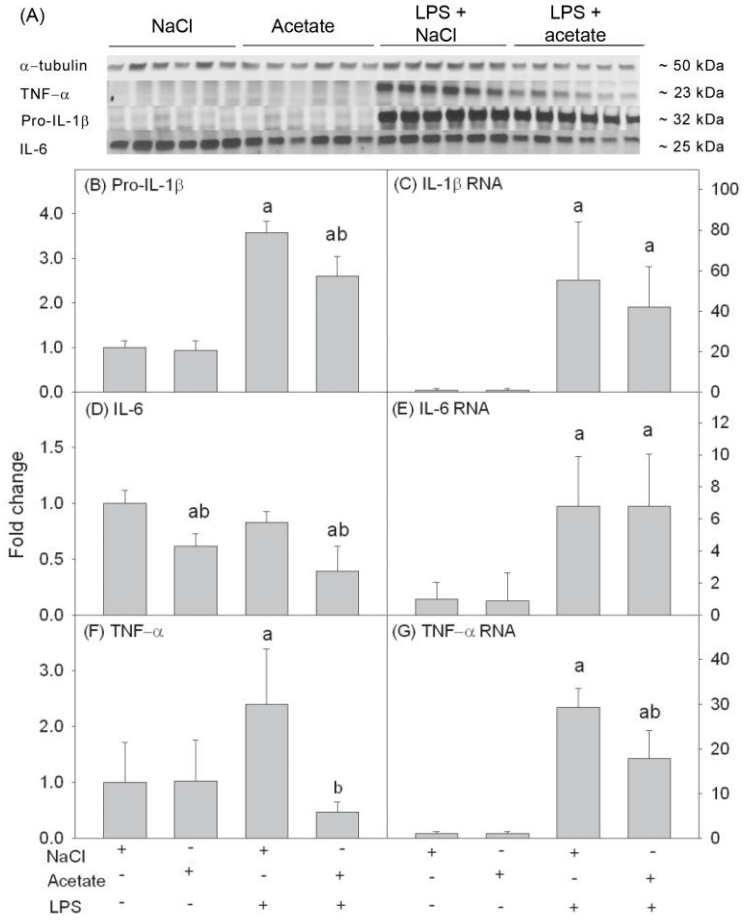

Figure 23. Acetate treatment and the expression of pro-inflammatory cytokines in LPS-stimulated primary astrocytes.

Changes in the pro-inflammatory cytokines pro-IL-1β, IL-6, and TNF-α in primary mouse astrocyte cell culture stimulated for 4 hr with LPS 6.25 ng/ml and/or 12 mM sodium acetate, with 12 mM NaCl as control. Panel A shows representative images of the Western blots. Panels B, D and F show the optical densities of the pro-inflammatory cytokines pro-IL-1β, IL-6 and TNF-α, respectively, normalized to the loading control α-tubulin (n = 6). Panels C, E and G show the changes in the mRNA levels of the pro-inflammatory cytokines IL-1β, IL-6 and TNF-α, quantified by qrt-PCR and normalized to β-actin (n = 6). Bars represent means $\pm$ SD where statistical significance (a = compared to NaCl, and b = compared to LPS) was set at $p \leq 0.05$, as determined by One Way ANOVA followed by Tukey's post-hoc test.

Acetate Reverses LPS-induced p38 Phosphorylation and Decreases Basal Levels of ERK1/2 Phosphorylation in Primary Astrocyte Culture

MAPK inflammatory cascade is evidently involved in neuroinflammation and pro-inflammatory cytokine production. Specific lysine acetylation was shown to activate a MAPK phosphatase-1, which in turn deactivates MAPK signaling. This sparked our interest to study the effects of acetate on LPS-induced MAPK phosphorylation, and determine whether this is a potential mechanism of the anti-inflammatory effect of acetate in primary astrocytes. Whole cell lysates were used for Western blot analysis, and p38, phosphorylated p38, JNK, phosphorylated JNK, ERK1/2, and phosphorylated ERK1/2 were detected as protein bands corresponding with the molecular weights of around 38, 38, 46 and 54, 46 and kDa, 42 and 46, and 42 and 46 kDa, respectively (Figure 25A).

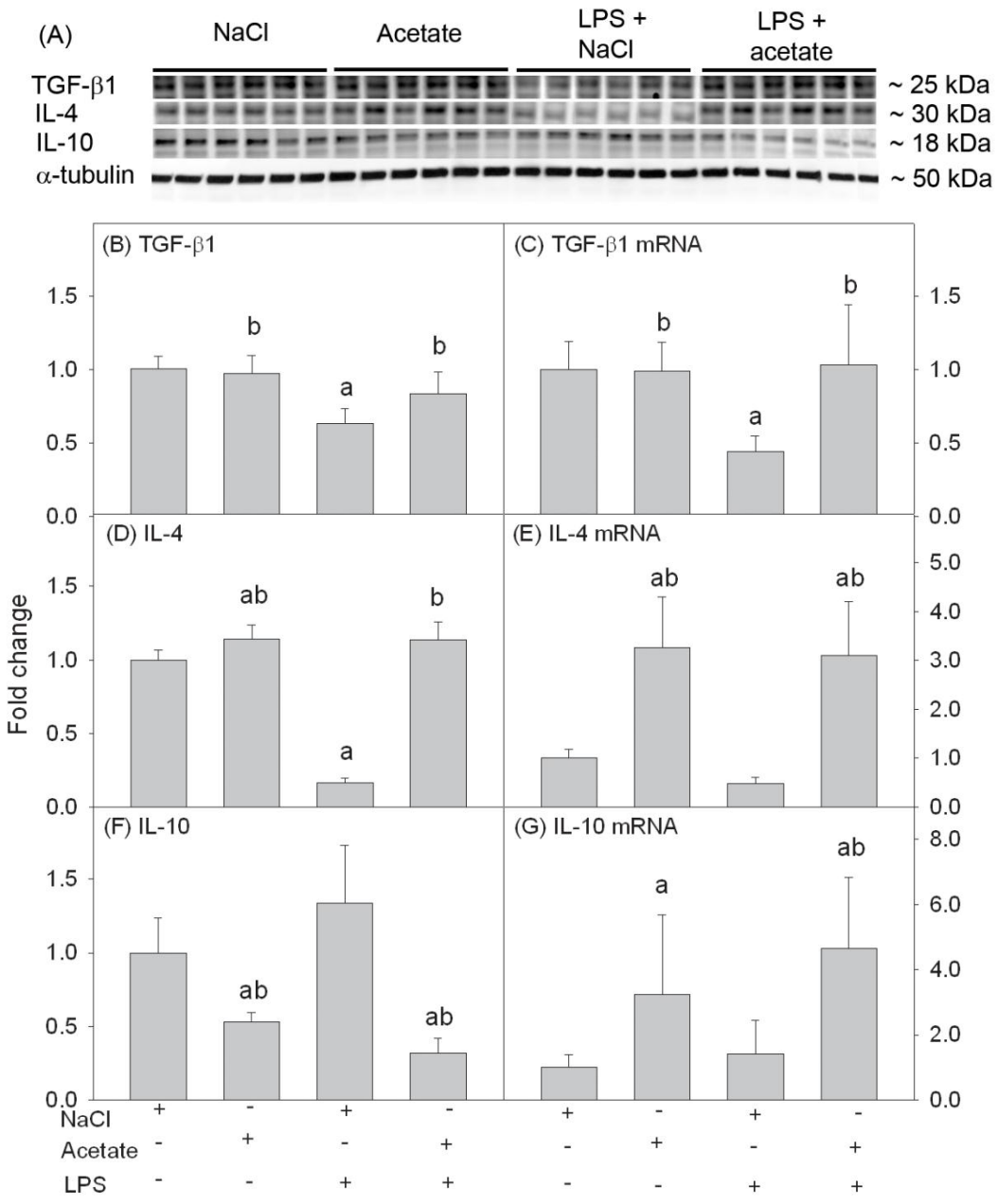

Figure 24. Acetate treatment and the expression of the anti-inflammatory cytokines in LPS- stimulated primary astrocytes.

Changes in the anti-inflammatory cytokines TGF-β1, IL-4, and IL-10 in primary mouse astrocyte cell culture stimulated for 4 hr with LPS 6.25 ng/ml and/or 12

mM sodium acetate, with 12 mM NaCl as control. Panel A shows representative images of the Western blots. Panels B, D and F show the optical densities of the anti-inflammatory cytokines TGF-β1, IL-4, and IL-10, respectively, normalized to the loading control α-tubulin (n = 6). Panels C, E and G show the changes in the mRNA levels of the anti-inflammatory cytokines TGF-β1, IL-4, and IL-10, quantified by qrt-PCR and normalized to β-actin (n = 6). Bars represent means $\pm$ SD where statistical significance (a = compared to NaCl, and b = compared to LPS) was set at $p \leq 0.05$, as determined by One Way ANOVA followed by Tukey's post-hoc test.

LPS increased p38 phosphorylation by 1.5-fold which was returned to control level with acetate (Figure 25B). Neither LPS not acetate had an effect on JNK phosphorylation (Figure 25C). While LPS did not alter ERK1/2 phosphorylation, the basal levels of phosphorylated ERK1/2 were decreased by acetate treatment in the presence and absence of LPS by almost 2-fold (Figure 25D). These data demonstrate that acetate and LPS selectively modulate MAPK phosphorylation in primary astrocytes *in vitro*, which can potentially represent a mechanism for the anti-inflammatory effect of acetate treatment in astrocytes. This is different from microglia where at 4 hr following LPS stimulation, MAPK p38 and JNK phosphorylation is increased and is not altered by acetate treatment, and phosphorylated ERK1/2 that is increased by acetate treatment only in the presence of LPS (Soliman et al. 2012a).

Acetate reverses LPS-induced elevated NF-κB p65 protein level, and decreases the basal levels of p65 phosphorylation at serine 536 in primary astrocyte culture.

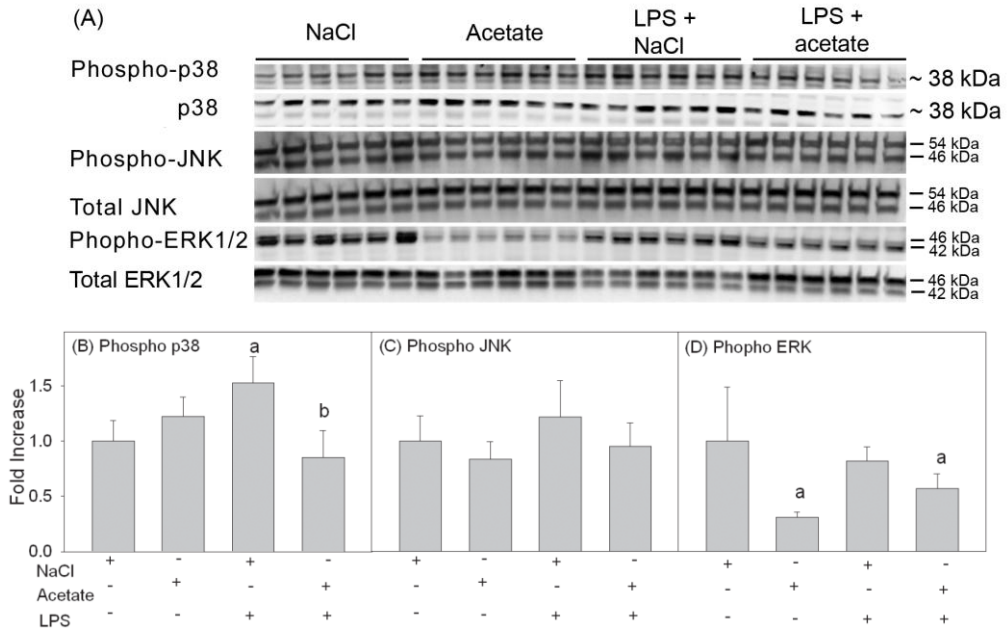

Figure 25. Acetate treatment and MAPK phosphorylation in LPS-stimulated primary astrocytes.

Changes in the phosphorylation state of MAPK p38, JNK and ERK1/2 in primary mouse astrocyte cell culture stimulated for 4 hr with LPS 6.25 ng/ml and/or 12 mM sodium acetate, with 12 mM NaCl as control. Panel A shows representative images of the Western blots. Panels B, C and D show the optical densities of phosphorylated MAPK p38, JNK and ERK1/2 normalized to the loading controls MAPK p38, JNK and ERK1/2, respectively (n = 6). The data represent the means ± SD where statistical significance (a = compared to NaCl and b = compared to LPS) was set at $p \leq 0.05$, as determined by One Way ANOVA followed by Tukey's post-hoc test.

NF-κB is a major player in neuroinflammation and the biosynthesis of pro-inflammatory mediators. NF-κB p65 subunit is also regulated by a wide range of post-translational modifications which have diverse functional consequences (Huang et al.

2010a). In the light of this, we quantified the effects of LPS and acetate treatment on NF-κB p65 protein levels and selected post-translational modifications using total cell lysates for Western blot analysis. Total NF-κB p65 protein, acetylated p65 at lysine 310, and phosphorylated p65 at serine residues 468 and 536 were detected as protein bands corresponding to the molecular weight 65 kDa (Figure 26). We found that while LPS increased the protein levels of NF-κB p65 by 1.5-fold, acetate treatment reduced it back to control levels (Figure 26B). Moreover, acetate treatment reduced the basal level of phosphorylated p65 at serine 536 (Figure 26D). Neither LPS nor acetate treatment altered acetylated p65 at lysine 310 or phosphorylated p65 at serine 468 (Figure 26C and E). These data suggest that acetate treatment can alter NF-κB p65 protein and selected post-translational modifications, which may explain the anti-inflammatory effect of acetate treatment in LPS-challenged primary astrocytes.

Acetate Treatment and the Protein Levels of Phospholipases in LPS-stimulated BV-2 Microglia

To determine the effect of LPS and acetate treatment on the phosphorylation level of $cPLA_2$ and the protein levels of total $cPLA_2$, $sPLA_2$ IIA and selected PLC isoforms in BV-2 microglia, cells were treated with 6.25 ng/ml LPS in the presence and absence of 12 mM sodium acetate, and compared the results to cells treated with 12 mM NaCl as a control group. Using whole cell lysates for Western blot analysis, $cPLA_2$, phosphorylated $cPLA_2$, $sPLA_2$ IIA, PLCβ1, PLCγ1, and PLCδ1 were detected as protein bands corresponding to the molecular weight of 85, 85, 18, 150, 155, and 85 kDa, respectively (Figure 27A). The protein levels of total $cPLA_2$ were not different between groups (Figure 27B), whereas phosphorylated $cPLA_2$ was increased with LPS

1.5-fold which was not altered by acetate treatment (Figure 27C). The protein levels of $sPLA_2$ IIA, PLCγ1 and PLCδ1 were not altered by either LPS or acetate treatment (Figure 27D, F and G). By contrast, LPS decreased PLCβ1 by 2-fold which was reversed to control levels with acetate treatment (Figure 27E). These data suggest that acetate treatment can alter $cPLA_2$ phosphorylation and the protein levels of enzymes involved in eicosanoid signaling in BV-2 microglia.

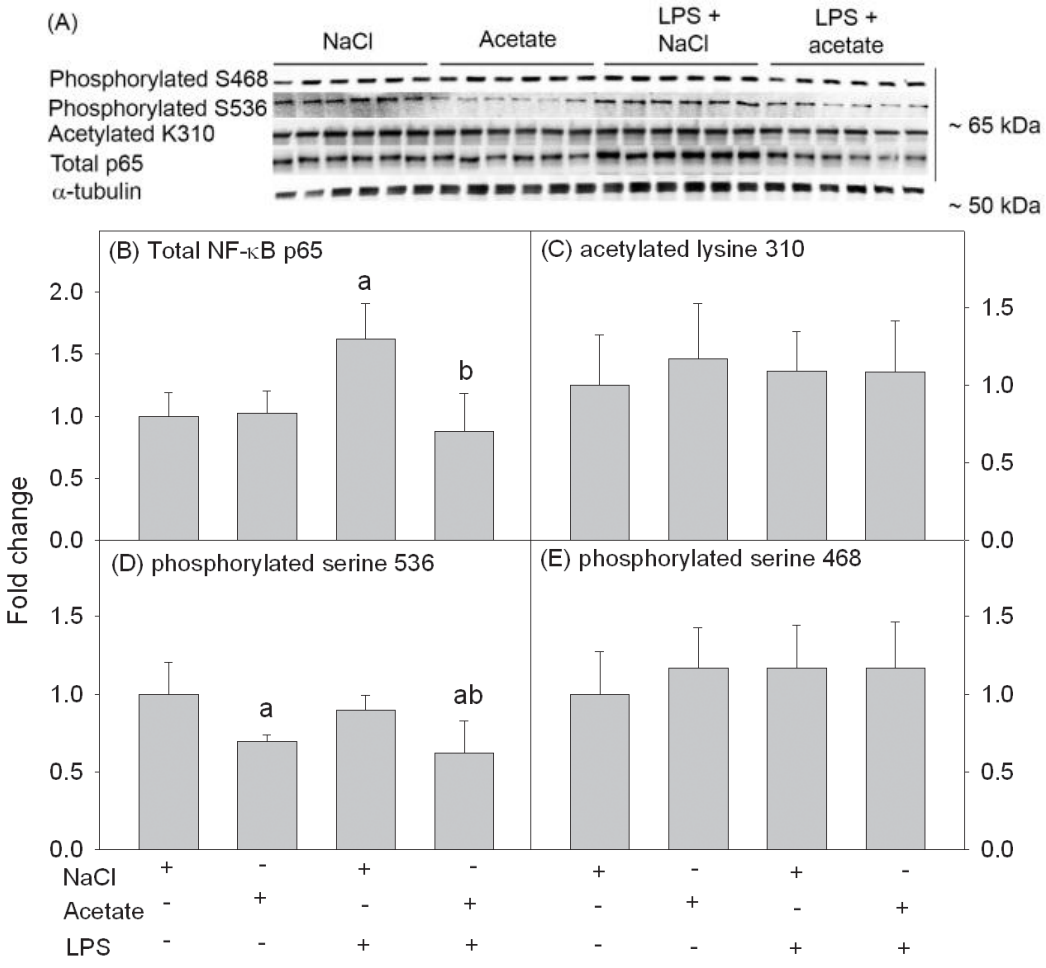

Figure 26. Acetate treatment and NF-κB p65 protein levels and modifications in LPS-stimulated primary astrocytes.

Changes in the protein level and phosphorylation and acetylation states of NF-κB p65 in primary mouse astrocyte cell culture stimulated for 4 hr with LPS 6.25 ng/ml and/or 12 mM sodium acetate, with 12 mM NaCl as control. Panel A shows representative images of the Western blots. Panel B shows the optical density of total NF-κB p65 normalized to the loading control α-tubulin. Panels C, D and E show the optical densities of acetylated p65 at lysine 310, phosphorylated p65 at S536, and phosphorylated p65 at serine 468, respectively (n = 6). The data represent the means ± SD where statistical significance (a = compared to NaCl and b = compared to LPS) was set at $p \leq 0.05$, as determined by One Way ANOVA followed by Tukey's post-hoc test.

Acetate Treatment and the Protein Levels of Phospholipases in LPS-stimulated Primary Astrocytes

To determine the effect of LPS and acetate treatment on the phosphorylation of $cPLA_2$ and the protein levels of total $cPLA_2$, $sPLA_2$ IIA and selected PLC isoforms in astrocytes, primary astrocyte cultures were treated with 6.25 ng/ml LPS in the presence and absence of 12 mM sodium acetate, and compared the results to cells treated with 12 mM NaCl as a control group. Whole cell lysates were used for Western blot analysis (Figure 28A). The protein levels of total $cPLA_2$ were not different between groups (Figure 28B), whereas LPS increased phosphorylated $cPLA_2$ by 2-fold which was reversed to control levels by acetate treatment (Figure 28C). Acetate treatment decreased the protein levels of $sPLA_2$ IIA and PLCβ1 by 20% only in the presence of LPS (Figure 28D and E). PLCγ1 and PLCδ1 protein levels were not altered by either LPS or acetate treatment (Figure 28F and G). These data suggest that acetate treatment

can alter $cPLA_2$ phosphorylation and the protein levels of enzymes involved in the eicosanoid signaling in primary astrocytes in a pattern different from BV-2 microglia.

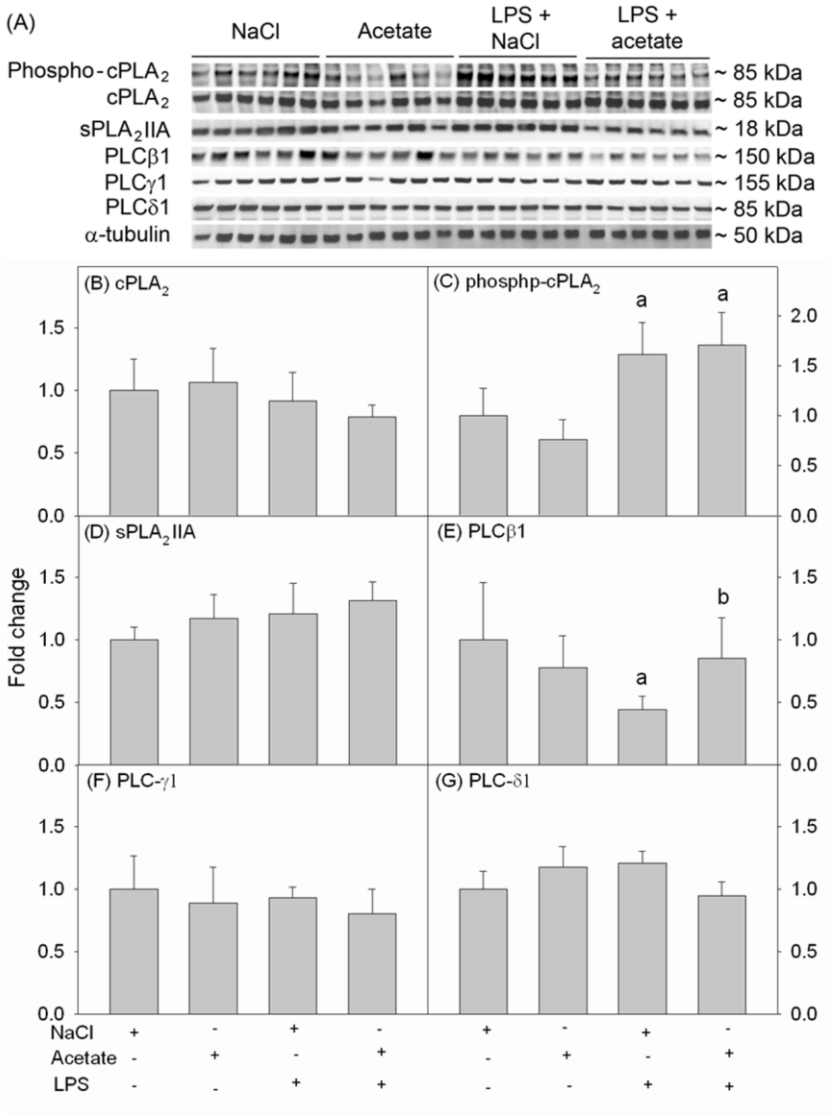

Figure 27. Acetate treatment and phospholipases phosphorylation and protein levels in LPS-stimulated BV-2 microglia.

Figure 27 shows the changes in the levels of $cPLA_2$ phosphorylation and total $cPLA_2$, $sPLA_2$ IIA, PLCβ1, PLCγ1 and PLCδ1 protein levels in BV-2 microglia

cultures stimulated for 4 hr with LPS 6.25 ng/ml and/or 12 mM sodium acetate, with 12 mM NaCl as control. Panel A shows representative images of the Western blots. Panels B, D, E, F and G show the optical densities total $cPLA_2$, $sPLA_2$ IIA, PLCβ1, PLCγ1 and PLCδ1 normalized to the loading control α-tubulin. Panel C shows the optical density of phosphorylated $cPLA_2$ normalized to total $cPLA_2$. Bars represent means $\pm$ SD where statistical significance (a = compared to NaCl, b = compared to LPS, n = 6 per group) was set at $p \leq 0.05$, as determined by One Way ANOVA followed by Tukey's post-hoc test.

Acetate Treatment and Cox-1 and 2 Levels in LPS-stimulated BV-2 Microglia and Primary Astrocytes Culture

To determine the effect of acetate treatment downstream of $cPLA_2$, the protein levels of Cox-1 and 2 were measured in both LPS-stimulated BV-2 microglia and primary astrocyte cell cultures. Using whole cell lysates for Western blot analysis, Cox-1 and 2 were detected as protein bands corresponding to the molecular weights of 70 and 72 kDa, respectively (Figure 29A). In BV-2 microglia cultures, LPS increased Cox-1 level by 1.5-fold which was completely reversed to control levels with acetate (Figure 29B), and Cox-2 by 4-fold which was only partially attenuated by acetate treatment (Figure 29C). In astrocyte cultures, LPS increased the protein levels of Cox-1 by 1.5-fold which was reversed to control levels with acetate treatment (Figure 29D) and Cox-2 by about 2.9-fold which was not altered by acetate treatment (Figure 29E). However, the basal levels of Cox-2 were reduced by 2-fold by acetate treatment only in the absence of LPS (Figure 29E). These data suggest that acetate treatment

differentially modulates the levels of Cox-1 and 2 in LPS-challenged BV-2 microglia and primary astrocytes cultures.

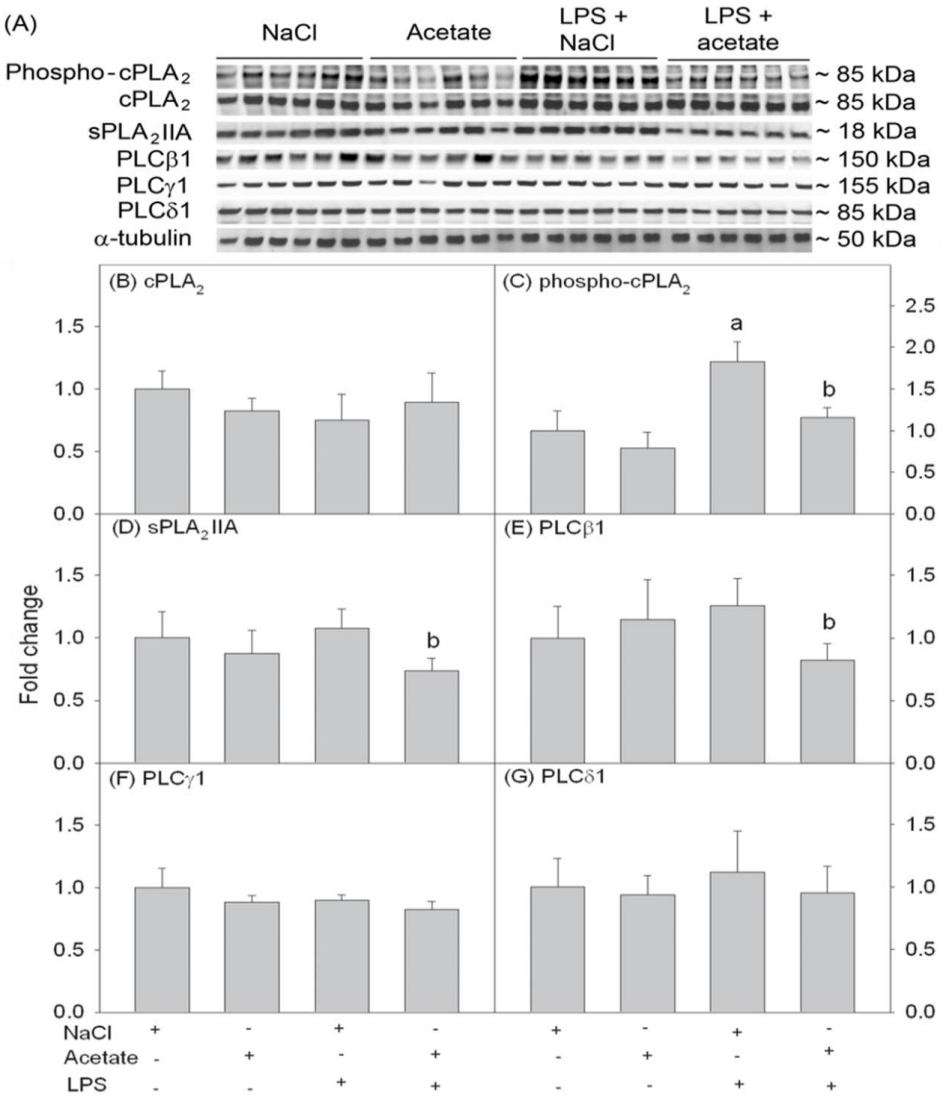

Figure 28. Acetate treatment and phospholipases phosphorylation and protein levels in LPS-stimulated primary astrocytes.

Figure 28 shows the changes in the levels of $cPLA_2$ phosphorylation and total $cPLA_2$, $sPLA_2$ IIA, PLCβ1, PLCγ1 and PLCδ1 protein levels in primary astrocyte cell cultures stimulated for 4 hr with LPS 6.25 ng/ml and/or 12 mM sodium acetate, with 12 mM NaCl as control. Panel A shows representative images of the Western blots. Panels B, D, E, F and G show the optical densities total $cPLA_2$, $sPLA_2$ IIA, PLCβ1, PLCγ1 and PLCδ1 normalized to the loading control α-tubulin. Panel C shows the optical density of phosphorylated $cPLA_2$ normalized to total $cPLA_2$. Bars represent means ± SD where statistical significance (a = compared to NaCl, b = compared to LPS, n = 6 per group) was set at $p \leq 0.05$, as determined by One Way ANOVA followed by Tukey's post-hoc test.

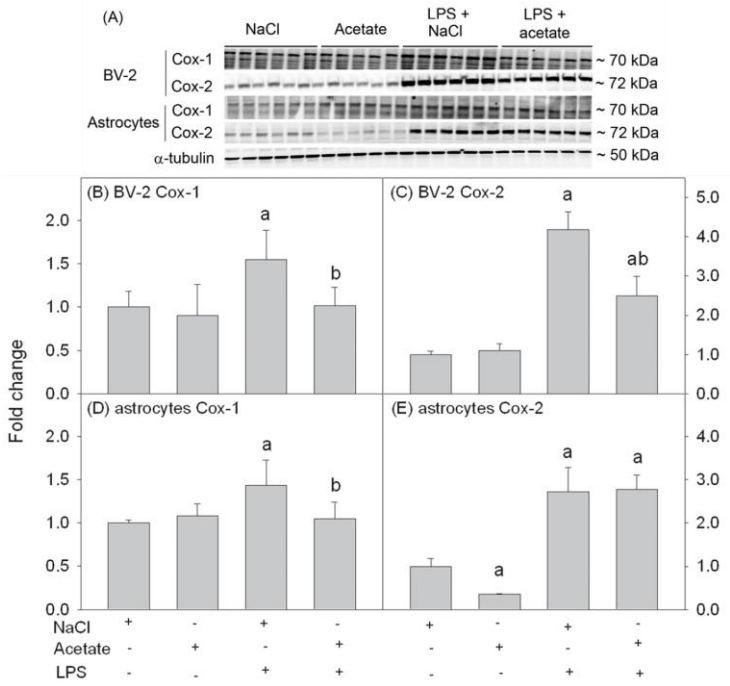

Figure 29. Acetate treatment and the protein levels of cyclooxygenases in LPS-stimulated BV-2 microglia and primary astrocytes.

Figure 29 shows the changes in the total Cox-1 and Cox-2 protein levels in BV-2 microglia and primary astrocyte cell cultures stimulated for 4 hr with LPS 6.25 ng/ml and/or 12 mM sodium acetate, with 12 mM NaCl as control. Panel A shows representative images of the Western blots. Panels B and C show the optical densities of Cox-1 and Cox 2, respectively normalized to the loading control α-tubulin in BV-2 microglial cell cultures. Panels D and E show the optical densities of Cox-1 and Cox 2, respectively normalized to the loading control α-tubulin in primary astrocyte cell cultures. Bars represent means $\pm$ SD where statistical significance (a = compared to NaCl, b = compared to LPS, n = 6 per group) was set at $p \leq 0.05$, as determined by One Way ANOVA followed by Tukey's post-hoc test.

Acetate Treatment and the Production of Prostaglandin E_2 in LPS-stimulated BV-2 Microglia and Primary Astrocyte Cultures

Having demonstrated the ability of acetate treatment to alter $cPLA_2$ phosphorylation and $sPLA_2$ IIA, Cox-1 and 2 protein levels, we proceeded to determine whether acetate treatment had functional effects in terms of PG release. The media from LPS-stimulated BV2-microglia and primary astrocyte cultures were used to quantify PGE_2 using enzyme immunoassay kit. PGE_2 levels were not altered by either LPS or acetate treatment in BV-2 microglia cultures (Figure 30A), whereas LPS increased PGE_2 levels by 4-fold in astrocyte cultures which was completely reversed to control levels with acetate treatment (Figure 30B). These data suggest that acetate treatment can differentially modulate PGE_2 release, which may contribute to the anti-inflammatory effect of acetate in LPS-stimulated astrocytes.

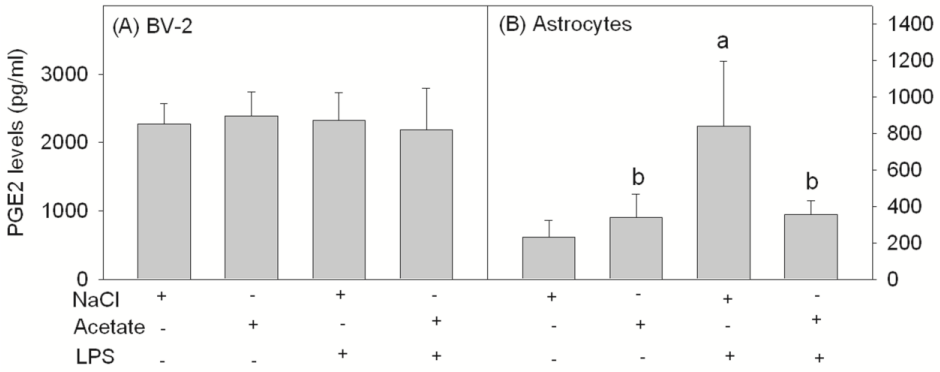

Figure 30. Acetate treatment and the release of prostaglandin E_2 in LPS-stimulated BV-2 microglia and primary astrocytes.

Figure 30 shows the changes in the levels of PGE_2 secreted in the media of BV-2 microglia (panel A) and primary astrocyte cell cultures (panel B) stimulated for 4 hr with LPS 6.25 ng/ml and/or 12 mM sodium acetate, with 12 mM NaCl as control. PGE_2 levels were measured using enzyme immunoassay. Bars represent means $\pm$ SD where statistical significance (a = compared to NaCl, b = compared to LPS, n = 6 per group) was set at $p \leq 0.05$, as determined by One Way ANOVA followed by Tukey's post-hoc test.

Acetate Treatment and the Enrichment of Acetylated H3K9 around the Transcription Start Sites of Inflammatory Genes in LPS-stimulated BV-2 Microglia Cell Cultures

Acetate treatment increases H3K9 acetylation *in vivo* (Soliman & Rosenberger 2011, Soliman et al. 2012b) and *in vitro* (Soliman et al. 2012a), reverses LPS-induced increase in NF-κB p65 protein but not IL-1β mRNA, and increases IL-4 mRNA (Soliman et al. 2012a). Because histone acetylation changes are associated with alterations in gene expression (Rice & Allis 2001, Strahl & Allis 2000), the enrichment of acetylated H3K9 around the promoters of *ptgs1*, *ptgs2* (coding for Cox-1 and Cox-2,

respectively), *p65*, *il4* and *il1b* genes was measured using chromatin immunoprecipitation. Five different primer sets were prepared for each of these genes, except *il1b* (4 primer sets) spanning different genomic stretches between -750 base pairs and +1000 base pairs (Table 1). Acetate treatment increased acetylated H3K9 as detected using primer sets # 2, 3 and 5 for *ptgs1* (Figure 31A) and primer set # 5 for *ptgs2* (Figure 31B). In addition, acetate treatment was found to increase acetylated H3K9 as detected using primer sets # 1, 2 and 4 for *p65* (Figure 31C), and primer sets # 2, 3 and 4 for *il1b* (Figure 31E) and did not alter acetylation H3K9 at *il4* (Figure 31D). LPS did not alter the levels of acetylated H3K9, except for a small reduction observed using primer set # 2 for *ptgs1* which was reversed to control levels with acetate treatment (Figure 31A). These data suggest that acetate treatment alters acetylated H3K9 at the promoters of genes involved in inflammatory signaling, which may potentially influence inflammatory gene expression.

During the preparation of these primer sets, we used the mouse genome browser of the University of California, Santa Cruz at http://genome.ucsc.edu/cgi-bin/hgGateway; the December 2011 assembly. To calculate the properties of the primers (length, melting temperature, and GC content), we used the online oligonucleotide properties calculator available at http://www.basic.northwestern.edu/biotools/oligocalc.html. The (-) and (+) signs mean upstream and downstream, respectively in reference to the transcription start site. For each gene, we designed 2 primer sets spanning genomic sequences upstream to the transcription start site (up to 750 base pairs), 2 primer sets spanning genomic sequences downstream to the

transcription start site (up to 1000 base pairs) and one primer set spanning the transcription start site.

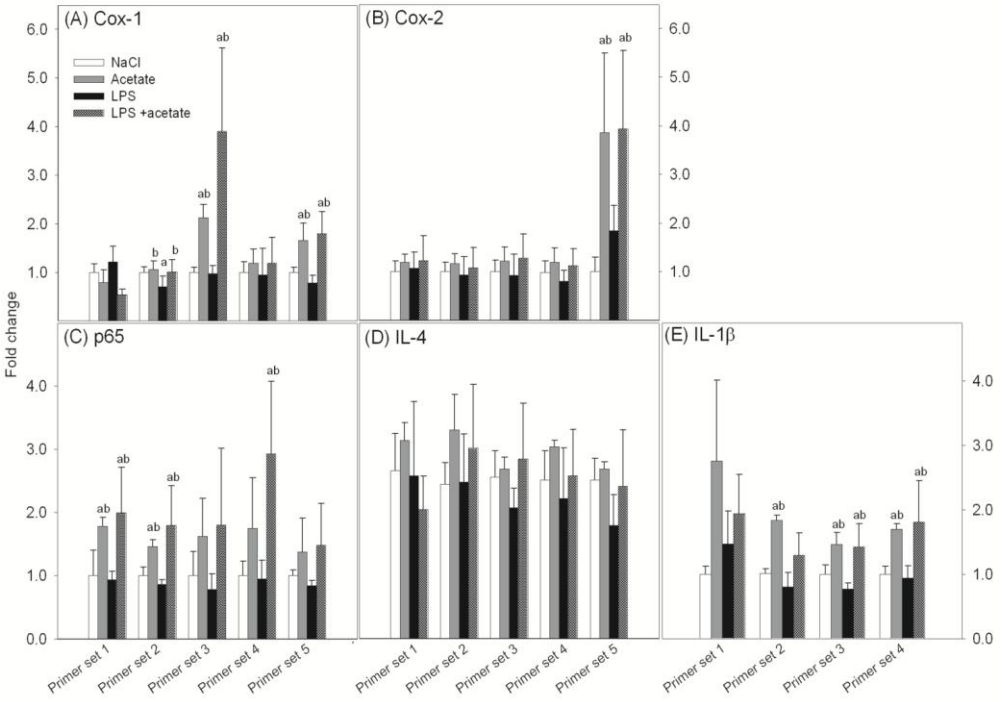

Figure 31: Acetate treatment and the enrichment of acetylated H3K9 around the transcription start sites of inflammatory genes in LPS-stimulated BV-2 microglia cultures.

Figure 31 shows the changes in the levels of enrichment of acetylated H3K9 at *ptgs1* (panel A), *ptgs2* (panel B), *p65* (panel C), *il4* (panel D), and *il1b* (panel E) genes measured by chromatin immunoprecipitation analysis followed by qrt-PCR, in BV-2 microglial cell cultures stimulated for 4 hr with LPS 6.25 ng/ml and/or 12 mM sodium acetate, with 12 mM NaCl as control. Bars represent means $\pm$ SD where statistical significance (a = compared to NaCl, b = compared to LPS, n = 3 per group) was set at $p \leq 0.05$, as determined by One Way ANOVA followed by Tukey's post-hoc test.

Table 1

Table Listing the Nucleotide Sequence of the Primers used in the Chromatin Immunoprecipitation Analysis

Gene	Primer Set		Sequence	Start	End	Length	Melting Temperature (° C)	Amplicon Size (bp)
ptgs1	Primer Set #1	Forward	CAA CTC CCC TCA CCT TTA ACT AT	-736	-714	23	60.9	288
		Reverse	CTT GCT GGT CCT CGG TGT AT	-468	-449	20	60.5	
	Primer Set #2	Forward	TCA TGT CTG ACC TGG CCT CT	-393	-374	20	60.5	257
		Reverse	TGG GAT ATA GCA AAC TGA GGC	-157	-137	21	59.5	
	Primer Set #3	Forward	GCA TTT CTG ACA CTG TAA AAA GAT C	-129	-105	25	60.9	261
		Reverse	GGG AGT GGA TGG ATG TGC AA	+112	+131	20	60.5	

Table 1 (continued)

Gene	Primer Set		Sequence	Start	End	Length	Melting Temperature (° C)	Amplicon Size (bp)
ptgs1	Primer Set #4	Forward	ACA CCC TCG GTC CTG CTC1	+296	+313	18	60.8	274
		Reverse	AGA ACC TGT CTC TGC TTC CC	+550	+569	20	60.5	
	Primer Set #5	Forward	TTG GGG AGG AAG CGG CAG	+668	+685	18	60.8	221
		Reverse	ACT TGG GGC TGT TAT CGC AC	+869	+888	20	60.1	
ptgs2	Primer Set #1	Forward	CTA TGT AAC AGC AGG GGG AAA AT	-720	-698	23	60.9	243
		Reverse	GCA CAC AGC TAC CGG TTA ATT T	-499	-478	22	60.1	
	Primer Set #2	Forward	TGA GCT TTT AGG CCC CCA CT	-373	-354	20	60.5	199
		Reverse	AGG CTT TTA CCC ACG CAA ATG A	-196	-175	22	60.1	

Table 1 (continued)

Gene	Primer Set		Sequence	Start	End	Length	Melting Temperature (° C)	Amplicon Size (bp)
Ptgs2	Primer Set #3	Forward	AAA GTT GGT GGG GGT TGG G	-131	-113	19	59.5	264
		Reverse	GCA GCG CAG AGC AGC AC	+116	+132	17	59.8	
	Primer Set #4	Forward	CTG CAA CCC ACT TTC AGG TTT	+265	+285	21	59.5	270
		Reverse	CGA CCT AGT GCA ATA GTC AAA ATT	+511	+534	24	60.3	
	Primer Set #5	Forward	TTA TCA TTG TAA AGT TGA CCC ATA GT	+750	+775	26	60.1	244
		Reverse	AGG AAG ATA CCC CAG GAA AAA CT	+971	+993	23	60.9	
P65	Primer Set #1	Forward	CAA CTC CCC TCA CCT TTA ACT AT	-743	-720	24	60.3	209
		Reverse	CTT GCT GGT CCT CGG TGT AT	-557	-535	23	60.9	

Table 1 (continued)

Gene	Primer Set		Sequence	Start	End	Length	Melting Temperature (° C)	Amplicon Size (bp)
P65	Primer Set #2	Forward	TCA TGT CTG ACC TGG CCT CT	-518	-499	20	60.5	201
		Reverse	TGG GAT ATA GCA AAC TGA GGC	-336	-318	19	61.6	
	Primer Set #3	Forward	GCA TTT CTG ACA CTG TAA AAA GAT C	-93	-71	23	60.9	186
		Reverse	GGG AGT GGA TGG ATG TGC AA	+75	+92	18	60.8	
	Primer Set #4	Forward	ACA CCC TCG GTC CTG CTC	+146	+163	18	60.8	148
		Reverse	AGA ACC TGT CTC TGC TTC CC	+272	+293	22	60.1	
	Primer Set #5	Forward	TTG GGG AGG AAG CGG CAG	+538	+555	18	60.8	255
		Reverse	ACT TGG GGC TGT TAT CGC AC	+773	+792	20	60.5	

Table 1 (continued)

Gene	Primer Set		Sequence	Start	End	Length	Melting Temperature (° C)	Amplicon Size (bp)
il1β	Primer Set #1	Forward	CAA CTC CCC TCA CCT TTA ACT AT	-749	-730	20	60.5	253
		Reverse	CTT GCT GGT CCT CGG TGT AT	-516	-496	20	60.5	
	Primer Set#2	Forward	TCA TGT CTG ACC TGG CCT CT	-450	-429	22	60.1	241
		Reverse	TGG GAT ATA GCA AAC TGA GGC	-229	-210	20	60.5	
	Primer Set #3	Forward	GCA TTT CTG ACA CTG TAA AAA GAT C	-125	-103	23	60.9	237
		Reverse	GGG AGT GGA TGG ATG TGC AA	+89	+111	23	60.9	
	Primer Set #4	Forward	TTG GGG AGG AAG CGG CAG	+550	+575	26	60.1	266
		Reverse	ACT TGG GGC TGT TAT CGC AC	+794	+815	22	60.1	

Table 1 (continued)

Gene	Primer Set		Sequence	Start	End	Length	Melting Temperature (° C)	Amplicon Size (bp)
il4	Primer Set #1	Forward	CAA CTC CCC TCA CCT TTA ACT AT	-748	-729	20	60.5	251
		Reverse	CTT GCT GGT CCT CGG TGT AT	-517	-498	20	60.5	
	Primer Set #2	Forward	TCA TGT CTG ACC TGG CCT CT	-449	-427	23	60.9	236
		Reverse	TGG GAT ATA GCA AAC TGA GGC	-239	-214	26	60.1	
	Primer Set #3	Forward	GCA TTT CTG ACA CTG TAA AAA GAT C	-113	-91	23	60.9	218
		Reverse	GGG AGT GGA TGG ATG TGC AA	+82	+104	23	60.9	
	Primer Set #4	Forward	ACA CCC TCG GTC CTG CTC	+151	+173	23	60.9	278
		Reverse	AGA ACC TGT CTC TGC TTC CC	+404	+428	25	60.9	

Table 1 (continued)

Gene	Primer Set		Sequence	Start	End	Length	Melting Temperature (° C)	Amplicon Size (bp)
il4	Primer Set #5	Forward	TTG GGG AGG AAG CGG CAG	+602	+624	23	60.9	134
		Reverse	ACT TGG GGC TGT TAT CGC AC	+713	+735	23	60.9	

Acetate Treatment Modulates the Expression of a Selected Subset of Inflammatory Genes

We addressed the question of whether acetate treatment alters global gene expression or the expression of selective inflammatory genes. Using qrt-PCR array, we quantified the effect of long-term acetate treatment on the expression of 84 genes that are involved in the innate and adaptive immune responses in rat brain. Only six genes out of a total of 84 showed more than 0.5-fold change from the control values. These 6 genes were *aodra2a*, *il1b*, *il1rn*, *mapk14*, *nfkb1* and *tnf* which code for adenosine A2a receptor, IL-1β, IL-1 receptor antagonist, MAPK p38, NF-κB 105 kDa protein subunit and TNF (Table 2). The change in only adenosine A2a receptor expression was statistically significant. These results support the findings that acetate treatment can alter the expression of genes involved in the inflammatory and immune responses and suggest that acetate treatment modulates gene expression in a selected subset of genes and does not induce global gene expression changes.

Table 2 shows the gene symbols, description and fold changes elicited by long-term acetate supplementation in the expression of 84 genes involved in the innate and adaptive immune responses in rat brain, (n = 2). The last five genes coding for a large ribosomal subunit protein P1, hypoxanthine phosphoribosyltransferase 1, ribosomal protein L13A, lactate dehydrogenase A, β-actin are controls. Data analysis was performed using SABiosciences online data analysis tool.

Table 2

Acetate Treatment and Expression of Genes involved Innate and Adaptive Immune Responses

#	Symbol	Description	Fold Change
1	Adora2a	Adenosine A2a receptor	8.66
2	C5	Complement component 5	1.14
3	C8a	Complement component 8, alpha polypeptide	1.14
4	Camp	Cathelicidin antimicrobial peptide	0.93
5	Casp1	Caspase 1	1.44
6	Casp4	Caspase 4, apoptosis-related cysteine peptidase	1.34
7	Cc12	Chemokine (C-C motif) ligand 2	1.90
8	Ccr3	Chemokine (C-C motif) receptor 3	1.14
9	Cd14	CD14 molecule	1.14
10	Cd1d1	CD1d1 molecule	1.14
11	Cd55	Cd55 molecule	1.34
12	Cfp	Complement factor properdin	1.26
13	Chuk	Conserved helix-loop-helix ubiquitous kinase	0.69
14	Clec7a	C-type lectin domain family 7, member a	1.14
15	Colec12	Collection sub-family member 12	0.57
16	Crjp	C-reactive protein, pentraxin-related	1.14

Table 2 (continued)

#	Symbol	Description	Fold Change
17	Cxcr4	Chemokine (C-X-C motif) receptor 4	1.14
18	Cybb	Cytochrome b-245, beta plypeptide	1.05
19	Defb4	Defensin beta 4	1.14
20	Dmbt1	Deleted in malignant brain tumors 1	1.14
21	Fn1	Fibronectin 1	0.61
22	Hmox1	Heme oxygenase (decycling) 1	1.23
23	Ifna1	Interferon-alpha 1	1.14
24	Ifnb1	Interferon beta 1, fibroblast	1.14
25	Ifngr1	Interferon gamma receptor 1	1.10
26	Ifngr2	Interferon gamma receptor 2	0.69
27	Ikbkb	Inhibitor of kappa light polypeptide gene enhancer in B-cells, kinase beta	0.83
28	I110	Interleukin 10	1.14
29	I112rb2	Interleukin 12 receptor, beta 2	0.68
30	I11a	Interleukin 1 alpha	1.04
31	I11b	Interleukin 1 beta	1.54
32	I11f10	Interleukin 1 family, member 10	1.14
33	I11f5	Interleukin 1 family, member 5 (delta)	1.14
34	I11f6	Interleukin 1 family, member 6	1.14

Table 2 (continued)

#	Symbol	Description	Fold Change
35	I11f8	Interleukin 1 family, member 8	1.14
36	I11fp	Interleukin 1 family, member 9	1.14
37	I11r1	Interleukin 1 receptor, type I	0.94
38	I11r2	Interleukin 1 receptor, type II	1.14
39	I11rap	Interleukin 1 receptor accessory protein	1.14
40	I11rap12	Interleukin 1 receptor accessory protein-like 2	0.75
41	I11r12	Interleukin 1 receptor-like 2	1.14
42	I11m	Interleukin 1 receptor antagonist	0.48
43	I16	Interleukin 6	1.14
44	Irak1	Interleukin-1 receptor-associated kinase 1	0.64
45	Irak2	Interleukin-1 receptor-associated kinase 2	1.14
46	Irf1	Interferon regulatory factor 1	0.91
47	Lalba	Lactalbumin, alpha	1.14
48	Lbp	Lipopolysaccharide binding protein	1.14
49	Lck	Lymphocyte-specific protein tyrosine kinase	1.14
50	Ly96	Lymphocyte antigen 96	0.97
51	Lyz2	Lysozyme 2	0.65
52	Mapk14	Mitogen activated protein kinase 14	2.36

Table 2 (continued)

#	Symbol	Description	Fold Change
53	Mapk8	Mitogen-activated protein kinase 8	0.60
54	Mif	Macrophage migration inhibitory factor	1.17
55	Myd88	Myeloid differentiation primary response gene 88	0.74
56	Ncf4	Neutrophil cytosolic factor 4	1.14
57	Nfkb1	Nuclear factor of kappa light polypeptide gene enhancer in B-cells 1	2.97
58	Nfkb2	Nuclear factor of kappa light polypeptide gene enhancer in B-cells 2, p49/p100	1.15
59	Nfkbia	Nuclear factor of kappa light polypeptide gene enhancer in B-cells inhibitor, alpha	0.93
60	Nirc4	NLR family, CARD domain containing 4	1.14
61	Nos2	Nitric oxide synthase 2, inducible	1.14
62	Pglyrp1	Peptidoglycan recognition protein 1	1.05
63	Pglyrp3	Peptidoglycan recognition protein 3	1.14
64	Ppbp	Pro-platelet basic protein (chemokine (C-X-C motif) ligand 7)	1.14
65	Prg2	Proteoglycan 2, bone marrow	0.85
66	Proc	Protein C	1.14
67	Ptafr	Platelet-activating factor receptor	1.10
68	Serpina 1	Serpin peptidase inhibitor, clade A (alpha-1 antiproteinase, antitrypsin), member 1	1.15

Table 2 (continued)

#	Symbol	Description	Fold Change
69	Serpina 1	Serpin peptidase inhibitor, clade E (nexin, plasminogen activator inhibitor type 1), member 1	1.14
70	Sftpd	Surfactant protein D	1.14
71	LOC100363145	Stabilin 1	1.14
72	Tgfb1	Transforming growth factor, beta 1	0.69
73	T1r1	Toll-like receptor 1	1.30
74	T1r10	Toll-like receptor 10	1.14
75	T1r2	Toll-like receptor 2	0.97
76	T1r3	Toll-like receptor 3	0.76
77	T1r4	Toll-like receptor 4	0.72
78	T1r6	Toll-like receptor 6	1.03
79	T1r9	Toll-like receptor 9	1.14
80	Tnf	Tumor necrosis factor (TNF superfamily, member 2)	2.59
81	Tnfrsf1a	Tumor necrosis factor receptor superfamily, member 1 a	1.14
82	Tollip	Toll interacting protein	1.05
83	Traf6	Tnf receptor-associated factor 6	0.64
84	Trem1	Triggering receptor expressed on myeloid cells 1	1.14
85	Rplp1	Ribosomal protein, large, P1	1.16

Table 2 (continued)

#	Symbol	Description	Fold Change
86	Hprt1	Hypoxanthine phosphoribosyltransferase 1	0.96
87	Rp113a	Ribosomal protein L13A	1.08
88	Ldha	Lactate dehydrogenase A	0.71
89	Actb	Actin, beta	0.97

CHAPTER IV

DISCUSSION

Preferential Uptake and Utilization of Acetate

Acetate has long been used as a substrate to study glial metabolism (Thoren *et al.* 2005, Wyss *et al.* 2011, Wyss *et al.* 2009), particularly because it is preferentially utilized by astrocytes (Waniewski & Martin 1998, Hosoi *et al.* 2009, Muir *et al.* 1986). Peripherally-derived acetate crosses the blood brain barrier by simple diffusion (Oldendorf 1973, Terasaki 1992). The rate-limiting step of acetate utilization is its activation by acetyl-CoA synthetase to form acetyl-CoA. The transport of acetate into the cell is through a carrier that has similar biochemical properties to monocarboxylate transporters (MCTs), a number of which were cloned, differ in organ distribution, and have different substrate and inhibitor affinities (Garcia *et al.* 1994b, Garcia *et al.* 1994a). Earlier reports demonstrated MCT1 is expressed in astrocytes while MCT2 is expressed in the neurons (Broer *et al.* 1997, Pierre *et al.* 2000), and later reports demonstrated the cell type-specific expression of MCTs 1, 2 and 4 in the brain based on age (Rafiki *et al.* 2003). The presence of different MCT isoforms in astrocytes than in neurons explains the differential utilization of acetate by astrocytes, particularly because acetyl-CoA synthetase is not expressed differently between cell types and even has greater activity in neurons than in astrocytes. Altogether, the ability of astrocytes to utilize acetate is well-established; however, the novelty of our studies stems from

investigating the mechanisms by which acetate treatment can be anti-inflammatory in glial cells. We tested the hypothesis that acetate alters histone acetylation and disrupts inflammatory signaling *in vivo* and *in vitro*, as an attempt to explain the anti-inflammatory effects of acetate we observed in a rat model of LPS-induced neuroinflammation (Reisenauer et al. 2011).

Metabolic Channels for Acetyl-CoA Utilization

Acetate supplementation using glyceryl triacetate increases brain levels of acetate 17-fold 1 hr after treatment with a dose of 5.8 g/kg (Mathew et al. 2005). Glyceryl triacetate-derived acetate is converted to metabolically active acetyl-CoA by 30 min following treatment and brain levels remain significantly elevated for up to 4 hr (Reisenauer et al. 2011). Acetyl-CoA has numerous roles in metabolism and biological processes in brain. For example, in oligodendrocyte cytosol, acetyl-CoA is the source of the units of two carbon atoms used for fatty acid elongation which parallels myelin deposition (Bourre *et al.* 1977). In addition, it can be used as a substrate for ketone bodies, fatty acids and cholesterol biosynthesis, and oxidation in Krebs cycle for energy generation after condensing with oxaloacetate to form citrate (Fukao et al. 2004, McGarry & Foster 1980, Deutsch et al. 2002, Des Rosiers et al. 1991). Acetyltransferases use acetyl-CoA as acetyl donor for post-translational acetylation reactions on lysine and arginine residues which can lead to structural and functional consequences in proteins.

At the onset of these studies, we proposed that a possible therapeutic mechanism of action by which acetate reduces neuroinflammatory phenotype is by

altering brain histone acetylation. To test this hypothesis, we examined the ability of a single oral dose of glyceryl triacetate (6 g/kg) to effectively alter brain histone acetylation state. These results suggest that acetate supplementation significantly increases the acetylation of brain histones H3K9, H4K8, and H4K16 while having no effect on the acetylation state of brain histones H3K14, H4K5, or H4K12. Moreover, acetate supplementation inhibited HDAC activity and decreased HDAC2 protein levels in brain without altering HAT activity. In order to begin to determine the mechanism by which acetate supplementation decreases HDAC activity, we examined the protein levels of several HDAC. Of the known HDAC, class I and II HDAC are known to be primarily involved in the regulation of histone acetylation. While we did not observe significant changes in HDAC1, 3, 4, 5 or 7, we found HDAC2 levels were significantly decreased at 4 hr post-treatment. The decrease in HDAC activity reported in this study coincides with the time points measured when HDAC2 protein levels were decreased and brain histone acetylation states were increased. The temporal relationship between increased histone acetylation and HDAC inhibition suggests that HDAC inhibition is a possible mechanism by which acetate supplementation can alter brain histone acetylation state.

The temporal and histone specific changes found in this study suggest that specific inhibition of HDAC2 may lead to preferential and possible therapeutically beneficial increases in the acetylation of specific histone lysine residues. This premise is supported by studies showing that HDAC maintain substrate specificity in terms of the particular histone lysine residues they deacetylate. For example, Rpd3p

preferentially deacetylates histones H4K5 and H4K12 and promotes hypoacetylation in yeast (Peterson 2002) and the diacetylation of histone H4 follows a specific non-random pattern at H4K16 and H4K8 (Clarke et al. 1993, Thorne *et al.* 1990, Turner *et al.* 1989). On the other hand, the acetylation of histone H4K5 and H4K12 is mainly restricted to the newly synthesized histone H4, and that acetylation of H4K8 and H4K16 inhibits the acetylation of H4K5 and H4K12 (Makowski *et al.* 2001). This data provides support for the premise that site-specific acetylation of histones can regulate the acetylation of other substrate sites and that elevated brain acetyl-CoA may result in specific HDAC inhibition.

Mechanisms of Action of HDAC Inhibitors

The HDAC inhibitors SAHA, MS 275, valproic acid, and TSA work on the catalytic site of the enzyme. These inhibitors function by; (a) chelating or displacing the zinc ions, (b) forming a hydrophobic spacer spanning the entire length of the HDAC enzyme hydrophobic active site, (c) acting as a hydrophobic cap preventing substrate binding and, (d) inducing ubiquitination and subsequent proteasomal degradation of the enzyme (Santini *et al.* 2007). Acetate supplementation has not been described previously as an inhibitor of HDAC activity; however, we demonstrate that acetylation caused by acetate supplementation may be a result of an inhibition of HDAC activity and expression independent of HAT activation. HDAC inhibition by acetate supplementation can, in addition, be explained by the fact that the increased tissue levels of acetyl-CoA exert endpoint inhibition of HDAC activity, thus hindering the removal of acetyl groups from the N-terminal tail of histone. Nevertheless, because

the regulatory mechanisms controlling histone acetylation and HDAC enzyme activity are numerous, the results demonstrated with a single oral dose of acetate cannot exclude the possibility of acetate altering other mechanisms such as acetylation of non-histone proteins, inducting other post-translational modifications of histones and transcriptional factors, or altering the activity of other HDAC.

Histone Acetylation Correlates with Anti-inflammatory and Neuroprotective Properties

Translational research and clinical trials are being executed to test the effectiveness of HDAC inhibitors as alternatives to non-steroidal anti-inflammatory drugs as well as being anti-neoplastic through inducing a hyperacetylation state. The association of histone hyperacetylation with anti-inflammatory effects is clearly demonstrated by a wide range of studies showing that a number of HDAC inhibitors ameliorate symptoms of Huntington's disease, spinal and bulbar muscular atrophy, Alzheimer's and Parkinson's diseases, amyotrophic lateral sclerosis, spinal muscular atrophy, and Friedreich's ataxia (Adcock 2007, Blanchard & Chipoy 2005, Langley *et al.* 2005, Morrison *et al.* 2007). The functional significance of site-specific histone acetylation remains unclear; however, the acetylation of certain lysine residues has been associated with beneficial biological outcomes. For example, an increase in acetylated H3K9 following valproic acid treatment, a class I HDAC inhibitor, protects neurons against hypoxia-induced neuronal apoptosis (Li *et al.* 2008). Similarly, increased acetylated H3K9 is associated with attenuating microglial activation in an animal model of traumatic brain injury (Zhang et al. 2008). The preferential hyperacetylation of brain H4K16 is recognized as a central switch in higher-order

chromatin structure (Shogren-Knaak et al. 2006). When arranged into nucleosomal arrays, acetylated H4K16 inhibits the formation of higher-order 30 nm chromatin fibers and therefore leads to activation of gene expression. Moreover, H4K16 acetylation is thought to play a unique role in DNA repair due to its being defective in aging and neurodegenerative disorders (Li et al. 2010). In this regard, both H4K16 and H4K8 acetylation were increased following a single oral dose of glyceryl triacetate as well as with long-term acetate supplementation. All of which support the premise that specific alterations in histone acetylation can be potentially therapeutic. These results suggest that a potential mechanism by which acetate supplementation may be effective at attenuating neuroinflammation is by altering higher-order chromatin structure and reducing pro-inflammatory gene expression. In support of this notion, H4K12 acetylation, which was not altered in our model, is implicated in gene silencing (Braunstein *et al.* 1996). The acetylation state at H4K16 is also an epigenetic hallmark for certain cancers, including leukemia, lymphoma, and colorectal adenocarcinoma cell lines, in which H4K16 hyperacetylation is lost (Fraga *et al.* 2005, Fraga & Esteller 2005).

Discrepancies between the Effects of a Single Dose of Acetate and Long-term Acetate Supplementation

Long-term acetate supplementation decreases neuroglia activation and cholinergic cell loss in a rat model of neuroinflammation (Reisenauer et al. 2011). A single oral dose increases histone acetylation, decreases HDAC activity, and decreases HDAC2 protein levels (Soliman & Rosenberger 2011). For these reasons and because histone hyperacetylation is associated with anti-inflammatory phenotypes (Adcock

2007) and can alter gene expression (Strahl & Allis 2000), we proposed that acetate supplementation reverses LPS-induced histone acetylation changes, and is associated with reduction of the pro-inflammatory gene expression. To begin to test this hypothesis we quantified the ability of long-term acetate supplementation to increase brain histone acetylation, to alter HAT and HDAC enzyme activities, and to decrease the expression of the pro-inflammatory cytokine IL-1β in a rat model of LPS-induced neuroinflammation. Unlike a single dose of glyceryl triacetate, long-term acetate supplementation increased HAT activity and had no effect on total brain HDAC activity, with variable effects on brain HDAC class I & II expression. In agreement with our hypothesis, neuroinflammation reduced the proportion of brain H3K9 acetylation by 50% and increased IL-1β protein and mRNA levels by 1.3- and 10- fold, respectively, all of which were effectively reversed with long-term acetate supplementation.

Evaluating the effect of neuroinflammation on brain histone acetylation in parallel with the drug effect found in the control and treated rats suggest that H3K9 acetylation and possibly HDAC7 activity may be directly involved in injury progression in this model. For example, as outlined in figure 8B, LPS-induced neuroinflammation resulted in a direct reduction in H3K9 acetylation that was reversed with acetate supplementation. This finding is corroborated by other reports showing that the use of a HDAC inhibitor DMA-PB decreases microglial activation in a rat model of traumatic brain injury, and that this anti-inflammatory effect is associated with increased histone H3 acetylation (Zhang et al. 2008). Further, the proportion of

acetylated H3K9 is significantly lower in livers of aged rats, suggesting that the acetylation of H3K9 may be required to maintain essential cellular functions (Kawakami *et al.* 2009). Similarly, we found that the expression of HDAC7 was increased in rats subjected to LPS-induced neuroinflammation that was again reversed with long-term acetate supplementation. This suggests that mechanisms are in place that may account for injury- and treatment-specific changes in histone acetylation. In contrast, the acetylation state of H3K14 was not altered by acetate supplementation or LPS-induced neuroinflammation suggesting that H3K14 acetylation was not related to treatment or neuroinflammation.

Another discrepancy between the effects of a single oral dose of acetate versus long-term acetate supplementation is that a single treatment decreases brain HDAC activity, whereas long-term supplementation had no effect on total brain HDAC activity, despite multiple alterations in the expression of individual HDAC. This can be explained by the fact that HDAC assays performed in this study measured overall HDAC activity and were reflective of the sum of all the individual HDAC. Given the differences in HDAC expression (i.e. increased brain HDAC1, 2 & 7 and decreased brain HDAC3), we believe that the histone acetylation pattern found in this study is a reflection of the substrate specificity of the specific HDAC expressed following treatment despite no overall change in total brain HDAC activity. We speculate that the increased expression of HDAC1 and HDAC2 is a physiological response to long-term acetate supplementation and an increase in brain acetyl-CoA levels. Further, HDAC activity does not depend solely on the expression of HDAC, but rather work in

concert with co-regulatory repressive complexes to modify catalytic activity (de Ruijter et al. 2003). For example, cloned HDAC and purified HDAC do not have deacetylating activity *in vitro* due to the lack of other protein complexes found *in vivo* (Saha & Pahan 2006). Therefore, HDAC activity is not expected to increase unless the increase in HDAC expression is paralleled by an increase in the expression of co-regulatory complexes. Moreover, we do not exclude the possibility that other post-transcriptional or post-translational modifications of the expressed HDAC that render them less active, resulting in no overall change in total brain HDAC activity.

Pyruvate: Another Anti-inflammatory Metabolite

Another metabolite that has anti-inflammatory and neuroprotective properties is pyruvate. The supplementation of pyruvate, or its aliphatic ester ethyl pyruvate, decreases LPS and hydrogen peroxide-induced microglial activation and promotes neuronal survival (Kim *et al.* 2005). In addition, the administration of pyruvate provides protection against hippocampal neuronal injury following transient cerebral ischemia in rats (Lee *et al.* 2001). Pyruvate also boosts extracellular brain glucose levels and decreases contusion volume and neuronal death in a rat model of traumatic brain injury (Fukushima *et al.* 2009). Because acetate-derived acetyl-CoA can inhibit pyruvate dehydrogenase and lead to the accumulation of brain pyruvate, it is not unreasonable to suggest that the anti-inflammatory and neuroprotective effect of acetate may occur at least in part due to the accumulation of pyruvate. It will be interesting to test whether pyruvate, like acetate, can increase brain acetyl-CoA levels and alter histone acetylation and pro-inflammatory gene expression. To examine whether

acetate works through a mitochondrial process, we measured the effect of acetate on mitochondrial biogenesis but found no alteration in neuronal mitochondrial numbers following 28 days of acetate supplementation. This, however, does not exclude the possibility that acetate alters other mitochondrial processes such as tricarboxylic acid cycle, the energy state, or mitochondrial gene expression. In summary, long-term acetate supplementation reduced IL-1β expression *in vivo* by a mechanism that may involve a distinct site-specific pattern of histone acetylation and/or HDAC expression in brain. LPS-induced changes in H3K9 acetylation, the expression of HDAC7, and the pro-inflammatory cytokine IL-1β are potentially key mechanistic targets of acetate supplementation. Thus physical epigenetic changes and/or direct changes in protein acetylation may help to explain the functional consequences of acetate supplementation found in this rat model of neuroinflammation.

The data generated in the *in vitro* system were informative and inclusive as they comprised more pro-inflammatory cytokines as well as anti-inflammatory cytokines that could not be measured reliably *in vivo* because of the dilution of these molecules in whole brain homogenates. We demonstrated that acetate treatment reverses the LPS-induced reduction in H3K9 acetylation and decreases pro-inflammatory cytokines in microglia *in vitro*. Moreover, acetate treatment increased the transcription of the anti-inflammatory cytokines TGF-β1 and IL-4, suggesting that acetate-induced histone modulation may influence more strongly the expression of anti-inflammatory cytokines in this model considering histone hyperacetylation is conventionally linked to increased gene expression. We also demonstrated the time-dependent effects of LPS and acetate

treatment on MAPK activation. In addition, acetate treatment reduced LPS-induced increases in total NF-κB p65 protein level, serine 468 phosphorylation, and increased its acetylation at lysine 310. These data suggest that acetate metabolism can modulate cytokine balance in microglia toward a more anti-inflammatory state which correlates to increases in both histone and non-histone protein acetylation.

Possible Mechanisms by which Acetate may Interfere with Translation

The differential effect of acetate treatment on mRNA and protein levels suggests that the reduction in pro-inflammatory cytokines may be due to a disruption in mRNA translation rather than gene transcription or pro-inflammatory cytokine turnover. Translation involves the interaction of mRNA with various subsets of proteins which, we speculate, may be regulated by acetylation. For example, nuclear mRNA binds to nuclear proteins that transport mRNA to the cytosol. Some of these proteins repress translation by interfering with the binding of mRNA to ribosomal subunits (Wells 2006). Similarly, the integrity of mRNA is modulated by mRNA stabilizing proteins (Kohn *et al.* 1996). It is possible that acetylation may alter the expression and/or activity of mRNA-binding and/or stabilizing proteins. Of particular interest is cytosolic polyadenylation element-binding protein (CPEB) expressed both in neuroglia and neurons which prevents the formation of the translation initiation complex and represses translation (Theis *et al.* 2003, Mendez & Richter 2001). CPEB is regulated by phosphorylation (Atkins *et al.* 2004) however the effect that acetylation has on its activity remains unknown. Further, the eukaryotic initiation factor 5A (eIF5A), which regulates initiation and elongation, contains a polyamine-lysine

conjugated amino acid "hypusine" that is essential to its activity (Zanelli *et al.* 2006, Gregio *et al.* 2009, Saini *et al.* 2009) and is inactivated following acetylation by spermidine/spermine acetyltransferase 1 (Lee *et al.* 2011). In addition, acetylation by a histone acetyltransferase PCAF leads to eIF5A accumulation in the nucleus that prevents translocation to the cytosol and in turn disrupts translation (Ishfaq *et al.* 2012). All of which suggests that acetylation may be involved in the regulation of mRNA translation. Acetate treatment may also reduce pro-inflammatory cytokine levels but not mRNA by increasing protein turnover. A number of histone acetyltransferases possess intrinsic ubiquitin-conjugating activity and are associated with ubiquitin transferases in multiprotein complexes that stimulate degradation (Sadoul et al. 2008). Further, acetylation of the translation elongation factor (E2F1) (Galbiati *et al.* 2005) and the hypoxia-inducible factor 1α (HIF-1) at lysine 532 enhances their ubiquitination and degradation (Jeong *et al.* 2002). Thus, it is plausible that non-histone protein acetylation may alter mRNA translation and the turnover of pro-inflammatory cytokines in activated microglia. These speculations may potentially explain why acetate treatment reduces the levels of pro-inflammatory cytokine protein and not mRNA.

The Dynamic Balance between Pro- and Anti-inflammatory Cytokines

An increase in pro-inflammatory cytokine production is generally considered deleterious based on their involvement in a wide number of neurological and non-neurological disorders. IL-1β, among other cytokines, is expressed in brain at low levels under physiological conditions and contributes to the control of metabolism

(Grossberg *et al.* 2011), temperature regulation (Huang *et al.* 2010b), synaptic plasticity and neuronal transmission (Vitkovic *et al.* 2000). However, IL-1β is produced in high levels in many pathological conditions that include ischemic stroke (Legos *et al.* 2000), Alzheimer's disease (Griffin *et al.* 1989, Shaftel et al. 2008), Down syndrome (Griffin et al. 1989), multiple sclerosis (McGuinness *et al.* 1997), Parkinson's disease (Parish *et al.* 2002), epilepsy (Pernot *et al.* 2011), amyotrophic lateral sclerosis (Meissner *et al.* 2010), and HIV-associated dementia (Zhao *et al.* 2001). Co-cultures of primary rat cortical neurons with LPS-activated microglia results in neuronal death which can be largely blocked using the naturally occurring IL-1 receptor antagonist IL-1ra (Li *et al.* 2003). Not surprisingly, suppression of pro-inflammatory cytokines is associated with improved behavioral and cognitive endpoints in animal models of neurodegenerative diseases (Hu *et al.* 2007, Lloyd *et al.* 2008). All of which suggests that IL-1β has an important role in the progression of neuroinflammation (Basu *et al.* 2004). Upon injury, activated microglia produce inflammatory mediators which lead to activation and proliferation of astrocytes. Likewise, activated astrocytes release inflammatory mediators, leading to further inter-glial communication, that if left unchecked results in neuronal bystander lysis (Streit et al. 1999). IL-1β is a major signaling molecule and is involved in both neuronal-glial and inter-glial interactions which can increase microglial proliferation in mixed glial cultures, but not in isolated microglia cultures (Ganter *et al.* 1992), bolstering the notion that microglial activation is at least in part dependent on interactions with neighboring astrocytes (Kim *et al.*). Therefore, disruption of the IL-1β system using anti-IL-1β antibodies, receptor blockade, or

interfering with activation by enzymatic cleavage ameliorates neuroinflammation and delays neurodegeneration (Labow *et al.* 1997).

In a mouse model of septic shock, the histone deacetylase inhibitor SAHA increases H3K9 acetylation and inhibits TNF-α and IL-1β gene expression in lung tissue (Li *et al.* 2009). This supports the premise that the reduction in the proportion of H3K9 is indeed associated with the LPS-induced neuroinflammation, and that increased H3K9 acetylation can be linked to reducing the pro-inflammatory cytokines expression. However, pro-inflammatory cytokine expression in microglia is controlled directly by p38α MAPK downstream of the toll-like receptor 4 complex and is modulated by inhibitors selective for this kinase (Bachstetter *et al.*). Further, p38α MAPK is associated with other regulatory kinases that are potentially modified post-translationally by acetylation reactions. For example, HDAC inhibition increases the acetylation of MAPK- phosphatase 1 that promotes complex formation between MAPK phosphatase-1 and p38α MAPK. This results in a reduction in phosphorylated p38α MAPK and a reduction in cytokine formation (Cao et al. 2008). Mechanistically, it is not known whether the net anti-inflammatory effect of HDAC inhibition is the result of alterations in pro-inflammatory gene expression or a direct result of modulating the acetylation state of accessory proteins involved in toll-like receptor signaling. Therefore, it is not clear at this point as to whether the treatment effect found *in vivo* on IL-1β expression, on IL-6 *in vitro* in LPS-stimulated microglia, and on TNF-α in LPS-stimulated astrocytes is a direct result of decreasing p38α MAPK phosphorylation or an indirect effect by modulating gene expression.

On the other hand, IL-4, IL-10, and TGF-β1 share features of anti-inflammatory and neuroprotective actions that can be attributed to downregulating glial production of pro-inflammatory cytokines and/or attenuating their secondary release. IL-4 reduces the production of inflammatory mediators, including inducible nitric oxide (NO) synthase, TNF-α, IL-1β, cyclooxygenase 2, and macrophage chemoattractant protein-1 by activated microglia *in vivo* and *in vitro* (Ledeboer et al. 2000, Furlan *et al.* 2000). In addition, TGF-β has a neuroprotective effect by regulating Bad (pro-apoptotic) and Bcl-2 and Bcl-x1 (anti-apoptotic) proteins (Dhandapani & Brann 2003). Further, anti-inflammatory cytokines reduce the expression levels of the pro-inflammatory cytokines in LPS-stimulated microglial-astroglial co-cultures (Ledeboer et al. 2000). Endogenous and exogenous TGF-β1 and β2 suppress the production of NO but not IL-1β, IL-6 or TNF-α and exogenous IL-4 downregulates NO, IL-6 and TNF-α, but not IL-1β (Ledeboer et al. 2000). Our findings showing that LPS stimulation upregulated IL-10 is not counterintuitive, because stimulation of an inflammatory response can lead to upregulation of both conventional pro-inflammatory and anti-inflammatory mediators as a biological self-checking mechanism. In this regard, IL-10 inhibits the LPS-induced increase of IL-1β and TNF-α (Sawada *et al.* 1999) and IL-10 release by LPS-stimulated microglia increases simultaneously with TNF-α (Seo *et al.* 2004). The multiplicity of receptors, signaling cascades, cellular and subcellular targets, and various experimental designs all demonstrate the complexity of how anti-inflammatory cytokines can regulate the transcription and/or translation of the pro-inflammatory cytokines.

A dynamic balance exists between the pro- and anti-inflammatory cytokines, both of which are generated upon exposure to injury or infection. The duration and net effect of interactions between these opposing molecular groups determines the outcome of the immune response. Pathologies arise from shifting this dynamic balance in one direction or the other. For example, excessive pro-inflammatory cytokines are linked to neuroinflammation and degeneration as mentioned earlier, while excessive anti-inflammatory cytokines are conversely associated with susceptibility to systemic infections (Kasai *et al.* 1997, Munoz *et al.* 1991).

Non-histone Targets of Acetylation

Lysine acetylation is a common post-translational modification that occurs on both histones as well as non-histone proteins. Histone acetylation is conventionally linked to alteration of gene expression. Non-histone targets of acetylation include cytoskeletal proteins and transcription and nuclear import factors. Acetylation of these targets have many functional consequences including altering subcellular localization, DNA-binding, transcriptional activity, protein-protein interaction and protein stability (Sadoul et al. 2008, Glozak et al. 2005). Acetyltransferases use acetyl-CoA as acetyl donor for post-translational acetylation reactions on lysine and arginine residues which can lead to structural and functional consequences in proteins. The functional consequences of acetylation depend on where exactly within the protein acetylation takes place. For example, NF-κB p65 acetylation at lysines 218, 221 and 310 increases nuclear localization, while acetylation at 122 and 123 reduces the binding affinity of p65 to DNA which promotes IκB-p65 interaction and nuclear export (Chen et al. 2002,

Huang et al. 2010a). These examples give an idea on the intricacy of reactions and functional consequences based of acetylation. We have demonstrated that, in LPS-stimulated primary astrocyte cell cultures, acetate treatment decreases the basal levels of NF-κB p65 phosphorylation at serine 536 while not altering p65 phosphorylation at serine 468 or acetylation at lysine 310. In this regard, phosphorylation of serine 536 lowers the affinity of p65 to IκBα leading to NF- κB translocation into the nucleus and enhanced activity (Buss *et al.* 2004, Bohuslav *et al.* 2004). Therefore, acetate treatment-mediated reduction in p65 phosphorylation at 536 may be responsible in part for the anti-inflammatory effect of acetate supplementation on LPS-activated astrocytes we observed *in vivo* (Reisenauer et al. 2011). Because p65 phosphorylation at serine 536 stimulates subsequent acetylation at lysine 310 (Hoberg *et al.* 2006, Chen *et al.* 2005b), this could explain why acetate does not increase acetylation at lysine 310 in astrocytes, unlike in microglia. Regardless, since post-translational modifications of NF-κB have diverse functional consequences (Huang et al. 2010a), further experiments need to be performed to determine the effect of acetate treatment on the different functional aspects of NF-κB in both LPS-stimulated microglia and astrocyte cultures.

MAPK signaling -another example of non-histone targets of acetylation- is inducible by pro-inflammatory cytokines and also regulates their transcription and translation. For example, MAPK signaling regulates the production of IL-8 in response to IL-1 and osmotic shock (Shapiro & Dinarello 1995), and regulates the production of IL-6 in response to TNF-α (Beyaert *et al.* 1996). Furthermore, interferon-β reduces traumatic spinal cord injury-induced ERK hyperphosphorylation and is associated with

functional recovery (Ito *et al.* 2009). Inhibition of MAPK p38 and ERK reduces edema and the inflammatory mediator matrix metalloproteinase-9 after brain trauma (Mori *et al.* 2002), the infarct size (Sugino *et al.* 2000), iNOS, TNF-α, and cyclooxygenase-2 expression (Piao *et al.* 2003) in ischemia, and the neurological deficits after transient (Legos *et al.* 2001) and permanent (Barone *et al.* 2001) ischemia. Animals with genetic deletion of one of the MAPK accessory proteins show diminished IL-6 and TNF-α production in response to LPS stimulation (Kotlyarov *et al.* 1999).

Earlier studies demonstrated that a MAPK phosphatase is activated by certain lysine acetylation which leads to inactivation of MAPK signaling pathway, providing an important link between acetylation and phosphorylation in the regulation of neuroinflammation (Cao et al. 2008). Because MAPK signaling can be altered by acetylation, we studied whether acetate treatment alters MAPK phosphorylation (activation) in LPS-stimulated BV-2 microglia and primary astrocyte cell cultures. We have showed that acetate reduces LPS-induced MAPK p38 phosphorylation and basal level phosphorylation of ERK1/2 in astrocytes which may be attributable to acetylation of MAPK phosphatase-1. In BV-2 microglia, the effect of LPS on MAPK phosphorylation in BV-2 microglia was time-dependent, as was the ability of acetate treatment to reduce LPS-induced p38 and JNK phosphorylation. LPS increased phosphorylated p38 at 4 hr and phosphorylated JNK at 2 and 4 hr, whereas acetate treatment reduced phosphorylated p38 and JNK only at 2, but not 4, hr. We did not observe an increase in MAPK activation at 0.5 or 1 hr unlike other studies (Schumann et al. 1996, Kraatz et al. 1998). However, this may be due to our using a lower

concentration of LPS or may demonstrate a cell-type specific response. These data are important in the light of the role that MAPK signaling has in neuropathologies. While the therapeutic effect of acetate supplementation is demonstrated in the *in vivo* studies (Reisenauer et al. 2011), these present results further strengthen our understanding of the possible therapeutic mechanism(s) involved in modulating cytokine expression by increasing acetate metabolism. Therefore, because the effect of acetate treatment on the LPS-induced MAPK p38 phosphorylation in BV-2 microglia is transient, the effect of acetate treatment on cytokine release may be due to the synergistic effect of other possible mechanisms.

NF-κB -another example of non-histone targets of acetylation- is acetylated on p65 subunit which modulates nuclear translocation, DNA binding, and transcriptional activity (Chen et al. 2001, Chen et al. 2002, Huang et al. 2010a). Our studies showed that acetate treatment induced p65 hyperacetylation at lysine 310 in LPS-stimulated BV-2 microglia. This is of interest because p65 interacts with HDAC1, 2 and 3, but only HDAC3 deacetylates p65 (Kiernan et al. 2003, Chen et al. 2001) which is downregulated with long-term acetate supplementation (Figure 11). Therefore, the effect that acetate metabolism has on HDAC3 expression may help to explain the hyperacetylation of p65 at lysine 310 observed in this study. The acetylation of p65 may be associated with anti-inflammatory outcomes as it represses transcriptional activity, reduces binding to κB-DNA, and facilitates its interaction with IκB that increases p65 export to the cytoplasm. Because acetylated p65 accumulates in the cytoplasm suggests that post-activation turn-off of NF-κB-dependent transcription is

regulated, at least in part, by acetylation (Kiernan et al. 2003). However, β-amyloid toxicity increases hyperacetylated p65 at lysine 310 in microglia, which is reversed by sirtuin 1 over-expression and stimulation (Chen *et al.* 2005a). This suggests that changes in the activity and expression of the of the sirtuins and class I HDAC can differentially modulate NF-κB-mediated inflammatory phenotype, possibly as a result of differing inflammatory stimulation or differing intercellular regulation points. Alternately, acetate treatment-induced p65 hyperacetylation in the presence of LPS may be linked to pro-inflammatory signaling that is generally outweighed by the other anti-inflammatory mechanisms. Regardless, the functional consequences of post-translational modification of p65 are diverse and specific to the modification and the residue involved (Huang et al. 2010a). Future studies are necessary to determine the impact that acetylation of p65 has on NF-κB functionality in this model.

Acetate-mediated Global and Gene-specific Epigenetic and Expression Modulation

Whereas acetate treatment alters histone acetylation at histones H3K9, H4K8 and H4K16 after a single oral dose and long-term supplementation, LPS alters only acetylated H3K9 in our *in vivo* experimental paradigm where it reduces acetylated H3K9 by 2-fold and acetate treatment reverses it to a hyperacetylation state (Soliman et al. 2012b). Because of this as well as other reports implicating H3K9 in neuroinflammation and neuroglial activation (Govindarajan *et al.* 2011, Silva *et al.* 2012, Zhang et al. 2008), we chose to focus on this epigenetic marker for our later *in vitro* experiments. In LPS-stimulated microglia, acetate treatment also reverses LPS-induced H3K9 hypoacetylation similar to that found *in vivo* (Soliman et al. 2012a). In

contrast, in LPS-stimulated astrocytes, acetate treatment increases H3K9 acetylation in the presence and absence of LPS, but LPS itself does not alter acetylated H3K9. For this reason, we decided to carry out our chromatin immunoprecipitation analysis with BV-2 microglia cultures, where LPS is altered by both LPS and acetate treatment.

Acetate treatment reverses LPS-induced increases in Cox-1, Cox-2 and NF-κB p65 protein levels, IL-1β protein and not mRNA, and increases IL-4 mRNA. In an attempt to determine whether acetate treatment-induced global H3K9 hyperacetylation is involved in the regulation of these inflammatory mediators at the gene levels, we measured H3K9 acetylation at the promoters of these genes of interest using chromatin immunoprecipitation. The enrichment levels of acetylated H3K9 were increased around the promoter regions for the genes coding for Cox-1 and 2, IL-1β and NF-κB p65, but not IL-4, all of which were largely unaffected by LPS. This suggests that acetate-induced H3K9 acetylation may potentially contribute to the effect of treatment on the expression of these specific genes. Alternatively, the effect of acetate treatment on gene expression can possibly be linked to acetylation of non-histone transcription factors as discussed earlier, or other acetate treatment-mediated histone acetylation changes such as H4K8 or H4K16. These results warrant more experiments to evaluate the involvement of other histone markers in the acetate-treatment mediated gene expression changes.

Since histone acetylation is conventionally associated with enhanced gene expression (Strahl & Allis 2000), we speculate that the increases in H3K9 acetylation may be instrumental in upregulating the transcription of anti-inflammatory cytokines,

as found in our studies. Interestingly, LPS did not alter H3K9 acetylation in astrocytes unlike our other results showing that LPS infusion over 28 days decreases H3K9 acetylation by 50% in whole brains from a rat model of neuroinflammation (Soliman et al. 2012b) and in LPS-stimulated primary and BV-2 microglia. This can potentially be attributed to the different overall acetate concentrations (and thus acetate-derived acetyl-CoA) *in vivo* and *in vitro*, or the *in vivo* results representing the combined effects in all cell types in the brain. Our data also demonstrate a correlation between acetate treatment-induced inhibition of pro-inflammatory cytokine release and hyperacetylation of H3K9 and p65 at lysine 310.

H3K9 can also be modified by methylation where methylated H3K9 is associated with gene repression, contrary to acetylated H3K9 that is associated with active gene expression (Rice & Allis 2001). In this regard, the enrichment of methylated H3K9 at the promoter region of opioid receptors is linked to a decrease in opioid receptor transcription in mice fed a high fat diet (Vucetic *et al.* 2011). Similarly, genome-wide mapping demonstrates that an increase H3K9 acetylation corresponds with areas of transcription activity (Shin *et al.* 2012). H3 methylation is more predominant in areas of enriched acetylated H4, unlike methylated H4 which is more evident in less acetylated chromatin regions (Annunziato et al. 1995). The functional outcome of this interplay regarding gene expression control and the individual genes involved is not clearly known, but sheds the light on the intricacy of the post-translational modifications of histones. It is also possible that H3K9 hyperacetylation may alter the expression and/or activity of effector proteins involved in translation,

which may help to explain the decrease in pro-inflammatory cytokines in the absence of a reduction in their mRNA levels.

To address non-specific effects of acetate on gene expression, we performed an rt-PCR array to determine the simultaneous changes in 84 genes involved in both the innate and adaptive immune responses. The expression of only six genes was altered by more than 0.5-fold. Only four genes did show more than a 2–fold change; adenosine receptor A2a, MAPK p38, TNF-α, and IL-1 receptor antagonist suggesting that acetate supplementation can influence the expression of genes involved in adaptive and innate immune responses. None of these changes were statistically significant, with the exception of adenosine A2a mRNA which was increased by 8 fold. The importance of this experiment is that it shows that acetate treatment alters the expression of selected genes and does not induce global gene expression changes.

Astrocytes Involvement in the Inter-glial Communication in Neuroinflammation

Astrocytes possess a number of physiological functions including regulation of blood flow, fluid, ion and transmitter homeostasis, modulation of synaptic functions, and supporting the blood brain barrier (Sofroniew & Vinters 2010). The immune functions of the astrocytes are recognized as astrocytes are an abundant source of pro-inflammatory cytokines and other as inflammatory mediators in brain injury and infection (Sofroniew & Vinters 2010, Dong & Benveniste 2001, Gorina et al. 2009, Gorina et al. 2011) and reactive astrogliosis is a pathological component of numerous neurological discords (Hamby & Sofroniew 2010, Sofroniew & Vinters 2010). Furthermore, glial communication plays a crucial role in sustaining a

neuroinflammatory response and can eventually lead to neuronal bystander death if left unchecked (Tian et al. 2012, Hamby & Sofroniew 2010, Streit et al. 1999). This crosstalk also involves beneficial effects; for example, astrocytic factors upregulate microglia-derived anti-oxidants and thus reduce microglial reactive oxygen species generation (Min *et al.* 2006). Likewise, astrocyte-conditioned media rapidly reduce interferon-γ-stimulated microglia-derived inflammatory mediators such as iNOS (Kim et al. 2010) and stimulate microglial release of the pro-survival mediator brain-derived neurotrophic factor (Yang *et al.* 2012). Downregulating the astrocytes-derived inflammatory response protects neurons from the potential of excessive uncontrolled pro-inflammatory cytokines (Hamby & Sofroniew 2010). In addition, it can disrupt neuroglia communication and mutual activation, and therefore further averts neuronal damage. We demonstrated that acetate treatment reduces pro-inflammatory cytokine levels in a rat model of neuroinflammation, and *in vitro* in LPS-stimulated microglia and astrocytes, which can explain the attenuation of LPS-induced glial activation observed with acetate supplementation *in vivo* (Reisenauer et al. 2011).

The Differences between the Effects of Acetate Treatment in Microglia and Astrocyte Cultures

Interestingly, throughout our cumulating work, we have observed many neuroglial cell type-specific similarities as well as discrepancies in terms of their response to acetate treatment and LPS challenge. Similarities include acetate treatment reducing LPS-induced microglial and astrocyte activation *in vivo*, increasing H3K9 acetylation, upregulating anti-inflammatory cytokine IL-4 and TGF-β1 mRNA, and returning LPS-induced NF-κB p65 and Cox-1 protein levels to control levels in both

cell types *in vitro*. Moreover, acetate treatment reduces pro-inflammatory cytokines IL-1β, IL-6 and TNF-α protein but not mRNA in both cell types, suggesting that treatment decreases pro-inflammatory cytokine levels mainly by interfering with translation of mRNA rather than modulating transcription, or by stimulating protein turnover. Differences between the astroglial and microglia responses include LPS reducing H3K9 acetylation by 2-fold, increasing IL-6 by 1.3-fold, increasing JNK phosphorylation by 2-fold, and decreasing PLCβ1 protein level only in microglia. Moreover, whereas MAPK p38 phosphorylation is increased by LPS both in microglia and astrocytes, it is reduced by acetate treatment at 4 hr in astrocytes cell cultures only. In addition, acetate treatment increases NF-κB p65 acetylation at lysine 310 by 3.5 fold, and reverses LPS-induced increases in phosphorylation at serine 468 of p65 and Cox-2 protein level only in microglial cell culture, whereas only in astrocytes does acetate treatment decrease $sPLA_2$ IIA, PLCβ1, LPS-induced $cPLA_2$ phosphorylation and PGE_2 release, and basal levels of NF-κB p65 phosphorylation at 536. ERK1/2 phosphorylation increases by acetate treatment only in the presence of LPS in microglia cultures, and is reduced beyond control levels with acetate treatment in astrocyte cultures. All of which demonstrates clear cell type-specific responses to acetate treatment despite the similar overall anti-inflammatory outcome evidenced by the reduction in the LPS-induced activation *in vivo* and the shift of the inflammatory cytokine balance toward a more anti-inflammatory state *in vitro* and *in vivo*. This is further supported by other reports showing the distinctive responses of astrocytes and microglia to injury, infection, inflammation and other anti-inflammatory agents (Lee *et*

al. 2010, Lu *et al.* 2010). Because acetate treatment reverses the LPS-induced MAPK p38 phosphorylation and the basal levels of phosphorylated ERK1/2 in astrocyte and not in microglial cultures, we speculate that interruption of MAPK signaling plays a stronger role in the anti-inflammatory effect of acetate treatment in astrocytes. Conversely, because H3K9 acetylation in reduced by LPS and reversed with acetate treatment in microglia, it is possible that the epigenetic mechanisms are more influential in microglia. This premise is promising for the potential of selectively downregulating MAPK signaling in only one cell type without impeding its physiological functions in other cell types, as opposed to universal inhibitors of MAPK signaling. This adds to the advantage of acetate treatment being safe and well-tolerated. In this regard, clinical trials using glyceryl triacetate to induce acetate supplementation in patients with Canavan's disease show that it does not produce biochemical or metabolic abnormalities (Madhavarao et al. 2009, Segel *et al*. 2011). Likewise, animal studies using larger doses of glyceryl triacetate show that acetate supplementation is well-tolerated and cause no apparent toxicity (Mathew et al. 2005).

In vivo, the discrepancy in the glial responses to acetate treatment, which partially reduces LPS-mediated microglial activation while completely reducing astrocyte activation, may be attributed to astrocytes being more efficient at the uptake and/or utilization of acetate, or the continual LPS stimulation to which microglia may be more sensitive. This could potentially explain why acetate treatment interrupts more inflammatory reactions in astrocytes than it does it microglia as demonstrated by the selective effect of acetate on MAPK, $cPLA_2$ phosphorylation, $sPLA_2$ IIA, PLCβ1 and

PGE_2 release in astrocyte. These speculations pave the road for further studies determining other cell type-specific mechanism of the anti-inflammatory effect of acetate.

Eicosanoid Signaling Alteration in the Light of MAPK and Cytokine Changes

To broaden our understanding of the mechanisms of the anti-inflammatory effect of acetate *in vivo*, we studied the effect of acetate treatment on eicosanoid signaling known to be associated with neuroinflammatory and neurodegenerative conditions (Lima et al. 2012, Sun et al. 2010) in BV-2 microglia and primary astrocyte cultures following LPS stimulation. Acetate treatment did not alter LPS-induced $cPLA_2$ phosphorylation and reversed LPS-induced reduction in PLCβ1 and increases in Cox-1 and Cox-2 in BV-2 microglia. In LPS-stimulated primary astrocytes, acetate treatment reduced $sPLA_2$ IIA, PLCβ1 in the presence of LPS and reversed the LPS-induced $cPLA_2$ phosphorylation and Cox-1 levels while not altering LPS-increased Cox-2. Further, acetate treatment reversed LPS-elevated PGE_2 secretion in astrocyte, which was not altered in BV-2 microglia by either LPS or acetate treatment. The enrichment levels of acetylated H3K9 were measured at the promoters of the genes for Cox-1 and 2 and were found to be increased by acetate treatment and largely unaltered by LPS stimulation. These data suggest that acetate treatment can modulate eicosanoid signaling in neuroglial cell type-distinct mechanisms, which may potentially involve H3K9 acetylation.

Of interest, acetate reduces $sPLA_2$ IIA and LPS-induced $cPLA_2$ phosphorylation in astrocytes and not BV-2 microglia. Because $cPLA_2$ is a substrate for

phosphorylation by MAPK p38 (Hiller & Sundler 1999, Kramer et al. 1996) and ERK (Hiller & Sundler 1999), both of which are inhibited by acetate treatment in astrocytes and not BV-2 microglia, it is possible that acetate treatment reverses $cPLA_2$ phosphorylation primarily by reducing MAPK p38 and ERK activity. In addition, acetate treatment reduces LPS-induced elevations of TNF-α and IL-1β, both of which upregulate $cPLA_2$ phosphorylation (Jupp et al. 2003) and $sPLA_2$ IIA level and activity (Adibhatla & Hatcher 2007) which may contribute to the reduction of $cPLA_2$ phosphorylation with acetate treatment. Although plausible in astrocytes, this does not explain why acetate treatment does not reduce LPS-induced $cPLA_2$ phosphorylation in BV-2 microglia in this study, since acetate treatment reduces IL-1β and TNF-α in both LPS-stimulated BV-2 microglia and astrocyte cultures. The complete attenuation of LPS-induced PGE_2 in astrocytes and not in BV-2 microglia by acetate treatment can potentially be due to completely reducing $cPLA_2$ phosphorylation only in astrocytes. These data do not exclude the possibility of alterations regarding the enzyme activities and membrane translocation.

Conclusion

In conclusion, these studies significantly broadened our understanding of the specific molecular and cellular effects of acetate treatment in *in vivo* and *in vitro* models of inflammation. We have optimized *in vitro* microglia and astrocyte systems that reproduce the main findings from a rat model of neuroinflammation. Specific key inflammatory mediators have been identified that can be altered by acetate treatment in neuroglial cell type-specific patterns in microglia and astrocyte. Moreover, these

results describe epigenetic changes both on the global and gene-specific levels, shifting of the inflammatory cytokine balance towards a more anti-inflammatory phenotype, and modulation of certain signaling transduction pathways by acetate treatment. Future studies will test the effect of acetate treatment on the behavioral deficits in animal models of neurodegenerative diseases such as a triple transgenic mouse model of Alzheimer's disease, the functional consequences of NF-κB modifications, and the changes in other histone targets and their modifications.

REFERENCES

Adcock, I. M. (2007) HDAC inhibitors as anti-inflammatory agents. *British journal of pharmacology, 150***,** 829-831.

Adibhatla, R. M. and Hatcher, J. F. (2007) Secretory phospholipase A2 IIA is up-regulated by TNF-alpha and IL-1alpha/beta after transient focal cerebral ischemia in rat. *Brain research, 1134***,** 199-205.

Anderson, J. D., Lowary, P. T. and Widom, J. (2001) Effects of histone acetylation on the equilibrium accessibility of nucleosomal DNA target sites. *J Mol Biol, 307***,** 977-985.

Annunziato, A. T., Eason, M. B. and Perry, C. A. (1995) Relationship between methylation and acetylation of arginine-rich histones in cycling and arrested HeLa cells. *Biochemistry, 34,* 2916-2924.

Aravalli, R. N., Peterson, P. K. and Lokensgard, J. R. (2007) Toll-like receptors in defense and damage of the central nervous system. *Journal of neuroimmune pharmacology : the official journal of the Society on NeuroImmune Pharmacology, 2,* 297-312.

Arents, G., Burlingame, R. W., Wang, B. C., Love, W. E. and Moudrianakis, E. N. (1991) The nucleosomal core histone octamer at 3.1 A resolution: a tripartite protein assembly and a left-handed superhelix. *Proceedings of the National Academy of Sciences of the United States of America, 88,* 10148-10152.

Ariyannur, P. S., Moffett, J. R., Madhavarao, C. N., Arun, P., Vishnu, N., Jacobowitz, D. M., Hallows, W. C., Denu, J. M. and Namboodiri, A. M. (2010) Nuclear-cytoplasmic localization of acetyl coenzyme a synthetase-1 in the rat brain. *The Journal of comparative neurology, 518,* 2952-2977.

Arun, P., Ariyannur, P. S., Moffett, J. R., Xing, G., Hamilton, K., Grunberg, N. E., Ives, J. A. and Namboodiri, A. M. (2010a) Metabolic acetate therapy for the treatment of traumatic brain injury. *Journal of neurotrauma, 27,* 293-298.

Arun, P., Madhavarao, C. N., Moffett, J. R. et al. (2010b) Metabolic acetate therapy improves phenotype in the tremor rat model of Canavan disease. *Journal of inherited metabolic disease, 33,* 195-210.

Atkins, C. M., Nozaki, N., Shigeri, Y. and Soderling, T. R. (2004) Cytoplasmic polyadenylation element binding protein-dependent protein synthesis is regulated by calcium/calmodulin-dependent protein kinase II. *J Neurosci, 24,* 5193-5201.

Avalos, J. L., Bever, K. M. and Wolberger, C. (2005) Mechanism of sirtuin inhibition by nicotinamide: altering the NAD(+) cosubstrate specificity of a Sir2 enzyme. *Molecular cell, 17,* 855-868.

Bachstetter, A. D., Xing, B., de Almeida, L., Dimayuga, E. R., Watterson, D. M. and Van Eldik, L. J. (2011) Microglial p38alpha MAPK is a key regulator of proinflammatory cytokine up-regulation induced by toll-like receptor (TLR) ligands or beta-amyloid (Abeta). *Journal of neuroinflammation, 8,* 79.

Balasubramaniyan, V., Boddeke, E., Bakels, R., Kust, B., Kooistra, S., Veneman, A. and Copray, S. (2006) Effects of histone deacetylation inhibition on neuronal differentiation of embryonic mouse neural stem cells. *Neuroscience, 143,* 939-951.

Balboa, M. A., Varela-Nieto, I., Killermann Lucas, K. and Dennis, E. A. (2002) Expression and function of phospholipase A(2) in brain. *FEBS letters, 531,* 12-17.

Baneres, J. L., Martin, A. and Parello, J. (1997) The N tails of histones H3 and H4 adopt a highly structured conformation in the nucleosome. *J Mol Biol, 273,* 503-508.

Barone, F. C., Irving, E. A., Ray, A. M. et al. (2001) SB 239063, a second-generation p38 mitogen-activated protein kinase inhibitor, reduces brain injury and neurological deficits in cerebral focal ischemia. *The Journal of pharmacology and experimental therapeutics, 296,* 312-321.

Basu, A., Krady, J. K. and Levison, S. W. (2004) Interleukin-1: a master regulator of neuroinflammation. *Journal of neuroscience research, 78,* 151-156.

Beyaert, R., Cuenda, A., Vanden Berghe, W., Plaisance, S., Lee, J. C., Haegeman, G., Cohen, P. and Fiers, W. (1996) The p38/RK mitogen-activated protein kinase pathway regulates interleukin-6 synthesis response to tumor necrosis factor. *The EMBO journal, 15,* 1914-1923.

Blanchard, F. and Chipoy, C. (2005) Histone deacetylase inhibitors: new drugs for the treatment of inflammatory diseases? *Drug Discov Today, 10,* 197-204.

Blasi, E., Barluzzi, R., Bocchini, V., Mazzolla, R. and Bistoni, F. (1990) Immortalization of murine microglial cells by a v-raf/v-myc carrying retrovirus. *Journal of neuroimmunology, 27,* 229-237.

Bocchini, V., Mazzolla, R., Barluzzi, R., Blasi, E., Sick, P. and Kettenmann, H. (1992) An immortalized cell line expresses properties of activated microglial cells. *Journal of neuroscience research, 31,* 616-621.

Bohuslav, J., Chen, L. F., Kwon, H., Mu, Y. and Greene, W. C. (2004) p53 induces NF-kappaB activation by an IkappaB kinase-independent mechanism involving phosphorylation of p65 by ribosomal S6 kinase 1. *The Journal of biological chemistry, 279,* 26115-26125.

Borun, T. W., Pearson, D. and Paik, W. K. (1972) Studies of histone methylation during the HeLa S-3 cell cycle. *The Journal of biological chemistry, 247,* 4288-4298.

Bourre, J. M., Paturneau-Jouas, M. Y., Daudu, O. L. and Baumann, N. A. (1977) Lignoceric acid biosynthesis in the developing brain. Activities of mitochondrial acetyl-CoA-dependent synthesis and microsomal malonyl-CoA chain-elongating system in relation to myelination. Comparison between normal mouse and dysmyelinating mutants (quaking and jimpy). *Eur J Biochem, 72,* 41-47.

Bradbury, E. M. (1992) Reversible histone modifications and the chromosome cell cycle. *Bioessays, 14,* 9-16.

Bradford, M. M. (1976) A rapid and sensitive method for the quantitation of microgram quantities of protein utilizing the principle of protein-dye binding. *Analytical biochemistry, 72,* 248-254.

Braunstein, M., Sobel, R. E., Allis, C. D., Turner, B. M. and Broach, J. R. (1996) Efficient transcriptional silencing in Saccharomyces cerevisiae requires a heterochromatin histone acetylation pattern. *Molecular and cellular biology, 16,* 4349-4356.

Broer, S., Rahman, B., Pellegri, G., Pellerin, L., Martin, J. L., Verleysdonk, S., Hamprecht, B. and Magistretti, P. J. (1997) Comparison of lactate transport in astroglial cells and monocarboxylate transporter 1 (MCT 1) expressing Xenopus laevis oocytes. Expression of two different monocarboxylate transporters in astroglial cells and neurons. *The Journal of biological chemistry, 272,* 30096-30102.

Buss, H., Dorrie, A., Schmitz, M. L., Hoffmann, E., Resch, K. and Kracht, M. (2004) Constitutive and interleukin-1-inducible phosphorylation of p65 NF-{kappa}B at serine 536 is mediated by multiple protein kinases including I{kappa}B kinase (IKK)-{alpha}, IKK{beta}, IKK{epsilon}, TRAF family member-associated (TANK)-binding kinase 1 (TBK1), and an unknown kinase and couples p65 to TATA-binding protein-associated factor II31-mediated interleukin-8 transcription. *The Journal of biological chemistry, 279,* 55633-55643.

Cao, W., Bao, C., Padalko, E. and Lowenstein, C. J. (2008) Acetylation of mitogen-activated protein kinase phosphatase-1 inhibits Toll-like receptor signaling. *The Journal of experimental medicine, 205,* 1491-1503.

Chen, F. E. and Ghosh, G. (1999) Regulation of DNA binding by Rel/NF-kappaB transcription factors: structural views. *Oncogene, 18,* 6845-6852.

Chen, J., Zhou, Y., Mueller-Steiner, S., Chen, L. F., Kwon, H., Yi, S., Mucke, L. and Gan, L. (2005a) SIRT1 protects against microglia-dependent amyloid-beta toxicity through inhibiting NF-kappaB signaling. *The Journal of biological chemistry, 280,* 40364-40374.

Chen, L., Fischle, W., Verdin, E. and Greene, W. C. (2001) Duration of nuclear NF-kappaB action regulated by reversible acetylation. *Science (New York, N.Y, 293,* 1653-1657.

Chen, L. F., Mu, Y. and Greene, W. C. (2002) Acetylation of RelA at discrete sites regulates distinct nuclear functions of NF-kappaB. *The EMBO journal, 21,* 6539-6548.

Chen, L. F., Williams, S. A., Mu, Y., Nakano, H., Duerr, J. M., Buckbinder, L. and Greene, W. C. (2005b) NF-kappaB RelA phosphorylation regulates RelA acetylation. *Molecular and cellular biology, 25,* 7966-7975.

Clarke, D. J., O'Neill, L. P. and Turner, B. M. (1993) Selective use of H4 acetylation sites in the yeast Saccharomyces cerevisiae. *The Biochemical journal, 294 (Pt 2),* 557-561.

Dang, W., Steffen, K. K., Perry, R., Dorsey, J. A., Johnson, F. B., Shilatifard, A., Kaeberlein, M., Kennedy, B. K. and Berger, S. L. (2009) Histone H4 lysine 16 acetylation regulates cellular lifespan. *Nature, 459,* 802-807.

de Ruijter, A. J., van Gennip, A. H., Caron, H. N., Kemp, S. and van Kuilenburg, A. B. (2003) Histone deacetylases (HDACs): characterization of the classical HDAC family. *The Biochemical journal, 370,* 737-749.

Dennis, E. A. (1994) Diversity of group types, regulation, and function of phospholipase A2. *The Journal of biological chemistry, 269,* 13057-13060.

Des Rosiers, C., David, F., Garneau, M. and Brunengraber, H. (1991) Nonhomogeneous labeling of liver mitochondrial acetyl-CoA. *The Journal of biological chemistry, 266,* 1574-1578.

Deutsch, J., Rapoport, S. I. and Rosenberger, T. A. (2002) Coenzyme A and short-chain acyl-CoA species in control and ischemic rat brain. *Neurochemical research, 27,* 1577-1582.

Dhandapani, K. M. and Brann, D. W. (2003) Transforming growth factor-beta: a neuroprotective factor in cerebral ischemia. *Cell biochemistry and biophysics, 39,* 13-22.

Dhawan, G., Floden, A. M. and Combs, C. K. (2012) Amyloid-beta oligomers stimulate microglia through a tyrosine kinase dependent mechanism. *Neurobiology of aging, 33,* 2247-2261.

DiDonato, J. A., Mercurio, F. and Karin, M. (2012) NF-kappaB and the link between inflammation and cancer. *Immunological reviews, 246,* 379-400.

Dong, Y. and Benveniste, E. N. (2001) Immune function of astrocytes. *Glia, 36,* 180-190.

Eberharter, A. and Becker, P. B. (2002) Histone acetylation: a switch between repressive and permissive chromatin. Second in review series on chromatin dynamics. *EMBO Rep, 3,* 224-229.

Farooqui, A. A. and Horrocks, L. A. (2005) Signaling and interplay mediated by phospholipases A2, C, and D in LA-N-1 cell nuclei. *Reprod Nutr Dev, 45,* 613-631.

Farooqui, A. A., Yang, H. C., Rosenberger, T. A. and Horrocks, L. A. (1997) Phospholipase A2 and its role in brain tissue. *Journal of Neurochemistry, 69,* 889-901.

Fraga, M. F., Ballestar, E., Villar-Garea, A. et al. (2005) Loss of acetylation at Lys16 and trimethylation at Lys20 of histone H4 is a common hallmark of human cancer. *Nature genetics, 37,* 391-400.

Fraga, M. F. and Esteller, M. (2005) Towards the human cancer epigenome: a first draft of histone modifications. *Cell cycle (Georgetown, Tex, 4,* 1377-1381.

Frantseva, M. V., Kokarovtseva, L. and Perez Velazquez, J. L. (2002) Ischemia-induced brain damage depends on specific gap-junctional coupling. *J Cereb Blood Flow Metab, 22,* 453-462.

Fujimori, Y., Murakami, M., Kim, D. K., Hara, S., Takayama, K., Kudo, I. and Inoue, K. (1992) Immunochemical detection of arachidonoyl-preferential phospholipase A2. *Journal of biochemistry, 111,* 54-60.

Fujino, T., Kondo, J., Ishikawa, M., Morikawa, K. and Yamamoto, T. T. (2001) Acetyl-CoA synthetase 2, a mitochondrial matrix enzyme involved in the oxidation of acetate. *The Journal of biological chemistry, 276,* 11420-11426.

Fukao, T., Lopaschuk, G. D. and Mitchell, G. A. (2004) Pathways and control of ketone body metabolism: on the fringe of lipid biochemistry. *Prostaglandins, leukotrienes, and essential fatty acids, 70,* 243-251.

Fukushima, M., Lee, S. M., Moro, N., Hovda, D. A. and Sutton, R. L. (2009) Metabolic and histologic effects of sodium pyruvate treatment in the rat after cortical contusion injury. *Journal of neurotrauma, 26,* 1095-1110.

Furlan, R., Bergami, A., Lang, R., Brambilla, E., Franciotta, D., Martinelli, V., Comi, G., Panina, P. and Martino, G. (2000) Interferon-beta treatment in multiple sclerosis patients decreases the number of circulating T cells producing interferon-gamma and interleukin-4. *Journal of neuroimmunology, 111,* 86-92.

Galbiati, L., Mendoza-Maldonado, R., Gutierrez, M. I. and Giacca, M. (2005) Regulation of E2F-1 after DNA damage by p300-mediated acetylation and ubiquitination. *Cell cycle (Georgetown, Tex, 4,* 930-939.

Ganter, S., Northoff, H., Mannel, D. and Gebicke-Harter, P. J. (1992) Growth control of cultured microglia. *Journal of neuroscience research, 33,* 218-230.

Garcia, C. K., Goldstein, J. L., Pathak, R. K., Anderson, R. G. and Brown, M. S. (1994a) Molecular characterization of a membrane transporter for lactate, pyruvate, and other monocarboxylates: implications for the Cori cycle. *Cell, 76,* 865-873.

Garcia, C. K., Li, X., Luna, J. and Francke, U. (1994b) cDNA cloning of the human monocarboxylate transporter 1 and chromosomal localization of the SLC16A1 locus to 1p13.2-p12. *Genomics, 23,* 500-503.

Glass, C. K., Saijo, K., Winner, B., Marchetto, M. C. and Gage, F. H. (2010) Mechanisms underlying inflammation in neurodegeneration. *Cell, 140,* 918-934.

Glozak, M. A., Sengupta, N., Zhang, X. and Seto, E. (2005) Acetylation and deacetylation of non-histone proteins. *Gene, 363,* 15-23.

Gorina, R., Font-Nieves, M., Marquez-Kisinousky, L., Santalucia, T. and Planas, A. M. (2011) Astrocyte TLR4 activation induces a proinflammatory environment through the interplay between MyD88-dependent NFkappaB signaling, MAPK, and Jak1/Stat1 pathways. *Glia, 59,* 242-255.

Gorina, R., Santalucia, T., Petegnief, V., Ejarque-Ortiz, A., Saura, J. and Planas, A. M. (2009) Astrocytes are very sensitive to develop innate immune responses to lipid-carried short interfering RNA. *Glia, 57,* 93-107.

Gorisch, S. M., Wachsmuth, M., Toth, K. F., Lichter, P. and Rippe, K. (2005) Histone acetylation increases chromatin accessibility. *Journal of cell science, 118,* 5825-5834.

Govindarajan, N., Agis-Balboa, R. C., Walter, J., Sananbenesi, F. and Fischer, A. (2011) Sodium butyrate improves memory function in an Alzheimer's disease mouse model when administered at an advanced stage of disease progression. *J Alzheimers Dis, 26,* 187-197.

Green, G. R., Collas, P., Burrell, A. and Poccia, D. L. (1995) Histone phosphorylation during sea urchin development. *Semin Cell Biol, 6,* 219-227.

Gregio, A. P., Cano, V. P., Avaca, J. S., Valentini, S. R. and Zanelli, C. F. (2009) eIF5A has a function in the elongation step of translation in yeast. *Biochemical and biophysical research communications, 380,* 785-790.

Griffin, W. S., Stanley, L. C., Ling, C., White, L., MacLeod, V., Perrot, L. J., White, C. L., 3rd and Araoz, C. (1989) Brain interleukin 1 and S-100 immunoreactivity are elevated in Down syndrome and Alzheimer disease. *Proceedings of the National Academy of Sciences of the United States of America, 86,* 7611-7615.

Grossberg, A. J., Zhu, X., Leinninger, G. M., Levasseur, P. R., Braun, T. P., Myers, M. G., Jr. and Marks, D. L. (2011) Inflammation-induced lethargy is mediated by suppression of orexin neuron activity. *J Neurosci, 31***,** 11376-11386.

Guan, J. S., Haggarty, S. J., Giacometti, E. et al. (2009) HDAC2 negatively regulates memory formation and synaptic plasticity. *Nature, 459,* 55-60.

Hamby, M. E. and Sofroniew, M. V. (2010) Reactive astrocytes as therapeutic targets for CNS disorders. *Neurotherapeutics, 7,* 494-506.

Hanisch, U. K. (2002) Microglia as a source and target of cytokines. *Glia, 40,* 140-155.

Hanisch, U. K. and Kettenmann, H. (2007) Microglia: active sensor and versatile effector cells in the normal and pathologic brain. *Nature neuroscience, 10,* 1387-1394.

Haumaitre, C., Lenoir, O. and Scharfmann, R. (2009) Directing cell differentiation with small-molecule histone deacetylase inhibitors: the example of promoting pancreatic endocrine cells. *Cell cycle (Georgetown, Tex, 8,* 536-544.

Hauss-Wegrzyniak, B., Dobrzanski, P., Stoehr, J. D. and Wenk, G. L. (1998a) Chronic neuroinflammation in rats reproduces components of the neurobiology of Alzheimer's disease. *Brain research, 780,* 294-303.

Hauss-Wegrzyniak, B., Lukovic, L., Bigaud, M. and Stoeckel, M. E. (1998b) Brain inflammatory response induced by intracerebroventricular infusion of lipopolysaccharide: an immunohistochemical study. *Brain research, 794,* 211-224.

Hauss-Wegrzyniak, B., Vraniak, P. D. and Wenk, G. L. (2000) LPS-induced neuroinflammatory effects do not recover with time. *Neuroreport, 11,* 1759-1763.

Helmy, A., De Simoni, M. G., Guilfoyle, M. R., Carpenter, K. L. and Hutchinson, P. J. (2011) Cytokines and innate inflammation in the pathogenesis of human traumatic brain injury. *Progress in neurobiology, 95,* 352-372.

Hezroni, H., Sailaja, B. S. and Meshorer, E. (2011) Pluripotency-related, VPA-induced genome-wide H3K9 acetylation patterns in embryonic stem cells. *The Journal of biological chemistry*.

Hiller, G. and Sundler, R. (1999) Activation of arachidonate release and cytosolic phospholipase A2 via extracellular signal-regulated kinase and p38 mitogen-activated protein kinase in macrophages stimulated by bacteria or zymosan. *Cellular signalling, 11,* 863-869.

Hoberg, J. E., Popko, A. E., Ramsey, C. S. and Mayo, M. W. (2006) IkappaB kinase alpha-mediated derepression of SMRT potentiates acetylation of RelA/p65 by p300. *Molecular and cellular biology, 26,* 457-471.

Hopkins, S. J. and Rothwell, N. J. (1995) Cytokines and the nervous system. I: Expression and recognition. *Trends in neurosciences, 18,* 83-88.

Hosoi, R., Matsuyama, Y., Hirose, S., Koyama, Y., Matsuda, T., Gee, A. and Inoue, O. (2009) Characterization of (14)C-acetate uptake in cultured rat astrocytes. *Brain research, 1253,* 69-73.

Howe, L., Auston, D., Grant, P., John, S., Cook, R. G., Workman, J. L. and Pillus, L. (2001) Histone H3 specific acetyltransferases are essential for cell cycle progression. *Genes & development, 15,* 3144-3154.

Hu, W., Ralay Ranaivo, H., Roy, S. M., Behanna, H. A., Wing, L. K., Munoz, L., Guo, L., Van Eldik, L. J. and Watterson, D. M. (2007) Development of a novel therapeutic suppressor of brain proinflammatory cytokine up-regulation that attenuates synaptic dysfunction and behavioral deficits. *Bioorganic & medicinal chemistry letters, 17,* 414-418.

Huang, B., Yang, X. D., Lamb, A. and Chen, L. F. (2010a) Posttranslational modifications of NF-kappaB: another layer of regulation for NF-kappaB signaling pathway. *Cellular signalling, 22,* 1282-1290.

Huang, K. F., Huang, W. T., Lin, K. C., Lin, M. T. and Chang, C. P. (2010b) Interleukin-1 receptor antagonist inhibits the release of glutamate, hydroxyl radicals, and prostaglandin E(2) in the hypothalamus during pyrogen-induced fever in rabbits. *European journal of pharmacology, 629,* 125-131.

Ishfaq, M., Maeta, K., Maeda, S., Natsume, T., Ito, A. and Yoshida, M. (2012) Acetylation regulates subcellular localization of eukaryotic translation initiation factor 5A (eIF5A). *FEBS letters,* DOI: 10.1016/j.febslet.2012.06.042.

Ito, M., Natsume, A., Takeuchi, H., Shimato, S., Ohno, M., Wakabayashi, T. and Yoshida, J. (2009) Type I interferon inhibits astrocytic gliosis and promotes functional recovery after spinal cord injury by deactivation of the MEK/ERK pathway. *Journal of neurotrauma, 26,* 41-53.

Jeong, J. W., Bae, M. K., Ahn, M. Y. et al. (2002) Regulation and destabilization of HIF-1alpha by ARD1-mediated acetylation. *Cell, 111,* 709-720.

Johnston, H., Boutin, H. and Allan, S. M. (2011) Assessing the contribution of inflammation in models of Alzheimer's disease. *Biochemical Society transactions, 39,* 886-890.

Jupp, O. J., Vandenabeele, P. and MacEwan, D. J. (2003) Distinct regulation of cytosolic phospholipase A2 phosphorylation, translocation, proteolysis and activation by tumour necrosis factor-receptor subtypes. *The Biochemical journal, 374,* 453-461.

Kaminska, B., Gozdz, A., Zawadzka, M., Ellert-Miklaszewska, A. and Lipko, M. (2009) MAPK signal transduction underlying brain inflammation and gliosis as therapeutic target. *Anat Rec (Hoboken), 292,* 1902-1913.

Kang, W. and Hebert, J. M. (2011) Signaling pathways in reactive astrocytes, a genetic perspective. *Molecular neurobiology, 43,* 147-154.

Kargas, G., Rudy, T., Spennetta, T., Takayama, K., Querishi, N. and Shrago, E. (1990) Separation and quantitation of long-chain free fatty acids in human serum by high-performance liquid chromatography. *Journal of chromatography, 526,* 331-340.

Kasai, T., Inada, K., Takakuwa, T. et al. (1997) Anti-inflammatory cytokine levels in patients with septic shock. *Research communications in molecular pathology and pharmacology, 98,* 34-42.

Kawakami, K., Nakamura, A., Ishigami, A., Goto, S. and Takahashi, R. (2009) Age-related difference of site-specific histone modifications in rat liver. *Biogerontology, 10,* 415-421.

Kiernan, R., Bres, V., Ng, R. W., Coudart, M. P., El Messaoudi, S., Sardet, C., Jin, D. Y., Emiliani, S. and Benkirane, M. (2003) Post-activation turn-off of NF-kappa B-dependent transcription is regulated by acetylation of p65. *The Journal of biological chemistry, 278,* 2758-2766.

Kim, H. J., Rowe, M., Ren, M., Hong, J. S., Chen, P. S. and Chuang, D. M. (2007) Histone deacetylase inhibitors exhibit anti-inflammatory and neuroprotective effects in a rat permanent ischemic model of stroke: multiple mechanisms of action. *The Journal of pharmacology and experimental therapeutics, 321,* 892-901.

Kim, J. B., Yu, Y. M., Kim, S. W. and Lee, J. K. (2005) Anti-inflammatory mechanism is involved in ethyl pyruvate-mediated efficacious neuroprotection in the postischemic brain. *Brain research, 1060,* 188-192.

Kim, J. H., Min, K. J., Seol, W., Jou, I. and Joe, E. H. (2010) Astrocytes in injury states rapidly produce anti-inflammatory factors and attenuate microglial inflammatory responses. *Journal of Neurochemistry, 115,* 1161-1171.

Kim, J. S. and Shukla, S. D. (2006) Acute in vivo effect of ethanol (binge drinking) on histone H3 modifications in rat tissues. *Alcohol and alcoholism (Oxford, Oxfordshire), 41,* 126-132.

Kohn, D. T., Tsai, K. C., Cansino, V. V., Neve, R. L. and Perrone-Bizzozero, N. I. (1996) Role of highly conserved pyrimidine-rich sequences in the 3' untranslated region of the GAP-43 mRNA in mRNA stability and RNA-protein interactions. *Brain Res Mol Brain Res, 36,* 240-250.

Kotlyarov, A., Neininger, A., Schubert, C., Eckert, R., Birchmeier, C., Volk, H. D. and Gaestel, M. (1999) MAPKAP kinase 2 is essential for LPS-induced TNF-alpha biosynthesis. *Nature cell biology, 1,* 94-97.

Kraatz, J., Clair, L., Bellingham, J., Wahlstrom, K., Rodriguez, J. L. and West, M. A. (1998) Lipopolysaccharide pretreatment produces macrophage endotoxin tolerance via a serum-independent pathway. *The Journal of trauma, 45,* 684-691.

Krajewski, W. A. and Becker, P. B. (1998) Reconstitution of hyperacetylated, DNase I-sensitive chromatin characterized by high conformational flexibility of nucleosomal DNA. *Proceedings of the National Academy of Sciences of the United States of America, 95,* 1540-1545.

Kramer, R. M., Roberts, E. F., Um, S. L., Borsch-Haubold, A. G., Watson, S. P., Fisher, M. J. and Jakubowski, J. A. (1996) p38 mitogen-activated protein kinase phosphorylates cytosolic phospholipase A2 (cPLA2) in thrombin-stimulated platelets. Evidence that proline-directed phosphorylation is not required for mobilization of arachidonic acid by cPLA2. *The Journal of biological chemistry, 271,* 27723-27729.

Kumar, S., Boehm, J. and Lee, J. C. (2003) p38 MAP kinases: key signalling molecules as therapeutic targets for inflammatory diseases. *Nature reviews, 2,* 717-726.

Kuo, M. H., Brownell, J. E., Sobel, R. E., Ranalli, T. A., Cook, R. G., Edmondson, D. G., Roth, S. Y. and Allis, C. D. (1996) Transcription-linked acetylation by Gcn5p of histones H3 and H4 at specific lysines. *Nature, 383,* 269-272.

Labow, M., Shuster, D., Zetterstrom, M. et al. (1997) Absence of IL-1 signaling and reduced inflammatory response in IL-1 type I receptor-deficient mice. *J Immunol, 159,* 2452-2461.

Langley, B., Gensert, J. M., Beal, M. F. and Ratan, R. R. (2005) Remodeling chromatin and stress resistance in the central nervous system: histone deacetylase inhibitors as novel and broadly effective neuroprotective agents. *Current drug targets. CNS and neurological disorders, 4,* 41-50.

Lauritzen, I., Heurteaux, C. and Lazdunski, M. (1994) Expression of group II phospholipase A2 in rat brain after severe forebrain ischemia and in endotoxic shock. *Brain research, 651,* 353-356.

Ledeboer, A., Breve, J. J., Poole, S., Tilders, F. J. and Van Dam, A. M. (2000) Interleukin-10, interleukin-4, and transforming growth factor-beta differentially regulate lipopolysaccharide-induced production of pro-inflammatory cytokines and nitric oxide in co-cultures of rat astroglial and microglial cells. *Glia, 30,* 134-142.

Lee, H., Villacreses, N. E., Rapoport, S. I. and Rosenberger, T. A. (2004) In vivo imaging detects a transient increase in brain arachidonic acid metabolism: a potential marker of neuroinflammation. *Journal of Neurochemistry, 91,* 936-945.

Lee, J. Y., Kim, Y. H. and Koh, J. Y. (2001) Protection by pyruvate against transient forebrain ischemia in rats. *J Neurosci, 21,* RC171.

Lee, S., Zhao, Y. Q., Ribeiro-da-Silva, A. and Zhang, J. (2010) Distinctive response of CNS glial cells in oro-facial pain associated with injury, infection and inflammation. *Molecular pain, 6,* 79.

Lee, S. B., Park, J. H., Folk, J. E., Deck, J. A., Pegg, A. E., Sokabe, M., Fraser, C. S. and Park, M. H. (2011) Inactivation of eukaryotic initiation factor 5A (eIF5A) by specific acetylation of its hypusine residue by spermidine/spermine acetyltransferase 1 (SSAT1). *The Biochemical journal, 433,* 205-213.

Legos, J. J., Erhardt, J. A., White, R. F., Lenhard, S. C., Chandra, S., Parsons, A. A., Tuma, R. F. and Barone, F. C. (2001) SB 239063, a novel p38 inhibitor, attenuates early neuronal injury following ischemia. *Brain research, 892,* 70-77.

Legos, J. J., Whitmore, R. G., Erhardt, J. A., Parsons, A. A., Tuma, R. F. and Barone, F. C. (2000) Quantitative changes in interleukin proteins following focal stroke in the rat. *Neuroscience letters, 282,* 189-192.

Lehnardt, S. (2010) Innate immunity and neuroinflammation in the CNS: the role of microglia in Toll-like receptor-mediated neuronal injury. *Glia, 58,* 253-263.

Lehnardt, S., Massillon, L., Follett, P., Jensen, F. E., Ratan, R., Rosenberg, P. A., Volpe, J. J. and Vartanian, T. (2003) Activation of innate immunity in the CNS triggers neurodegeneration through a Toll-like receptor 4-dependent pathway. *Proceedings of the National Academy of Sciences of the United States of America, 100,* 8514-8519.

Levenson, J. M., O'Riordan, K. J., Brown, K. D., Trinh, M. A., Molfese, D. L. and Sweatt, J. D. (2004) Regulation of histone acetylation during memory formation in the hippocampus. *The Journal of biological chemistry, 279,* 40545-40559.

Li, X., Corsa, C. A., Pan, P. W., Wu, L., Ferguson, D., Yu, X., Min, J. and Dou, Y. (2010) MOF and H4 K16 acetylation play important roles in DNA damage repair by modulating recruitment of DNA damage repair protein Mdc1. *Molecular and cellular biology, 30,* 5335-5347.

Li, Y., Liu, B., Zhao, H. et al. (2009) Protective effect of suberoylanilide hydroxamic acid against LPS-induced septic shock in rodents. *Shock, 32,* 517-523.

Li, Y., Liu, L., Barger, S. W. and Griffin, W. S. (2003) Interleukin-1 mediates pathological effects of microglia on tau phosphorylation and on synaptophysin synthesis in cortical neurons through a p38-MAPK pathway. *J Neurosci, 23,* 1605-1611.

Li, Y., Yuan, Z., Liu, B., Sailhamer, E. A., Shults, C., Velmahos, G. C., Demoya, M. and Alam, H. B. (2008) Prevention of hypoxia-induced neuronal apoptosis through histone deacetylase inhibition. *The Journal of trauma, 64,* 863-870; discussion 870-861.

Lima, I. V., Bastos, L. F., Limborco-Filho, M., Fiebich, B. L. and de Oliveira, A. C. (2012) Role of prostaglandins in neuroinflammatory and neurodegenerative diseases. *Mediators of inflammation, 2012,* 946813.

Livak, K. J. and Schmittgen, T. D. (2001) Analysis of relative gene expression data using real-time quantitative PCR and the 2(-Delta Delta C(T)) Method. *Methods (San Diego, Calif, 25*, 402-408.

Lloyd, E., Somera-Molina, K., Van Eldik, L. J., Watterson, D. M. and Wainwright, M. S. (2008) Suppression of acute proinflammatory cytokine and chemokine upregulation by post-injury administration of a novel small molecule improves long-term neurologic outcome in a mouse model of traumatic brain injury. *Journal of neuroinflammation, 5,* 28.

Lu, X., Ma, L., Ruan, L., Kong, Y., Mou, H., Zhang, Z., Wang, Z., Wang, J. M. and Le, Y. (2010) Resveratrol differentially modulates inflammatory responses of microglia and astrocytes. *Journal of neuroinflammation, 7,* 46.

Luger, K., Mader, A. W., Richmond, R. K., Sargent, D. F. and Richmond, T. J. (1997) Crystal structure of the nucleosome core particle at 2.8 A resolution. *Nature, 389,* 251-260.

Madhavarao, C. N., Arun, P., Anikster, Y., Mog, S. R., Staretz-Chacham, O., Moffett, J. R., Grunberg, N. E., Gahl, W. A. and Namboodiri, A. M. (2009) Glyceryl triacetate for Canavan disease: a low-dose trial in infants and evaluation of a higher dose for toxicity in the tremor rat model. *Journal of inherited metabolic disease, 32,* 640-650.

Makowski, A. M., Dutnall, R. N. and Annunziato, A. T. (2001) Effects of acetylation of histone H4 at lysines 8 and 16 on activity of the Hat1 histone acetyltransferase. *The Journal of biological chemistry, 276,* 43499-43502.

Marmorstein, R. and Roth, S. Y. (2001) Histone acetyltransferases: function, structure, and catalysis. *Current opinion in genetics & development, 11,* 155-161.

Mathew, R., Arun, P., Madhavarao, C. N., Moffett, J. R. and Namboodiri, M. A. (2005) Progress toward acetate supplementation therapy for Canavan disease: glyceryl triacetate administration increases acetate, but not N-acetylaspartate, levels in brain. *The Journal of pharmacology and experimental therapeutics, 315,* 297-303.

McCampbell, A., Taye, A. A., Whitty, L., Penney, E., Steffan, J. S. and Fischbeck, K. H. (2001) Histone deacetylase inhibitors reduce polyglutamine toxicity. *Proceedings of the National Academy of Sciences of the United States of America, 98,* 15179-15184.

McGarry, J. D. and Foster, D. W. (1980) Regulation of hepatic fatty acid oxidation and ketone body production. *Annual review of biochemistry, 49,* 395-420.

McGuinness, M. C., Powers, J. M., Bias, W. B. et al. (1997) Human leukocyte antigens and cytokine expression in cerebral inflammatory demyelinative lesions of X-linked adrenoleukodystrophy and multiple sclerosis. *Journal of neuroimmunology, 75,* 174-182.

Meissner, F., Molawi, K. and Zychlinsky, A. (2010) Mutant superoxide dismutase 1-induced IL-1beta accelerates ALS pathogenesis. *Proceedings of the National Academy of Sciences of the United States of America, 107,* 13046-13050.

Mendez, R. and Richter, J. D. (2001) Translational control by CPEB: a means to the end. *Nature reviews, 2,* 521-529.

Merson, T. D., Binder, M. D. and Kilpatrick, T. J. (2010) Role of cytokines as mediators and regulators of microglial activity in inflammatory demyelination of the CNS. *Neuromolecular medicine, 12,* 99-132.

Min, K. J., Yang, M. S., Kim, S. U., Jou, I. and Joe, E. H. (2006) Astrocytes induce hemeoxygenase-1 expression in microglia: a feasible mechanism for preventing excessive brain inflammation. *J Neurosci, 26,* 1880-1887.

Mori, T., Wang, X., Aoki, T. and Lo, E. H. (2002) Downregulation of matrix metalloproteinase-9 and attenuation of edema via inhibition of ERK mitogen activated protein kinase in traumatic brain injury. *Journal of neurotrauma, 19,* 1411-1419.

Morrison, B. E., Majdzadeh, N. and D'Mello, S. R. (2007) Histone deacetylases: focus on the nervous system. *Cell Mol Life Sci, 64,* 2258-2269.

Mrak, R. E. (2009) Neuropathology and the neuroinflammation idea. *J Alzheimers Dis, 18,* 473-481.

Mu, C., Liu, H. and Zheng, G. C. (2007) [The modification and variants of histone]. *Mol Biol (Mosk), 41,* 395-407.

Muir, D., Berl, S. and Clarke, D. D. (1986) Acetate and fluoroacetate as possible markers for glial metabolism in vivo. *Brain research, 380,* 336-340.

Munoz, C., Carlet, J., Fitting, C., Misset, B., Bleriot, J. P. and Cavaillon, J. M. (1991) Dysregulation of in vitro cytokine production by monocytes during sepsis. *The Journal of clinical investigation, 88,* 1747-1754.

Nakase, T., Fushiki, S. and Naus, C. C. (2003) Astrocytic gap junctions composed of connexin 43 reduce apoptotic neuronal damage in cerebral ischemia. *Stroke; a journal of cerebral circulation, 34,* 1987-1993.

Oldendorf, W. H. (1973) Carrier-mediated blood-brain barrier transport of short-chain monocarboxylic organic acids. *The American journal of physiology, 224,* 1450-1453.

Olson, J. K. and Miller, S. D. (2004) Microglia initiate central nervous system innate and adaptive immune responses through multiple TLRs. *J Immunol, 173,* 3916-3924.

Parish, C. L., Finkelstein, D. I., Tripanichkul, W., Satoskar, A. R., Drago, J. and Horne, M. K. (2002) The role of interleukin-1, interleukin-6, and glia in inducing growth of neuronal terminal arbors in mice. *J Neurosci, 22,* 8034-8041.

Pearson, G., Robinson, F., Beers Gibson, T., Xu, B. E., Karandikar, M., Berman, K. and Cobb, M. H. (2001) Mitogen-activated protein (MAP) kinase pathways: regulation and physiological functions. *Endocrine reviews, 22,* 153-183.

Pekny, M. and Nilsson, M. (2005) Astrocyte activation and reactive gliosis. *Glia, 50,* 427-434.

Peleg, S., Sananbenesi, F., Zovoilis, A. et al. (2010) Altered histone acetylation is associated with age-dependent memory impairment in mice. *Science (New York, N.Y, 328,* 753-756.

Perkins, N. D., Felzien, L. K., Betts, J. C., Leung, K., Beach, D. H. and Nabel, G. J. (1997) Regulation of NF-kappaB by cyclin-dependent kinases associated with the p300 coactivator. *Science (New York, N.Y, 275,* 523-527.

Pernot, F., Heinrich, C., Barbier, L. et al. (2011) Inflammatory changes during epileptogenesis and spontaneous seizures in a mouse model of mesiotemporal lobe epilepsy. *Epilepsia*.

Peterson, C. L. (2002) HDAC's at work: everyone doing their part. *Molecular cell, 9,* 921-922.

Petrova, T. V., Akama, K. T. and Van Eldik, L. J. (1999) Selective modulation of BV-2 microglial activation by prostaglandin E(2). Differential effects on endotoxin-stimulated cytokine induction. *The Journal of biological chemistry, 274,* 28823-28827.

Phillis, J. W. and O'Regan, M. H. (2004) A potentially critical role of phospholipases in central nervous system ischemic, traumatic, and neurodegenerative disorders. *Brain Res Brain Res Rev, 44,* 13-47.

Piao, C. S., Kim, J. B., Han, P. L. and Lee, J. K. (2003) Administration of the p38 MAPK inhibitor SB203580 affords brain protection with a wide therapeutic window against focal ischemic insult. *Journal of neuroscience research, 73,* 537-544.

Pierre, K., Pellerin, L., Debernardi, R., Riederer, B. M. and Magistretti, P. J. (2000) Cell-specific localization of monocarboxylate transporters, MCT1 and MCT2, in the adult mouse brain revealed by double immunohistochemical labeling and confocal microscopy. *Neuroscience, 100,* 617-627.

Polach, K. J., Lowary, P. T. and Widom, J. (2000) Effects of core histone tail domains on the equilibrium constants for dynamic DNA site accessibility in nucleosomes. *J Mol Biol, 298,* 211-223.

Polevoda, B. and Sherman, F. (2002) The diversity of acetylated proteins. *Genome biology, 3,* 0006.0001-0006.0006.

Qian, L., Flood, P. M. and Hong, J. S. (2010) Neuroinflammation is a key player in Parkinson's disease and a prime target for therapy. *J Neural Transm, 117,* 971-979.

Rafiki, A., Boulland, J. L., Halestrap, A. P., Ottersen, O. P. and Bergersen, L. (2003) Highly differential expression of the monocarboxylate transporters MCT2 and MCT4 in the developing rat brain. *Neuroscience, 122,* 677-688.

Ransohoff, R. M. and Perry, V. H. (2009) Microglial physiology: unique stimuli, specialized responses. *Annual review of immunology, 27,* 119-145.

Redon, C., Pilch, D., Rogakou, E., Sedelnikova, O., Newrock, K. and Bonner, W. (2002) Histone H2A variants H2AX and H2AZ. *Current opinion in genetics & development, 12,* 162-169.

Reisenauer, C. J., Bhatt, D. P., Mitteness, D. J., Slanczka, E. R., Gienger, H. M., Watt, J. A. and Rosenberger, T. A. (2011) Acetate supplementation attenuates lipopolysaccharide-induced neuroinflammation. *Journal of Neurochemistry, 117,* 264-274.

Rice, J. C. and Allis, C. D. (2001) Histone methylation versus histone acetylation: new insights into epigenetic regulation. *Current opinion in cell biology, 13,* 263-273.

Rojanathammanee, L., Murphy, E. J. and Combs, C. K. (2011) Expression of mutant alpha-synuclein modulates microglial phenotype in vitro. *Journal of neuroinflammation, 8,* 44.

Rosenberger, T. A., Villacreses, N. E., Hovda, J. T., Bosetti, F., Weerasinghe, G., Wine, R. N., Harry, G. J. and Rapoport, S. I. (2004) Rat brain arachidonic acid metabolism is increased by a 6-day intracerebral ventricular infusion of bacterial lipopolysaccharide. *Journal of Neurochemistry, 88,* 1168-1178.

Rothwell, N. J. and Hopkins, S. J. (1995) Cytokines and the nervous system II: Actions and mechanisms of action. *Trends in neurosciences, 18,* 130-136.

Rouaux, C., Panteleeva, I., Rene, F., Gonzalez de Aguilar, J. L., Echaniz-Laguna, A., Dupuis, L., Menger, Y., Boutillier, A. L. and Loeffler, J. P. (2007) Sodium valproate exerts neuroprotective effects in vivo through CREB-binding protein-dependent mechanisms but does not improve survival in an amyotrophic lateral sclerosis mouse model. *J Neurosci, 27,* 5535-5545.

Ryu, H., Lee, J., Olofsson, B. A. et al. (2003) Histone deacetylase inhibitors prevent oxidative neuronal death independent of expanded polyglutamine repeats via an Sp1-dependent pathway. *Proceedings of the National Academy of Sciences of the United States of America, 100,* 4281-4286.

Sadoul, K., Boyault, C., Pabion, M. and Khochbin, S. (2008) Regulation of protein turnover by acetyltransferases and deacetylases. *Biochimie, 90,* 306-312.

Saha, R. N. and Pahan, K. (2006) HATs and HDACs in neurodegeneration: a tale of disconcerted acetylation homeostasis. *Cell death and differentiation, 13,* 539-550.

Saini, P., Eyler, D. E., Green, R. and Dever, T. E. (2009) Hypusine-containing protein eIF5A promotes translation elongation. *Nature, 459,* 118-121.

Sanders, B. D., Zhao, K., Slama, J. T. and Marmorstein, R. (2007) Structural basis for nicotinamide inhibition and base exchange in Sir2 enzymes. *Molecular cell, 25,* 463-472.

Santini, V., Gozzini, A. and Ferrari, G. (2007) Histone deacetylase inhibitors: molecular and biological activity as a premise to clinical application. *Curr Drug Metab, 8,* 383-393.

Sawada, M., Suzumura, A., Hosoya, H., Marunouchi, T. and Nagatsu, T. (1999) Interleukin-10 inhibits both production of cytokines and expression of cytokine receptors in microglia. *Journal of Neurochemistry, 72,* 1466-1471.

Schmitz, M. L., Mattioli, I., Buss, H. and Kracht, M. (2004) NF-kappaB: a multifaceted transcription factor regulated at several levels. *Chembiochem, 5,* 1348-1358.

Schumann, R. R., Pfeil, D., Lamping, N., Kirschning, C., Scherzinger, G., Schlag, P., Karawajew, L. and Herrmann, F. (1996) Lipopolysaccharide induces the rapid tyrosine phosphorylation of the mitogen-activated protein kinases erk-1 and p38 in cultured human vascular endothelial cells requiring the presence of soluble CD14. *Blood, 87,* 2805-2814.

Segel, R., Anikster, Y., Zevin, S., Steinberg, A., Gahl, W. A., Fisher, D., Staretz-Chacham, O., Zimran, A. and Altarescu, G. (2011) A safety trial of high dose glyceryl triacetate for Canavan disease. *Molecular genetics and metabolism, 103,* 203-206.

Seo, D. R., Kim, K. Y. and Lee, Y. B. (2004) Interleukin-10 expression in lipopolysaccharide-activated microglia is mediated by extracellular ATP in an autocrine fashion. *Neuroreport, 15,* 1157-1161.

Shaftel, S. S., Griffin, W. S. and O'Banion, M. K. (2008) The role of interleukin-1 in neuroinflammation and Alzheimer disease: an evolving perspective. *Journal of neuroinflammation, 5,* 7.

Shapiro, L. and Dinarello, C. A. (1995) Osmotic regulation of cytokine synthesis in vitro. *Proceedings of the National Academy of Sciences of the United States of America, 92,* 12230-12234.

Sharma, S. K. (2010) Protein acetylation in synaptic plasticity and memory. *Neuroscience and biobehavioral reviews, 34,* 1234-1240.

Shechter, D., Dormann, H. L., Allis, C. D. and Hake, S. B. (2007) Extraction, purification and analysis of histones. *Nature protocols, 2,* 1445-1457.

Shi, L. and Wu, J. (2009) Epigenetic regulation in mammalian preimplantation embryo development. *Reprod Biol Endocrinol, 7,* 59.

Shin, J. H., Li, R. W., Gao, Y., Baldwin, R. t. and Li, C. J. (2012) Genome-wide ChIP-seq mapping and analysis reveal butyrate-induced acetylation of H3K9 and H3K27 correlated with transcription activity in bovine cells. *Functional & integrative genomics, 12,* 119-130.

Shogren-Knaak, M., Ishii, H., Sun, J. M., Pazin, M. J., Davie, J. R. and Peterson, C. L. (2006) Histone H4-K16 acetylation controls chromatin structure and protein interactions. *Science (New York, N.Y, 311,* 844-847.

Silva, P. F., Garcia, V. A., Dornelles Ada, S. et al. (2012) Memory impairment induced by brain iron overload is accompanied by reduced H3K9 acetylation and ameliorated by sodium butyrate. *Neuroscience, 200,* 42-49.

Smith, W. L., DeWitt, D. L. and Garavito, R. M. (2000) Cyclooxygenases: structural, cellular, and molecular biology. *Annual review of biochemistry, 69,* 145-182.

Sofroniew, M. V. (2009) Molecular dissection of reactive astrogliosis and glial scar formation. *Trends in neurosciences, 32,* 638-647.

Sofroniew, M. V. and Vinters, H. V. (2010) Astrocytes: biology and pathology. *Acta neuropathologica, 119,* 7-35.

Soliman, M. L., Puig, K. L., Combs, C. K. and Rosenberger, T. A. (2012a) Acetate reduces microglia inflammatory signaling in vitro. *Journal of Neurochemistry, 123,* 555-567.

Soliman, M. L. and Rosenberger, T. A. (2011) Acetate supplementation increases brain histone acetylation and inhibits histone deacetylase activity and expression. *Molecular and cellular biochemistry, 352,* 173-180.

Soliman, M. L., Smith, M. D., Houdek, H. M. and Rosenberger, T. A. (2012b) Acetate supplementation modulates brain histone acetylation and decreases interleukin-1beta expression in a rat model of neuroinflammation. *Journal of neuroinflammation, 9,* 51.

Steffan, J. S., Bodai, L., Pallos, J. et al. (2001) Histone deacetylase inhibitors arrest polyglutamine-dependent neurodegeneration in Drosophila. *Nature, 413,* 739-743.

Sterner, D. E. and Berger, S. L. (2000) Acetylation of histones and transcription-related factors. *Microbiol Mol Biol Rev, 64,* 435-459.

Strahl, B. D. and Allis, C. D. (2000) The language of covalent histone modifications. *Nature, 403,* 41-45.

Streit, W. J., Walter, S. A. and Pennell, N. A. (1999) Reactive microgliosis. *Progress in neurobiology, 57,* 563-581.

Sugino, T., Nozaki, K., Takagi, Y., Hattori, I., Hashimoto, N., Moriguchi, T. and Nishida, E. (2000) Activation of mitogen-activated protein kinases after transient forebrain ischemia in gerbil hippocampus. *J Neurosci, 20,* 4506-4514.

Sun, G. Y., Shelat, P. B., Jensen, M. B., He, Y., Sun, A. Y. and Simonyi, A. (2010) Phospholipases A2 and inflammatory responses in the central nervous system. *Neuromolecular medicine, 12,* 133-148.

Suzuki, S., Tanaka, K. and Suzuki, N. (2009) Ambivalent aspects of interleukin-6 in cerebral ischemia: inflammatory versus neurotrophic aspects. *J Cereb Blood Flow Metab, 29,* 464-479.

Terasaki, T. (1992) [Studies on the mechanism of drug distribution in tissues]. *Yakugaku Zasshi, 112,* 887-905.

Theis, M., Si, K. and Kandel, E. R. (2003) Two previously undescribed members of the mouse CPEB family of genes and their inducible expression in the principal cell layers of the hippocampus. *Proceedings of the National Academy of Sciences of the United States of America, 100,* 9602-9607.

Thoren, A. E., Helps, S. C., Nilsson, M. and Sims, N. R. (2005) Astrocytic function assessed from 1-14C-acetate metabolism after temporary focal cerebral ischemia in rats. *J Cereb Blood Flow Metab, 25,* 440-450.

Thorne, A. W., Kmiciek, D., Mitchelson, K., Sautiere, P. and Crane-Robinson, C. (1990) Patterns of histone acetylation. *Eur J Biochem, 193,* 701-713.

Tian, L., Ma, L., Kaarela, T. and Li, Z. (2012) Neuroimmune crosstalk in the central nervous system and its significance for neurological diseases. *Journal of neuroinflammation, 9,* 155.

Turner, B. M., O'Neill, L. P. and Allan, I. M. (1989) Histone H4 acetylation in human cells. Frequency of acetylation at different sites defined by immunolabeling with site-specific antibodies. *FEBS letters, 253,* 141-145.

Vecsey, C. G., Hawk, J. D., Lattal, K. M. et al. (2007) Histone deacetylase inhibitors enhance memory and synaptic plasticity via CREB:CBP-dependent transcriptional activation. *J Neurosci, 27,* 6128-6140.

Vitkovic, L., Bockaert, J. and Jacque, C. (2000) "Inflammatory" cytokines: neuromodulators in normal brain? *Journal of Neurochemistry, 74,* 457-471.

Vitkovic, L., Maeda, S. and Sternberg, E. (2001) Anti-inflammatory cytokines: expression and action in the brain. *Neuroimmunomodulation, 9,* 295-312.

Vucetic, Z., Kimmel, J. and Reyes, T. M. (2011) Chronic high-fat diet drives postnatal epigenetic regulation of mu-opioid receptor in the brain. *Neuropsychopharmacology : official publication of the American College of Neuropsychopharmacology, 36,* 1199-1206.

Waniewski, R. A. and Martin, D. L. (1998) Preferential utilization of acetate by astrocytes is attributable to transport. *J Neurosci, 18,* 5225-5233.

Wells, D. G. (2006) RNA-binding proteins: a lesson in repression. *J Neurosci, 26,* 7135-7138.

Woo, M. S., Jang, P. G., Park, J. S., Kim, W. K., Joh, T. H. and Kim, H. S. (2003) Selective modulation of lipopolysaccharide-stimulated cytokine expression and mitogen-activated protein kinase pathways by dibutyryl-cAMP in BV2 microglial cells. *Brain Res Mol Brain Res, 113,* 86-96.

Wyss, M. T., Magistretti, P. J., Buck, A. and Weber, B. (2011) Labeled acetate as a marker of astrocytic metabolism. *J Cereb Blood Flow Metab, 31,* 1668-1674.

Wyss, M. T., Weber, B., Treyer, V., Heer, S., Pellerin, L., Magistretti, P. J. and Buck, A. (2009) Stimulation-induced increases of astrocytic oxidative metabolism in rats and humans investigated with 1-11C-acetate. *J Cereb Blood Flow Metab, 29,* 44-56.

Yang, H., Feng, G. D., Liang, Z., Vitale, A., Jiao, X. Y., Ju, G. and You, S. W. (2012) In vitro beneficial activation of microglial cells by mechanically-injured astrocytes enhances the synthesis and secretion of BDNF through p38MAPK. *Neurochemistry international, **61,*** 175-186.

Zanelli, C. F., Maragno, A. L., Gregio, A. P., Komili, S., Pandolfi, J. R., Mestriner, C. A., Lustri, W. R. and Valentini, S. R. (2006) eIF5A binds to translational machinery components and affects translation in yeast. *Biochemical and biophysical research communications, 348,* 1358-1366.

Zhang, B., West, E. J., Van, K. C., Gurkoff, G. G., Zhou, J., Zhang, X. M., Kozikowski, A. P. and Lyeth, B. G. (2008) HDAC inhibitor increases histone H3 acetylation and reduces microglia inflammatory response following traumatic brain injury in rats. *Brain research, 1226,* 181-191.

Zhang, K., Williams, K. E., Huang, L., Yau, P., Siino, J. S., Bradbury, E. M., Jones, P. R., Minch, M. J. and Burlingame, A. L. (2002) Histone acetylation and deacetylation: identification of acetylation and methylation sites of HeLa histone H4 by mass spectrometry. *Mol Cell Proteomics, 1,* 500-508.

Zhao, M. L., Kim, M. O., Morgello, S. and Lee, S. C. (2001) Expression of inducible nitric oxide synthase, interleukin-1 and caspase-1 in HIV-1 encephalitis. *Journal of neuroimmunology, 115,* 182-191.